Available online at www.sciencedirect.com
ScienceDirect
Coordination Chemistry Reviews 250 (2006) 2347–2410
COORDINATION CHEMISTRY REVIEWS
www.elsevier.com/locate/ccr

Review

Lanthanides and actinides: Annual survey of their organometallic chemistry covering the years 2001 and 2002

Jochen Gottfriedsen, Frank T. Edelmann *

Chemisches Institut der Otto-von-Guericke-Universität Magdeburg, D-39106 Magdeburg, Germany

Received 20 February 2006; accepted 21 February 2006
Available online 15 May 2006

Contents

* Corresponding author. Tel.: +49 391 6718327; fax: +49 391 6712933.
E-mail address: frank.edelmann@vst.uni-magdeburg.de (F.T. Edelmann).

0010-8545/$ – see front matter
doi:10.1016/j.ccr.2006.02.030

Keywords: Lanthanides; Actinides; Cyclopentadienyl complexes; Cyclooctatetraenyl complexes; Organometallic chemistry

1. Introduction

This review summarizes the progress in organo-*f*-element chemistry during the years 2001 and 2002. In 2002 both "Chemical Reviews" ("Frontiers in Lanthanide Chemistry") [1] and the "Journal of Organometallic Chemistry" published special issues devoted to (organo)lanthanide chemistry. Thus various important special aspects of organolanthanide chemistry have been covered in excellent recent review articles. Among the topics were "Chiral lanthanide complexes: coordination chemistry and applications" [2], "Synthesis, arrangement, and reactivity of arene-lanthanide compounds" [3], "Bis(pentafluorophenyl)mercury—a versatile synthon in organo-, organooxo-, and organoamido-lanthanoid chemistry" [4], "Synthesis and structural chemistry of non-cyclopentadienyl organolanthanide complexes" [5], "Chemistry of tris(pentamethylcyclopentadienyl) *f*-element complexes $(C_5Me_5)_3M$" [6], "The expansion of divalent organolanthanide reduction chemistry via new molecular divalent complexes and sterically induced reduction reactivity of trivalent complexes" [7], "Recent advances in *f*-element reduction chemistry" [8], "DFT studies of some structures and reactions of lanthanides complexes" [9], "$[(Tp^{tBu,Me})Yb(\mu\text{-}H)]_2$: a fecund precursor to a host of divalent, hydrotris(pyrazolyl)borate supported *f*-element complexes" [10], "Lanthanide(II) complexes bearing mixed linked and unlinked cyclopentadienyl—monodentate-anionic ligands" [11], "Asymmetric catalysis and amplification with chiral lanthanide complexes" [12], "A new era in divalent organolanthanide chemistry?" [13], "Aspects of non-classical organolanthanide chemistry" [14], "Organolanthanide chemistry in the gas phase" [15], "Chemistry of the lanthanides using pyrazolylborate ligands" [16], "Lanthanocene catalysts in selective organic synthesis" [17], "Mono(cyclopentadienyl) complexes of the rare-earth metals" [18], "Organolanthanides RLnX (R is alkyl, aryl, X is halogen) and lanthanide complexes with aromatic hydrocarbon dianions: synthesis, structure, and reactivity" [19], "Intramolecular coordination of Ln–O and Ln–N bonds in some new substituted lanthanocene complexes" [20] "Synthesis, structural characterization and catalytic behavior of one-atom bridged fluorenyl cyclopentadienyl lanthanocene complexes with C_s- or C_1-symmetry" [21], "Synthesis and reactivity of organolanthanoid complexes containing N and S ligands" [22], "Organo-rare-earth-metal initiated living polymerizations of polar and nonpolar monomers" [23], and "Insertions into lanthanide-ligand bonds in organolanthanide chemistry" [24]. Mikami et al. reviewed "Asymmetric catalysis with lanthanide complexes", including organometallic catalysts [25].

2. Lanthanides

2.1. Lanthanide carbonyls

A comparative density functional study on metal–ligand (M–L) interaction has been performed on $X_3Ln(CO)$ (X = F, I; Ln = La, Nd) species including scalar relativistic effects by means of the zero-order regular approximation (ZORA) Hamiltonian. The role of the halogen atoms in modeling the M–L interactions has been discussed for the π-ligand CO [26]. Reactions of neutral, ground-state yttrium atoms with formaldehyde,

acetaldehyde, and acetone (Y + RR′CO, where R,R′ = H, Me) were studied in crossed molecular beams, and carbonyl species of the type (R)(R′)Y(CO) and YCO have been discussed [27,28]. In a related study the reaction of ground-state Y atoms with ketene (H_2CCO) under formation of YCH_2, YCCO and YCHCO has been investigated [29].

2.2. Lanthanide hydrocarbyls

Whereas complexes of unsubstituted and substituted cyclopentadienyl ligands represent the vast majority of all published compounds in organolanthanide chemistry, examples of isolated and fully characterized (including X-ray structural analyses) compounds containing only σ-bonded alkyl and aryl ligands are still fairly rare. The first structurally characterized homoleptic lanthanide alkyls became available through the use of bulky mono-, bis- and tris(trimethylsilyl)-substituted methyl ligands. Simple unsolvated alkyls of the rare earth elements have not yet been synthesized.

Density functional B3LYP calculations have been employed to investigate potential energy surfaces for the reaction of scandium oxide with methane. ScO is not reactive with respect to methane at low and ambient temperatures. At elevated temperatures, the ScO + CH_4 reaction can proceed via a barrier of 22.4 kcal/mol to form a MeScOH molecule with exothermicity of 9.8 kcal/mol. MeScOH is not likely to decompose to the methyl radical and ScOH because this process is 58.9 kcal/mol exothermic [30]. DFT(B3PW91) calculations on the activation of CH_4 by models (Cl_2LnZ) of Cp^*_2LnZ (Z = H, Me) have been carried out for the entire lanthanide series. Cl_2LnZ appears to be a good model for Cp^*_2LnZ. It reproduces well the coordination around the lanthanide [31]. The potential energy surface and reaction mechanism corresponding to the reaction of ytterbium monocation with fluoromethane, involving $MeYbF^+$ as an intermediate, has been investigated by using density functional theory. The reaction represents a prototype of the activation of the C–F bond in fluorohydrocarbons by bare lanthanide cations [32].

2.2.1. Neutral homoleptic compounds

Anhydrous $SmCl_3$ reacts with $LiCH_2SiMe_3$ in THF yielding $Sm(CH_2SiMe_3)_3(THF)_3$ as yellow crystals in 50% yield. The single crystal structural analyses of the Sm compound as well as those of $Er(CH_2SiMe_3)_3(THF)_2$, $Yb(CH_2SiMe_3)_3(THF)_2$, and $Lu(CH_2SiMe_3)_3(THF)_2$ show the Sm atom in a *fac*-octahedral coordination and the heavier lanthanides Er, Yb, and Lu trigonal bipyramidally coordinated with three equatorial alkyl ligands and two axial THF molecules [33,34]. DFT calculations have also been carried out on the compounds $Ln[CH(SiR_2R')(SiR_3)]_3$ for Ln = La, Sm and (i) R = R′ = Me, (ii) R = H, R′ = Me, and (iii) R = R′ = H. The results were compared with the X-ray structures that are available from the literature for both metals and R = R′ = Me. The calculations correctly reproduced the experimental structural features in these complexes exhibiting the peculiar pyramidal coordination geometry. The results show significant increases in the Si–C bond lengths associated with β-Si–C agostic interactions, whereas little structural changes were found for γ-C–H agostic interactions. The latter are in fact repulsive [35]. Reactions of $Ln[CH(SiMe_3)_2]_3$ (Ln = Y, La) with 4 equiv. of nonafluorobiphenyl-2-ol (PBOH) in pentane results in rapid and quantitative formation of $Ln(PBO)_3(PBOH)$ complexes [36]. The metalation of $HP(SiMe_3)_2$ with $Y[CH(SiMe_3)_2]_3$ gave homoleptic, dimeric $[Y\{P(SiMe_3)_2\}_3]_2$ [37].

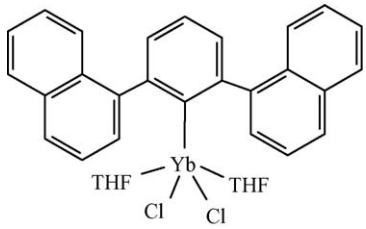

Scheme 1.

2.2.2. Anionic homoleptic compounds

The first homoleptic three-coordinate lanthanide(II) alkyl anions have been successfully prepared with the use of the sterically demanding bis(trimethylsilyl)methyl ligand. Red $[K(YbR_3)]_\infty$ was obtained in 87% yield by reacting ytterbium diiodide with KR in benzene (R = $CH(SiMe_3)_2$). Mixing LiR, YbI_2 and 2 equiv. of KR in a mixture of diethyl ether and a small amount of THF yielded the red lithium salt $[Li(THF)_4][YbR_3]$ in 52% yield. Both compound have been structurally characterized [38]. Several anionic scandium complexes containing 3-borane-1-alkylimidazol-2-ylidene derivatives have been prepared and structurally characterized [39].

2.2.3. Heteroleptic compounds

The synthetic and structural chemistry of non-cyclopentadienyl organolanthanide complexes have been reviewed by Edelmann et al. [5]. Marques et al. have published a review on the chemistry of the lanthanide using pyrazolylborate ligands [16].

The use of very bulky terphenyl-type ligands allowed the isolation and structural characterization of several monoarylanthanide dihalides [40]. Reactions of DmpLi (Dmp = 2,6-dimesitylphenyl) with $LnCl_3$ (Ln = Sc, Y, Yb) in a 1:1 molar ratio in THF at room temperature followed by crystallizaion from toluene/hexane at −30 °C produced $DmpLnCl_2(THF)_2$ (Ln = Sc, Yb) and $DmpYCl_2(THF)_3$, respectively. The molecular structures of these materials feature monomeric complexes with distorted-bipyramidal (Ln = Sc, Yb) or octahedral (Ln = Y) coordination geometry about the metal atom, with the two chlorine ligands occupying the axial positions [40]. The molecular structures of the terphenyl derivatives $DnpLnCl_2(THF)_2$ (Dnp = 2,6-di(1-naphthyl)phenyl; Ln = Y, Tm, Yb) have been reported (Scheme 1) [41].

Reaction of rare earth metal-alkyl complexes $Ln(CH_2SiMe_3)_3(THF)_3$ (Ln = Y, Lu) with $B(C_6X_5)_3$ (X = H, F) in the presence of crown ethers gave the ion pairs $[Ln(CH_2SiMe_3)(CE)(THF)_n][B(CH_2SiMe_3)(C_6X_5)_3]$ (CE = 12-crown-4, n = 1; CE = 15-crown-5, 18-crown-6,

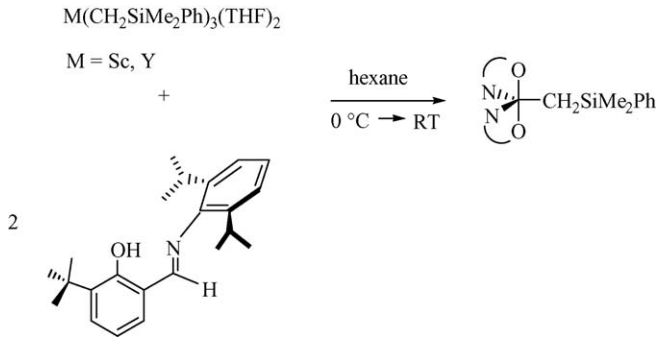

Scheme 2.

$n = 0$). The compound $[Lu(CH_2SiMe_3)_2(12\text{-crown-}4)(THF)][B(CH_2SiMe_3)Ph_3]$ was the first structurally characterized cationic lanthanide alkyl complex [42].

Similar reactions of $Ln(CH_2SiMe_3)_3(THF)_2$ (Ln = Sc, Y) with a bulky salicylaldiminato ligand as depicted in Scheme 2 led to diastereoselective formation of highly thermally stable L_2LnR complexes whose reactivity with dihydrogen to form Group 3 metal hydrides has been investigated. For the Y derivative a smooth and clean reaction with H_2 (4 atm, RT) was observed, leading to formation of the dimeric hydride. Fig. 1 illustrates the molecular structure of the scandium derivative [43].

Sterically demanding chelating diamide ligands have also been employed in the synthesis of monoalkyl lanthanide complexes. Yttrium triiodide reacts with the potassium salt $K_2[ArN(CH_2)_3NAr]$ (Ar = 2, 6-$Pr^i_2C_6H_3$) to yield a monoiodide complex and, by further reaction with $KCH(SiMe_3)_2$, the corresponding alkyl complex $[ArN(CH_2)_3NAr]Y[CH(SiMe_3)_2](THF)$, which has been structurally characterized by X-ray crystallography [44]. Several scandium hydrocarbyl complexes stabilized by diamido-donor ligands have been synthesized according to Scheme 3. The most suitable synthetic route is protonation of alkyl or aryl precursors by the free amines. Both monoorganoscandium complexes form thermally sensitive yellow solids [45].

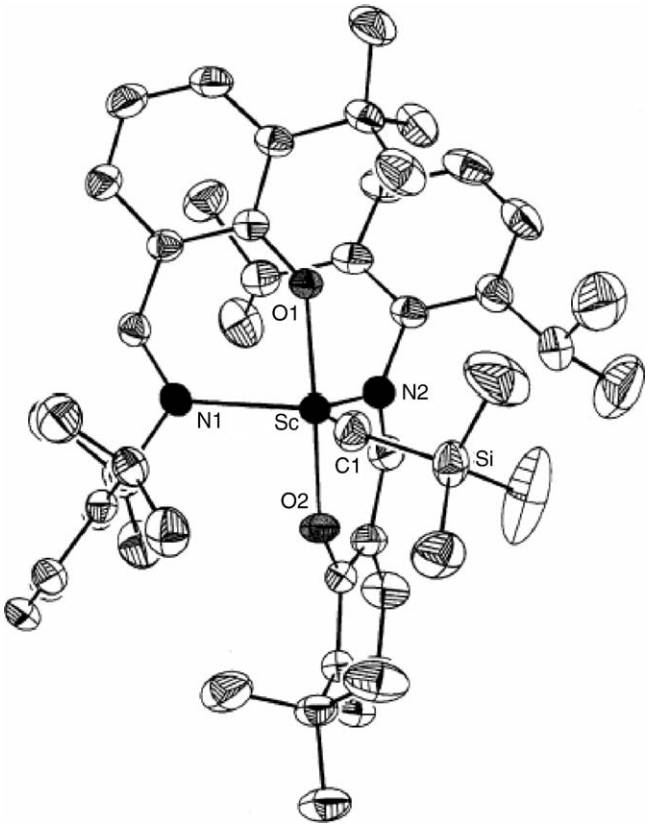

Fig. 1. Molecular structure of $[2\text{-}(2, 6\text{-}Pr^i_2C_6H_3N{=}CH)(6\text{-}Bu^t)C_6H_3O]_2Ln(CH_2SiMe_3)(THF)$ [47].

Related bis(alkyl) complexes of scandium and yttrium have become accessible with the use of a specially designed bulky iminophenolato ligand. The reaction of equimolar amounts of 2-(2,4,6-$Me_3C_6H_2N{=}CH$)(6-Bu^t)C_6H_3OH (=HL) with $Ln(CH_2SiMe_2Ph)_3(THF)_2$ (Ln = Sc, Y) under mild conditions gave $Ln(CH_2SiMe_2Ph)_3(THF)(L)$ (Scheme 4). The trigonal-bipyramidal structure of these dialkyls was conformed crystallographically for Ln = Sc. Whereas the scandium complex is stable in solution at room temperature, the yttrium derivative slowly disproportionates to give YL_3 which is also accessible from $Y(CH_2SiMe_3)_3(THF)_2$ and three HL [46]. A series of mono(salicylaldiminato) bis-alkyls of scandium and yttrium has been prepared analogously [47].

β-Diketiminato ("nacnac") ligands are becoming increasingly popular as ancillary ligands in organolanthanide chemistry. Scheme 5 summarizes typical synthetic routes leading to diorganoscandium complexes stabilized by bulky β-diketiminato ligands [48].

Unusual cationic scandium methyl complexes supported by a β-diketiminato ligand (=LBu^t) have also recently been reported. As depicted in Scheme 6, the monomeric dimethyl scandium precursor reacts with varying equivalents of $B(C_6F_5)_3$ to form different ion pairs. Upon reaction with 0.5 equiv. of borane, a μ-methyl dimer is formed, which is quite unstable and slowly evolves methane. When the dimethyl complex is treated with a full equivalent of $B(C_6F_5)_3$, however, a monomeric ion pair $[LBu^tScMe][MeB(C_6F_5)_3]$ is produced in excellent yield as a yellow, crystalline solid when precipitated from hexane. Even the second scandium methyl group can be abstracted to form the dicationic species as an analytically pure white solid. Fig. 2 shows the molecular structure of the ion pair complex $[LBu^tScMe][MeB(C_6F_5)_3]$, which exhibits complex dynamic behavior in solution [49].

A most remarkable achievement was the stabilization of a diamagnetic Sc^IBr molecule in a sandwich-like structure. The reaction of the β-diketiminato scandium derivative $LScBr_2$ (L = $Et_2NCH_2CH_2NC(Me)CHC(Me)NCH_2CH_2NEt_2$) with $(C_3H_5)MgBr$ gave the unexpected blue-green scandium complex $(LMgBr)_2ScBr$, the structure of which was established by X-ray analysis (Fig. 3), liquid and solid state NMR, EPR, UV–vis, and magnetic measurements as well as DFT calculations. Correlation of all results led to the conclusion that the formal oxidation state of scandium in this complex is *one* (Sc(I)) having no unpaired electrons [50].

Neutral and cationic yttrium and lanthanum alkyl complexes have also been prepared with related linked 1,4,7-

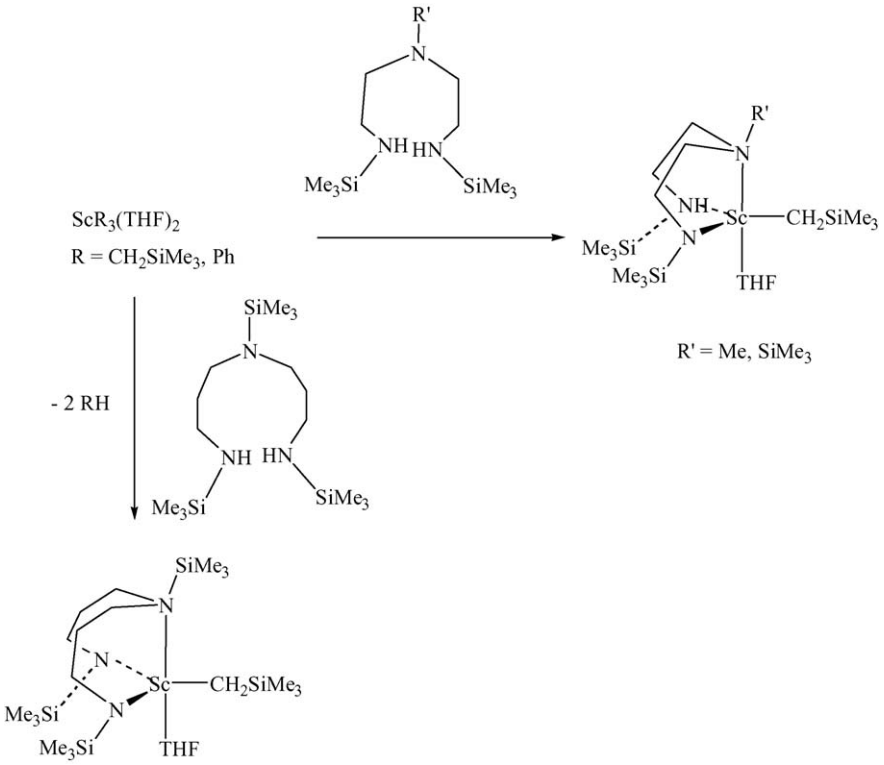

Scheme 3.

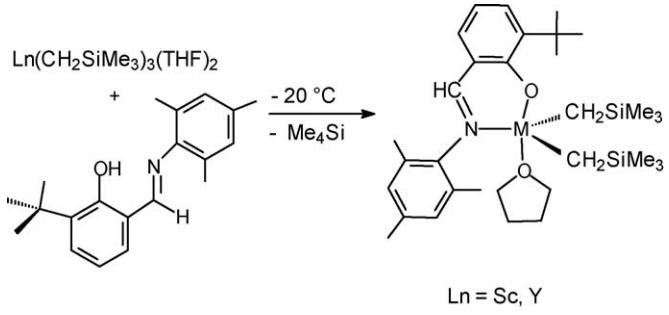

Scheme 4.

triazacyclononane-amide monoanionic ancillary ligands as illustrated in Scheme 7. An X-ray structure analysis of the neutral yttrium derivative with R = ^{i}Pr confirmed its identification as a monomeric, THF-free yttrium dialkyl (Fig. 4) [51].

Related new ligand sets for the stabilization of scandium and yttrium alkyls have been introduced. Typical reactions are summarized in Scheme 8. As a representative example, Fig. 5 shows the molecular structure of the monoalkyl derivative $(N_2NN')Sc(CH_2SiMe_3)$ $(N_2NN' = (2\text{-}C_5H_4N)CH_2N\text{-}\{CH_2CH_2NSiMe_3\}_2^{2-})$ [52,53].

Bulky guanidinato ligands have been successfully employed in the stabilization of yttrium alkyl complexes. Typical synthetic procedures are depicted in Scheme 9, while Fig. 6 illustrates the molecular structure of the σ-tertiary-butyl complex $[^{i}PrNC\{N(SiMe_3)_2\}N^{i}Pr]_2Y^{t}Bu$ [54].

The chemistry of organolanthanide complexes containing pyrazolylborate ancillary ligands have recently been reviewed by Marques et al. [16]. Reactions between $(Tp^{Me,Me})ScCl_2(THF)$ and $(Tp^{tBu,Me})ScCl_2$ ($Tp^{Me,Me}$ = tris(3,5-dimethylpyrazolyl)borate; $Tp^{tBu,Me}$ = tris(3-*t*-butyl-5-methylpyrazolyl)borate) with alkyllithium reagents RLi (R = Me, CH_2SiMe_3,

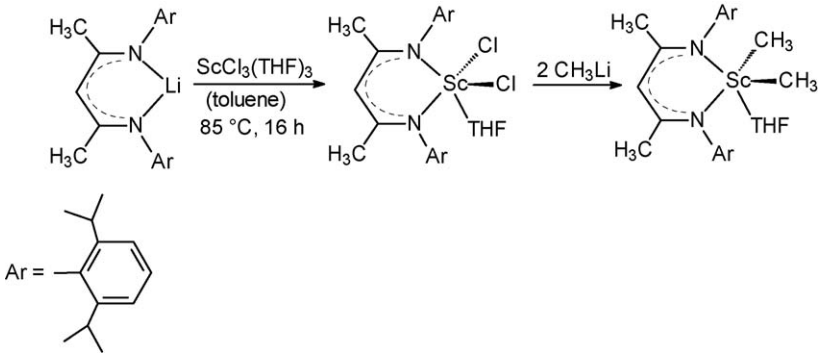

Scheme 5.

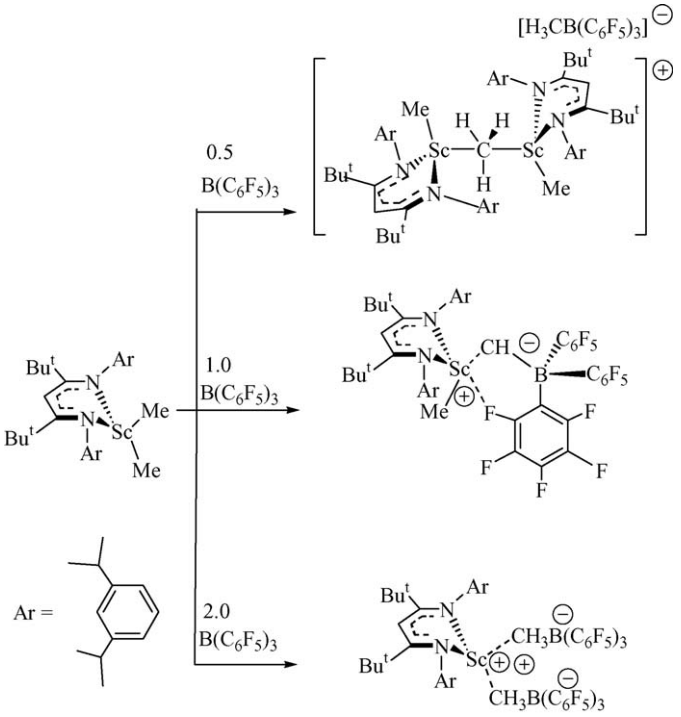

Scheme 6.

$CH(SiMe_3)_2$) mostly gave the lithium salts of the Tp ligands as the major products. Only the heteroleptic alkyl complex $(Tp^{Me,Me})Sc(CH_2SiMe_3)_2(THF)$ could be obtained contaminated with at least 10% $Li(Tp^{Me,Me})$ via this method. However, a salt-free elimination route involving reaction between in situ generated $Sc(CH_2SiMe_3)_3(THF)_2$ and the protonated ligands $Tp^{R,Me}H$ (R = Me, Bu^t) gave the desired dialkyl complexes $(Tp^{Me,Me})Sc(CH_2SiMe_3)_2(THF)$ and unsolvated $(Tp^{tBu,Me})Sc(CH_2SiMe_3)_2$ in 67 and 87% yield, respectively [16]. Addition of a stoichiometric amount of KR

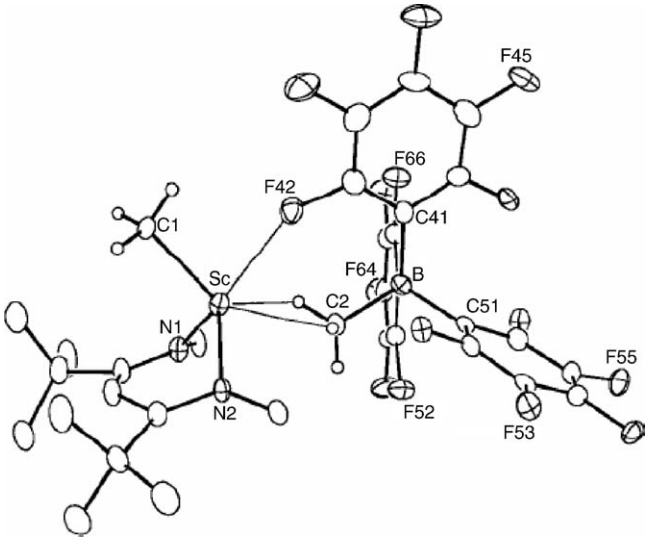

Fig. 2. Molecular structure of [LBu^{t}ScMe][$MeB(C_6F_5)_3$] [49].

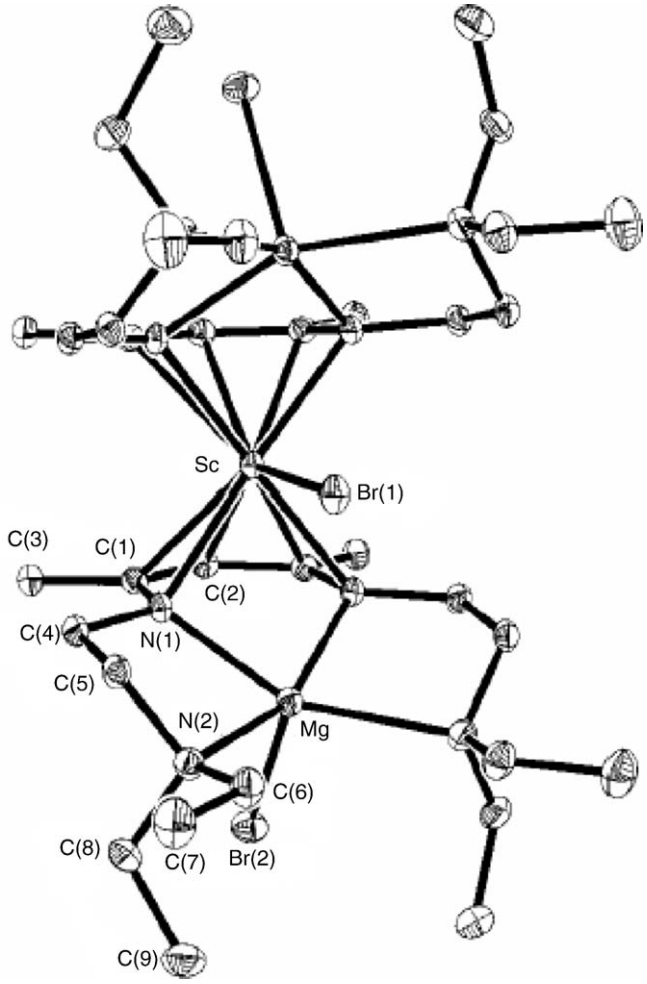

Fig. 3. Molecular structure of $(LMgBr)_2ScBr$ (L = $Et_2NCH_2CH_2NC(Me)CHC(Me)NCH_2CH_2NEt_2$) [50].

(R = $CH_2C_6H_4$-*o*-NMe_2, C_6H_4-*o*-CH_2NMe_2, CH_2Ph) to a solution of $Sm(Tp^{Me2})_2$ in toluene or THF led to the immediate formation of the insoluble, purple $Sm(Tp^{Me2})_2$ compound. However, when these reactions were carried out in the presence

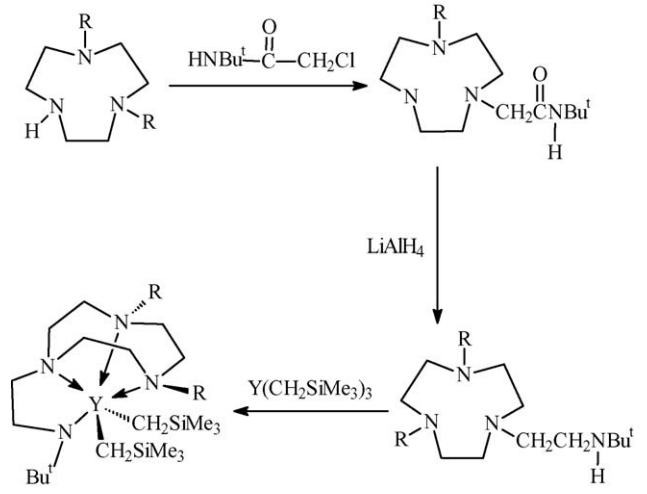

Scheme 7.

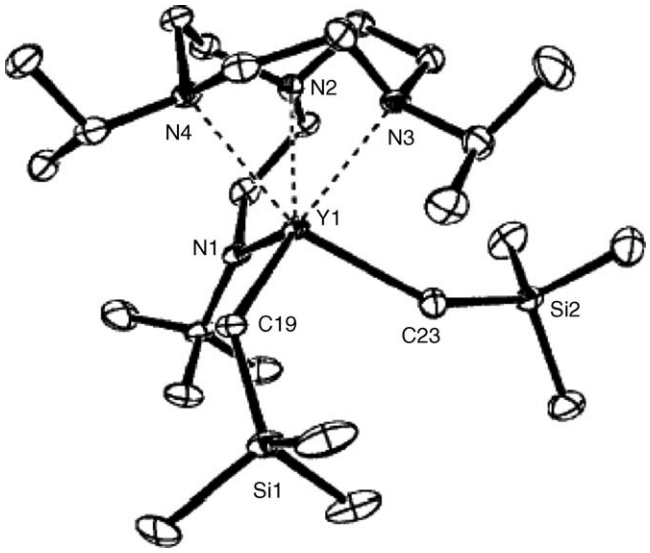

Fig. 4. Molecular structure of [*N*,*N*′-R_2-tacn-*N*″-$(CH_2)_2N^tBu$]$Y(CH_2SiMe_3)_2$ (R = ^{i}Pr, tacn = 1,4,7-triazacyclononane).

of protic substrates such as CpH or HC≡CPh, the compounds $(Tp^{Me2})_2SmCp$ and $(Tp^{Me2})_2SmC{\equiv}CPh$ were readily formed and isolated in good yields [55].

The reaction of $Ln[N(SiMe_3)_2]_3$ (Ln = Y, La, Ce, Pr, Nd, Sm, Eu, Tb, Dy, Ho, Tm, Yb) with 2 equiv. of cyclohexylisocyanide gave good yields of complexes of the composition $Ln[N(SiMe_3)_2]_3(CNC_6H_{11})_2$. The crystal, molecular, and electronic structure of the neodymium derivative have been investigated in detail. The structure of $Nd[N(SiMe_3)_2]_3(CNC_6H_{11})_2$ shows the five-coordinate Nd^{3+} ion in a nearly exact trigonal-bipyramidal environment with two CNC_6H_{11} molecules in the axial and the three $N(SiMe_3)_2$ ligands in the equatorial positions [56]. The same investigations have also been carried out on the corresponding praseodymium species $Pr[N(SiMe_3)_2]_3(CNR)_2$ (R = Bu^t, C_6H_{11}) [57].

2.3. Lanthanide alkenyl and alkynyl compounds

Reaction pathways for the Y-induced acetylene(HCCH)–vinylidene(CCH_2) rearrangement in the gas phase have been identified by density functional and coupled cluster calculations with basis set extrapolations [58].

Trivalent methyl and vinyl samarium derivatives supported by a calix-pyrrole ligand system (Et$_8$-calix-pyrrol)(R)Sm(μ^3-Cl)[Li(THF)]$_2$[Li$_2$(THF)$_3$] (R = Me, CH = CH$_2$) were prepared via reaction of (Et$_8$-calix-pyrrol)(Cl)Sm[Li$_2$(THF)$_3$] with the corresponding organolithium reagent. The dinuclear complex (Et$_8$-calix-pyrrol)Sm$_2${(μ-Cl)$_2$[Li(THF)$_2$]}$_2$ was alkylated in diethyl ether resulting in the formation of the isostructural alkyl complex (Et$_8$-calix-pyrrol)Sm$_2${(μ-CH$_3$)$_2$[Li(THF)$_2$]}$_2$. The nature of the substituents present on the calix-tetrapyrrole

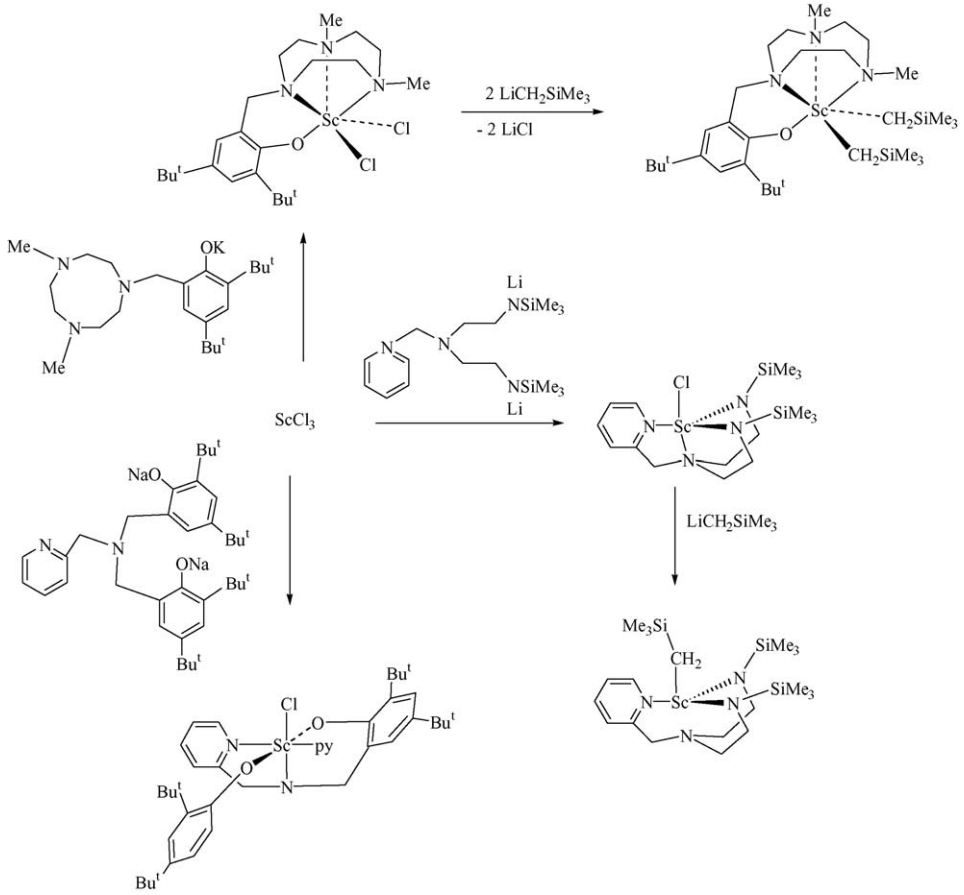

Scheme 8.

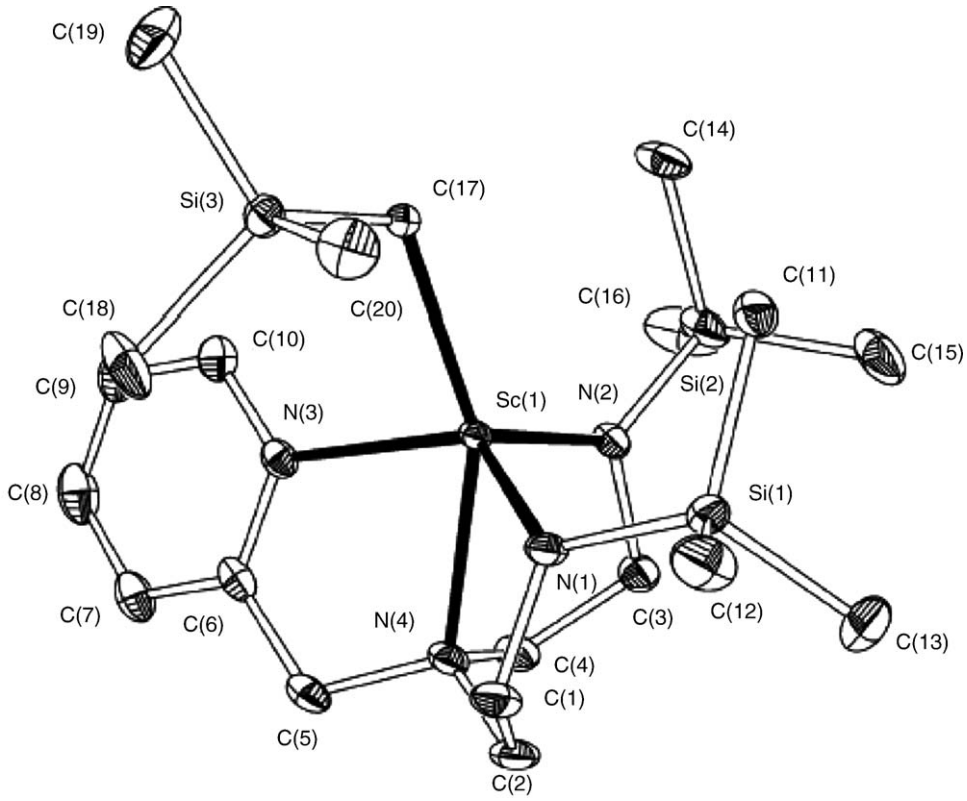

Fig. 5. Molecular structure of $(N_2NN')Sc(CH_2SiMe_3)$ $(N_2NN' = (2\text{-}C_5H_4N)CH_2N\{CH_2CH_2NSiMe_3\}_2^{2-})$ [53].

tetraanion ligand $\{[R_2C(C_4H_2N)]_4\}^{4-}$ (R = ($\{-CH_2\}_5-$)$_{0.5}$, Et) has been reported to greatly influence the type of reactivity of the corresponding Sm(II) compounds with acetylene, as illustrated in Scheme 10 [59].

2.4. Lanthanide allyls

A straightforward preparation of the dioxane adduct of tris(allyl)neodymium involves reaction of $NdI_3(THF)_{3.5}$

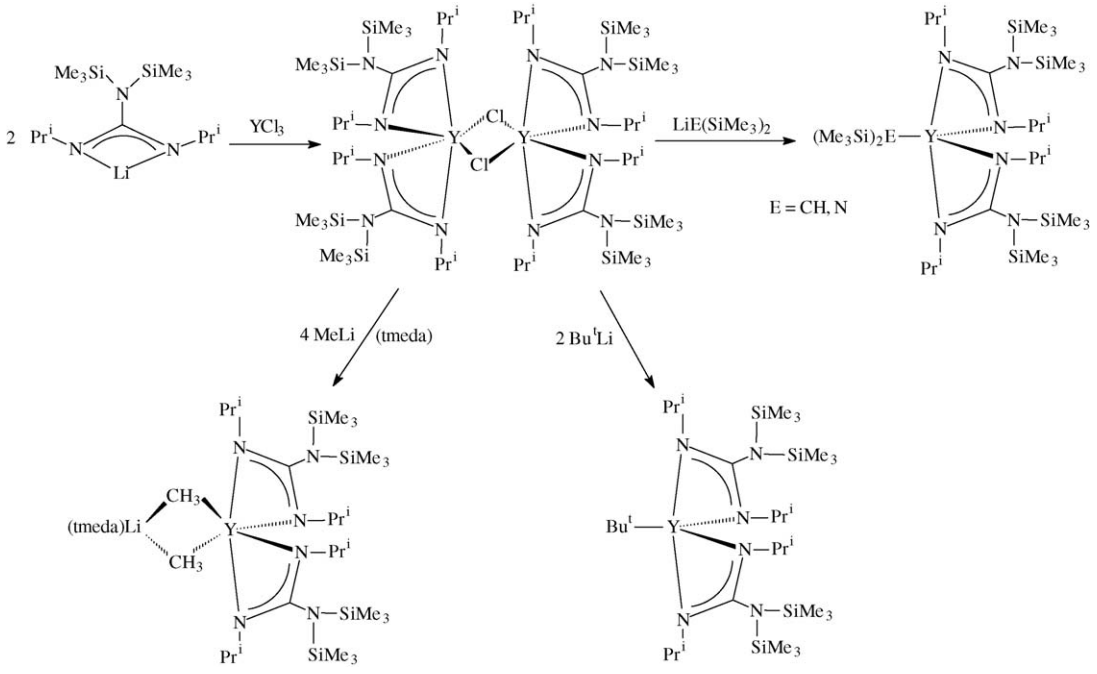

Scheme 9.

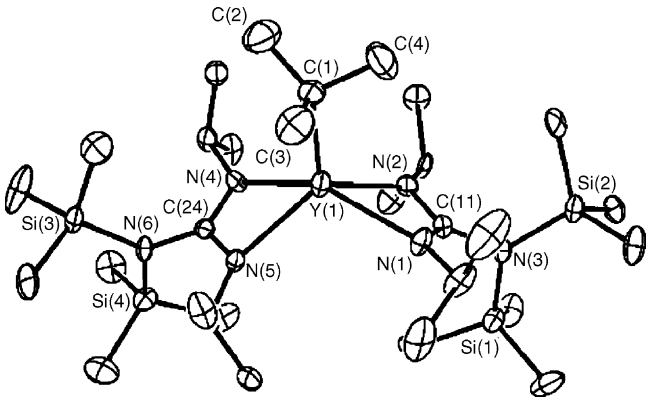

Fig. 6. Molecular structure of $[^{i}PrNC\{N(SiMe_3)_2\}N^{i}Pr]_2Y^{t}Bu$ [54].

with 3 equiv. of C_3H_5MgBr in THF, followed by recrystallization from dioxane. This procedure affords the halide-free product in more than 70% yield [60]. The synthesis of a cationic allylneodymium complex has also been achieved. In the first step, a comproportionation reaction between $Nd(\eta^3\text{-}C_3H_5)_3$(dioxane) and $NdCl_3(THF)_2$ (molar ratio 2:1) gave the bis(allyl)neodymium chloride complex $(\eta^3\text{-}C_3H_5)_2NdCl(THF)_x$, which was not isolated but treated in situ with $[Me_3NH][BPh_4]$ to afford grass-green $[(\eta^3\text{-}C_3H_5)NdCl(THF)_5][BPh_4]^{\bullet}THF$, which has been structurally characterized by an X-ray analysis. The crystal structure of this complex is depicted in Fig. 7 [60].

2.5. Lanthanide cyclopentadienyl complexes

Mono(cyclopentadienyl) complexes of the rare-earth metals have been comprehensively reviewed by Arndt and Okuda [18].

2.5.1. CpLnX compounds

Reactions of ytterbium naphthalene $(C_{10}H_8)Yb(THF)_2$ with 2-cyclopentadienylethanol, 1-cyclopentadienylpropan-2-ol, and 3-cyclopentadienyldimethylsilyl-*t*-butylamine have been studied as a convenient synthetic route to half-sandwich complexes of divalent ytterbium. In the case of the ligand 3-cyclopentadienyl-1-butoxy-2-propanol, $C_5H_4CH_2CH(OH)OBu^n$, the reaction with $(C_{10}H_8)Yb(THF)_2$ afforded the unusual tetranuclear, cubane-like complex $[\{C_5H_4CH_2CH(O)OBu^n\}Yb]_4$ in the form of ruby-red crystals, which have been characterized by an X-ray diffraction analysis. Fig. 8 shows the molecular structure of this compound [61].

Reactions of $Ln[N(SiMe_3)_2]_2(THF)_2$ (Ln = Sm, Yb) with 1 equiv. of $(C_5Me_4H)SiMe_2NHPh$ afforded the first linked cyclopentadienyl-anilido (or amido) lanthanide(II) complexes, $[Me_2Si(C_5Me_4)(NPh)]Ln(THF)_x$ (Ln = Sm, x = 0–1; Ln = Yb, x = 3) in 75–84% isolated yields (Scheme 11). Fig. 9 illustrates the molecular structure of $[Me_2Si(C_5Me_4)(NPh)]Yb(THF)_3$, verifying that this complex adopts a monomeric structure, in which the Yb(II) center is bonded to one chelating Cp-anilido ligand and three THF terminal ligands. The Yb–C(Cp) bond lengths range from 2.52 to 2.71 Å [62].

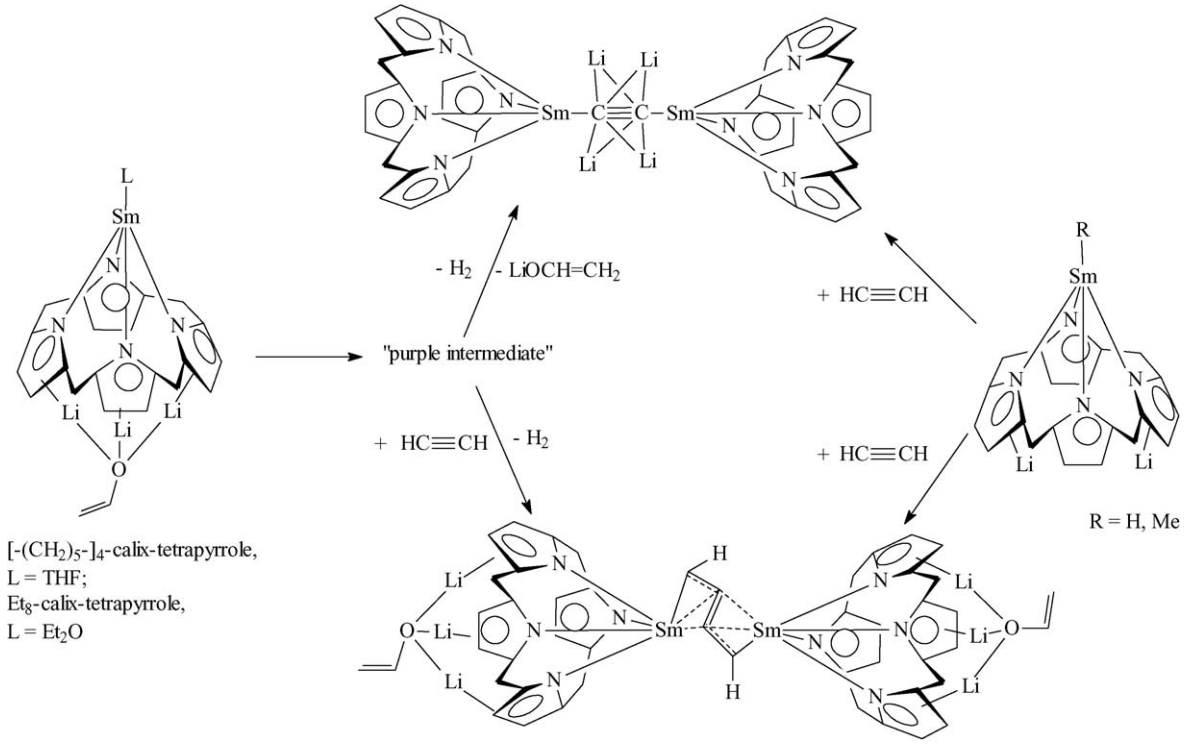

Organic substituents (either Et or -$(CH_2)_5$-) and THF coordinated to the Li atoms have been omitted for clarity

Scheme 10.

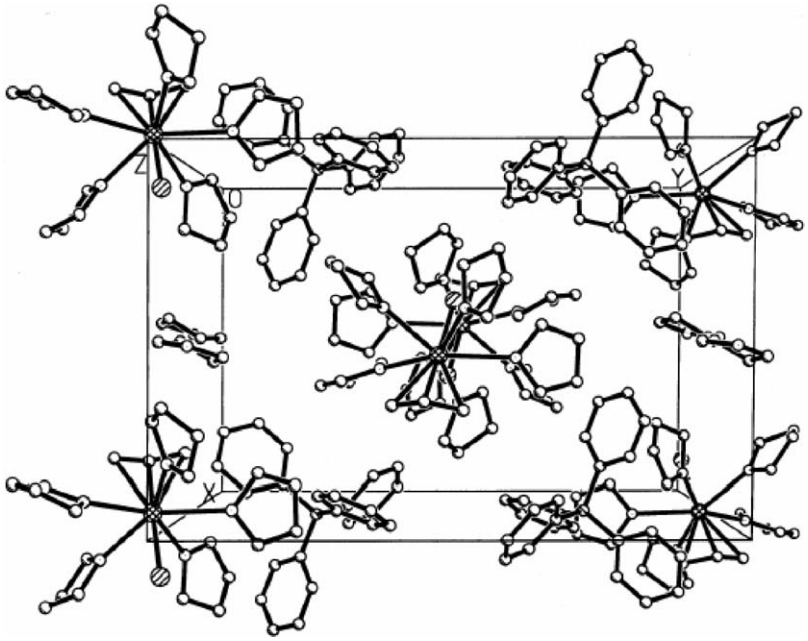

Fig. 7. Crystal structure of $[(\eta^3\text{-}C_3H_5)NdCl(THF)_5][BPh_4]\cdot THF$ [60].

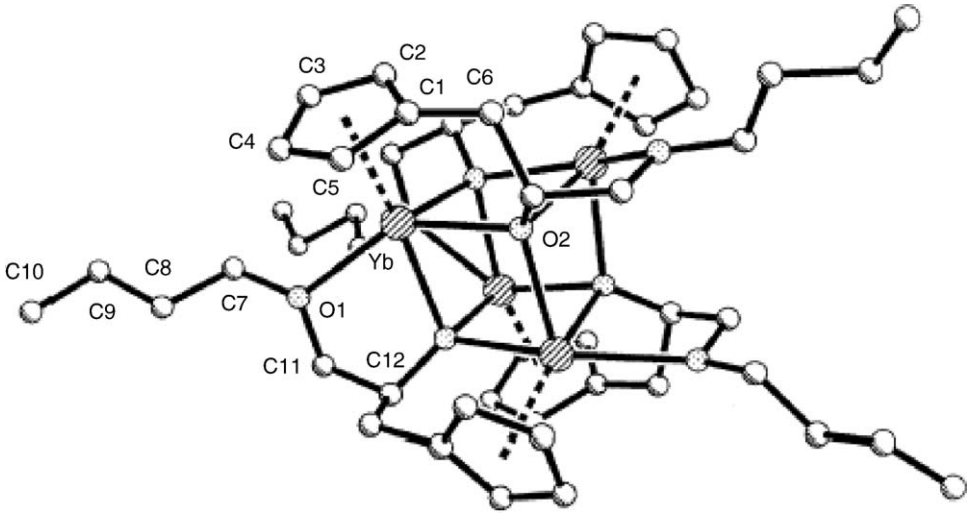

Fig. 8. Molecular structure of $[\{C_5H_4CH_2CH(O)OBu^n\}Yb]_4$ [61].

The synthesis, structures, and reactivity of the related silylene-linked cyclopentadienyl-phosphido lanthanide complexes have been studied. Scheme 12 illustrates the synthesis of the ligand precursors and the corresponding lanthanide(II) derivatives as well as reactions of the latter with 1,2-diiodoethane and benzophenone, which lead to binuclear lanthanide(III) species. As a representative example, the molecular structure of the divalent ytterbium species $[Me_2Si(C_5Me_4)(PAr)]Yb(THF)_3$ (Ar = $C_6H_2Bu^t{}_3$-2, 4, 6) is shown in Fig. 10 [63].

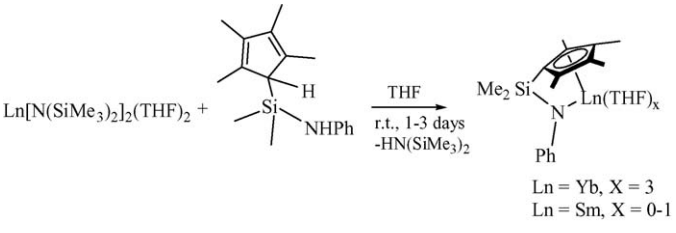

Scheme 11.

Two different synthetic routes leading to the iodo-bridged dimer $[(C_5HPr^i{}_4)Sm(\mu\text{-}I(THF)]_2$ have been reported [64]. The synthesis and characterization of divalent lanthanide complexes of a triazacyclononane-functionalized tetramethylcyclopentadienyl ligand have been reported [65]. Addition of $LnI_2(THF)_2$ (Ln = Sm, Yb) to $K[C_5Me_4SiMe_2(Pr^i{}_2\text{-tacn})]$ ($Pr^i{}_2$-tacn = 1, 4-diisopropyl-1, 4, 7-triazacyclononane) in THF yielded the monomeric organolanthanide $[C_5Me_4SiMe_2(Pr^i{}_2\text{-tacn})]SmI$ (dark red crystals, 85% yield) and $[C_5Me_4SiMe_2(Pr^i{}_2\text{-tacn})]YbI$ (red blocks, 80% yield) (Scheme 13). The crystal structures of both compounds have

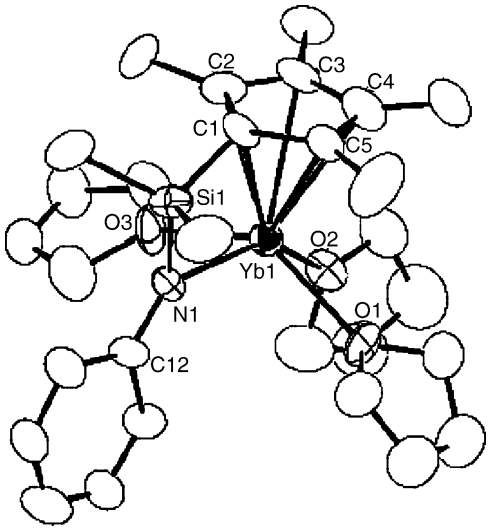

Fig. 9. Molecular structure of $[Me_2Si(C_5Me_4)(NPh)]Yb(THF)_3$ [62].

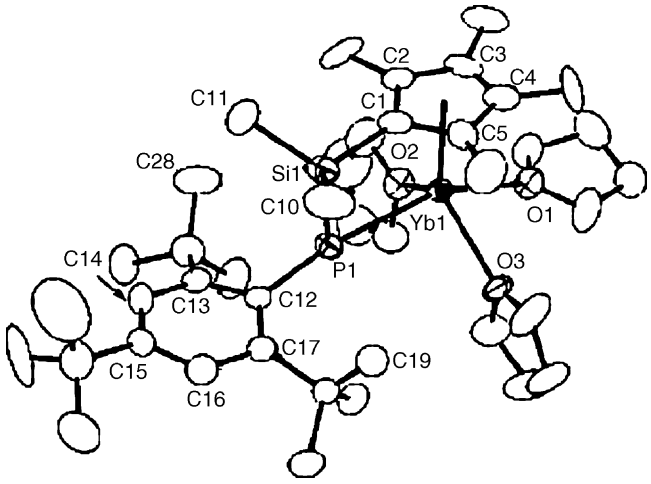

Fig. 10. Molecular structure of $[Me_2Si(C_5Me_4)(PAr)]Yb(THF)_3$ (Ar = $C_6H_2Bu^t_3$-2, 4, 6) [63].

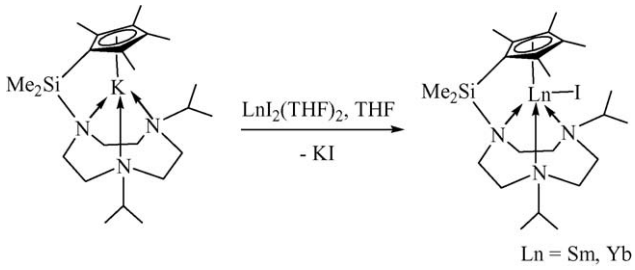

Scheme 13.

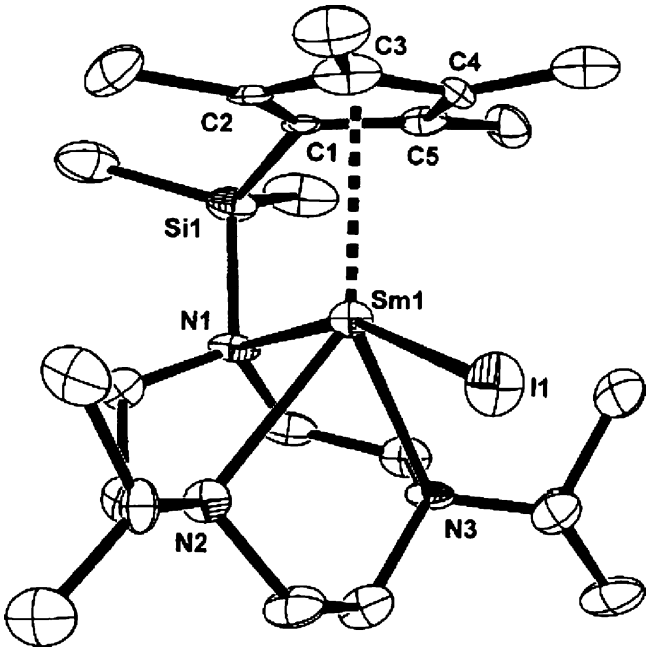

Fig. 11. Molecular structure of $[C_5Me_4SiMe_2(Pr^i_2\text{-tacn})]SmI$ (Pr^i_2-tacn = 1, 4-diisopropyl-1, 4, 7-triazacyclononane) [65].

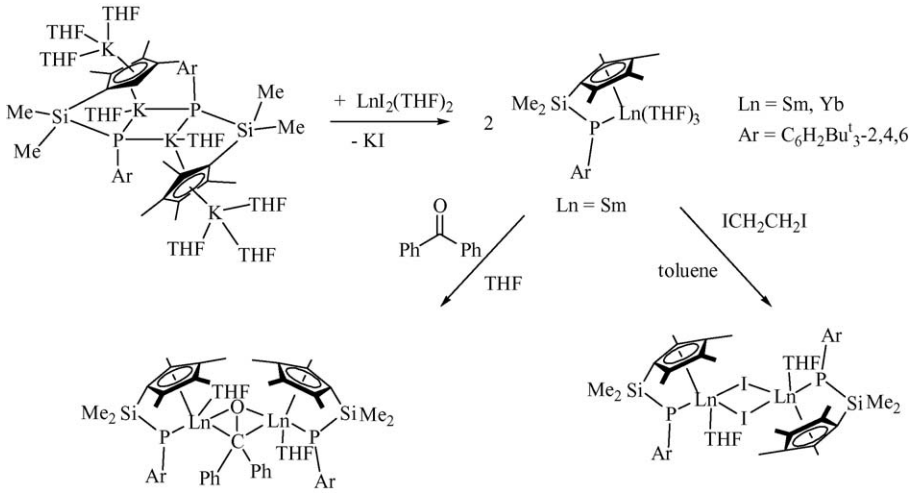

Scheme 12.

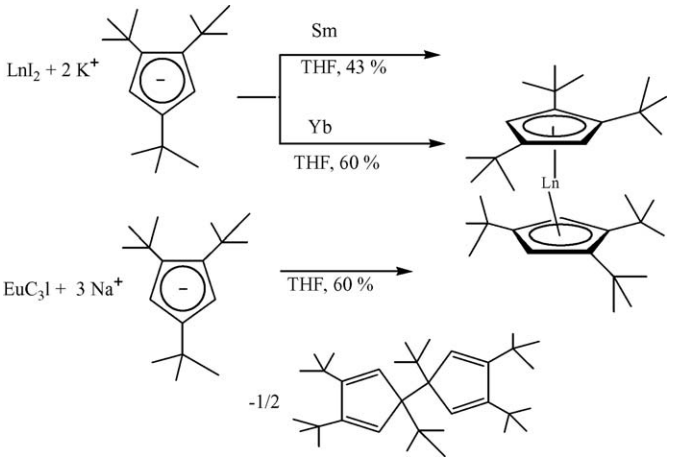

Scheme 14.

been explored. Fig. 11 shows an ORTEP view of the molecular structure of $[C_5Me_4SiMe_2(Pr^i_2\text{-tacn})]SmI$. The samarium center is bound to the cyclopentadienyl group, an iodide, and all three nitrogens of the triazacyclononane moiety. The geometry about the lanthanide center is best described as distorted trigonal-bipyramidal [65].

2.5.2. Cp_2Ln compounds

The one-pot reaction between SmX_2 (X = Cl, I) and Bu^tLi in THF at −40 °C, followed by the addition of NaCp resulted in a dark red solution, from which X-ray quality crystals of $Cp_2Sm(THF)_2$ could be obtained [66]. High yields of Cp_2Yb have been obtained from the reaction of YbI_2 with $CpCuPPh_3$ [67]. The hexa(*t*-butyl)metallocenes of Sm, Eu, and Yb have been prepared following the routes depicted in Scheme 14. 1:1-Adducts of the samarocene with THF and of the samarocene and ytterbocene with 2,6-$Me_2C_6H_3NC$ have also been prepared and characterized. The X-ray analysis confirmed that a single isocyanide ligand is bound in the middle of the open side of the metallocene wedge (Fig. 12) [68].

The reaction of CO with the divalent lanthanide decamethylmetallocenes Cp^*_2Ln (Ln = Sm, Eu, Yb) has been studied in toluene or methylcyclohexane solution in a high pressure infrared cell. In all cases the monocarbonyl complex Cp^*_2LnCO was observed to form under CO pressure. The CO stretching frequencies for Cp^*_2SmCO (2153 cm^{-1}) and Cp^*_2EuCO (2150 cm^{-1}) are greater than that of free CO (2134 cm^{-1} in toluene or methylcyclohexane). In contrast, Cp^*_2YbCO has ν(CO) 2114 cm^{-1}, below that of free CO. This 1:1 complex is formed at low CO pressure (<2 bar), while at higher CO pressures the 1:2 adduct $Cp^*_2Yb(CO)_2$ with an even lower ν(CO) value at 2072 cm^{-1} predominates [69–71].

Coordination of carbon monoxide and isocyanides to divalent ytterbocenes have been studied in detail. In the course of these investigations, the crystal structures of $Cp^*_2Yb(2,6\text{-}Me_2C_6H_3NC)_2$ (Fig. 13) $(C_5H_3Bu^t_2\text{-}1,3)_2Yb(2,6-Me_2C_6H_3NC)_2$ and $[C_5H_3(Me_3Si)_2\text{-}1,3]_2Yb(2,6\text{-}Me_2C_6H_3NC)_2$ have been determined [71].

In a successful attempt to expand divalent organolanthanide chemistry, the synthesis and structural characterization of the

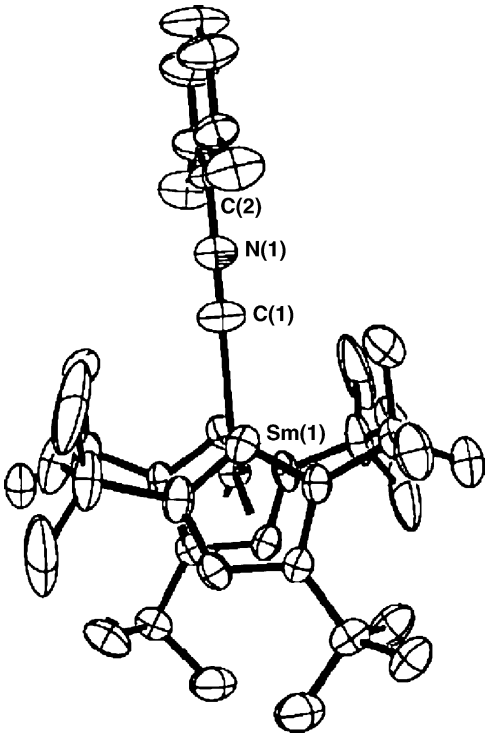

Fig. 12. Molecular structure of (1,2,4-$^tBu_3C_5H_2$)Sm(2,6-$Me_2C_6H_3NC$) [68].

first organothulium(II) complex has been achieved. While the reaction of $TmI_2(THF)_3$ with KCp^* under argon led to diethyl ether decomposition, the use of $KC_5H_3(SiMe_3)_2$ (=KCp″) in THF allowed the isolation of the organothulium(II) complex $Cp''_2Tm(THF)$ in 90% yield (Scheme 15). The purple crystalline compound was structurally characterized. An attempt to isolate the corresponding divalent dysprosium complex led to formation of the dark orange dysprosium(III) dinitrogen complex $(\mu\text{-}N_2)[Cp''_2Dy]_2$ (Scheme 15) [72].

2.5.3. $CpLnX_2$ compounds

The reduced lanthanide iodides of the composition LnIx (Ln = Sc, Y, La, Ce, Pr, Nd, Gd, Dy, Ho, Er; $x < 3$), obtained by the reaction of an excess of the appropriate metal with iodine at high temperature, react with cyclopentadiene to afford the complexes $CpLnI_2(THF)_3$ with yields up to 60% [73]. High yields of $CpSmI_2(THF)_2$ have been obtained from the reaction of $SmI_2(THF)_4$ with

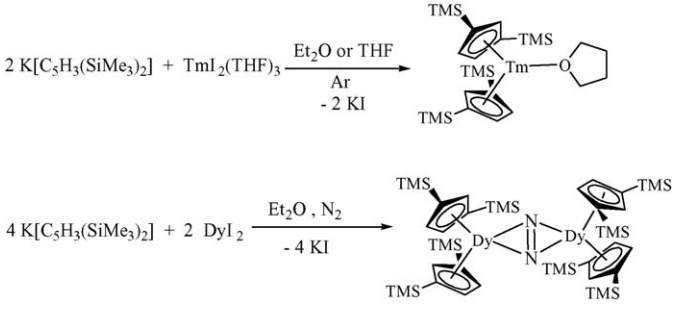

Scheme 15.

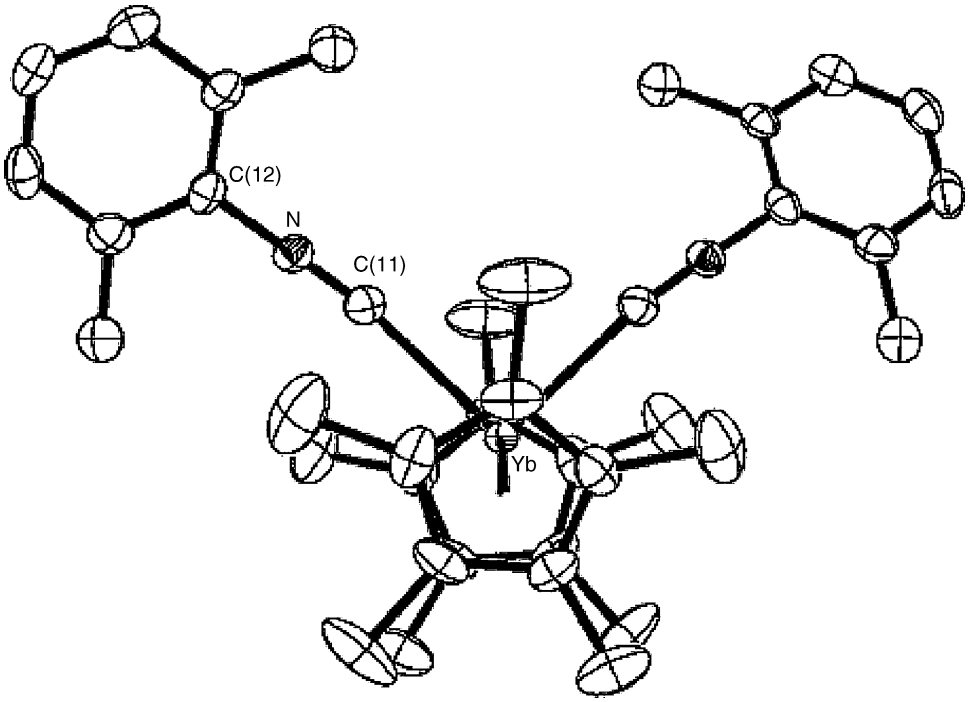

Fig. 13. Molecular structure of $Cp^*_2Yb(2,6\text{-}Me_2C_6H_3NC)_2$ [71].

$CpCuPPh_3$ [67]. Oxidative reactions of the ytterbium(II) thiocyanate complex $Yb(NCS)_2(THF)_2$ with TlCp or $Tl(C_5H_4Me)$ yielded the mono(cyclopentadienyl)ytterbium(III) derivatives $CpYb(NCS)_2(THF)_3$ and $(C_5H_4Me)Yb(NCS)_2(THF)_3$, respectively, in the form of orange crystals [74].

The preparation and reaction chemistry of β-diketiminato ytterbium complexes containing an additional cyclopentadienyl ligand have been investigated. Reaction of $Li[(DIPPh)_2nacnac]$ ($(DIPPh)_2nacnac$ = *N*,*N*-diisopropylphenyl-2,4-pentanediimine anion) with 1 equiv. of anhydrous $YbCl_3$ in THF afforded the dark red monomeric complex $[(DIPPh)_2nacnac]YbCl_2(THF)_2$ in high yield. Further treatment of this complex with $Na(C_5H_4Me)$ in a 1:1 molar ratio in THF gave the mixed-ligand ytterbium chloride $(C_5H_4Me)[(DIPPh)_2nacnac]YbCl$ (Fig. 14) as red crystals in 84% yield. This compound readily undergoes metathesis reactions with $LiNPh_2$ and $LiNPr^i_2$ in THF to form the compounds $(C_5H_4Me)[(DIPPh)_2nacnac]YbNPh_2$ and $(C_5H_4Me)[(DIPPh)_2nacnac]YbNPr^i_2$, respectively [75].

Sterically demanding chelating diamide ligands have also been employed in the synthesis of mono(cyclopentadienyl) lanthanide complexes. A typical synthetic route is outlined in Scheme 16. The structure of the product in solution and in the solid state is best described as a distorted tetrahedron [76].

A μ-hydroxo-bridged mono(cyclopentadienyl)lanthanide Schiff base complex was obtained as a partial hydrolysis product, when Cp_3Pr was allowed to react with bis(acetylacetone)

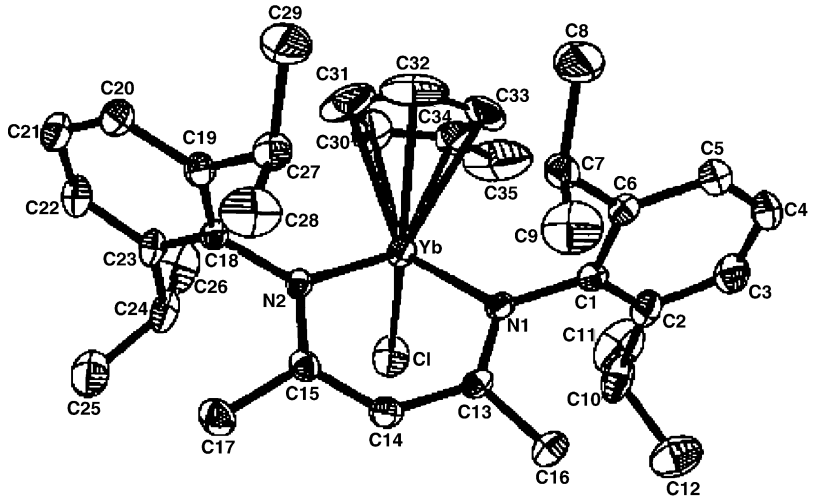

Fig. 14. Molecular structure of $(C_5H_4Me)[(DIPPh)_2nacnac]YbCl$ [75].

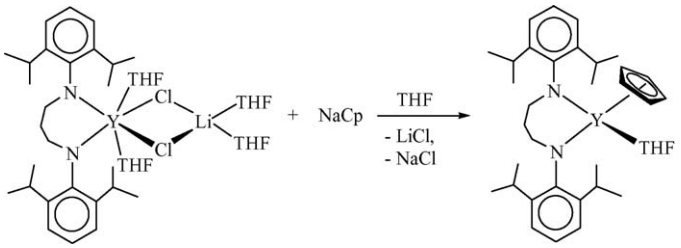

Scheme 16.

ethylenediamine. A representative structure is illustrated in Fig. 15 [77,78].

An organosamarium polyselenide cluster has been prepared via the reaction sequence shown in Scheme 17. Fig. 16 depicts the overall molecular structure of the dianion of $[Na(THF)_6]_2[Cp^t{}_6Sm_6(\mu_6\text{-}Se)(\mu\text{-}Se_2)_6]$, while the structure of the central $Se_{13}Sm_6$ core in this compound is highlighted in Fig. 17. The 13 selenium atoms in the dianion can be divided in three types: a central Se(1) atom which is coordinated to six Sm atoms, and six pairs of bridging Se units [Se(2)–Se(5a), Se(3)–Se(6), Se(4)–(7)] in which one Se atom is coordinated to three Sm atoms while the other one is connected with only two Sm atoms [79].

$[Me_2Si(C_5Me_4)(NBu^t)]LnN(SiMe_3)_2$ (Ln = Nd, Lu, Sm) and $[Me_2Si(C_5Me_4)\text{-}(NBu^t)]LnCH(SiMe_3)_2$ (Ln = Yb, Lu) complexes were synthesized by reaction of the corresponding homoleptic amides or alkyls with $[Me_2Si(C_5Me_4H)(NHBu^t)]$ (Scheme 18) [80].

Moderate yields (55%) of the mixed-ligand complex $(C_4H_4PPh_2)Sm(Tp^{Me2})(I)(THF)$ (Fig. 18, green-yellow crystals) were obtained from the redox reaction between SmI_2 and

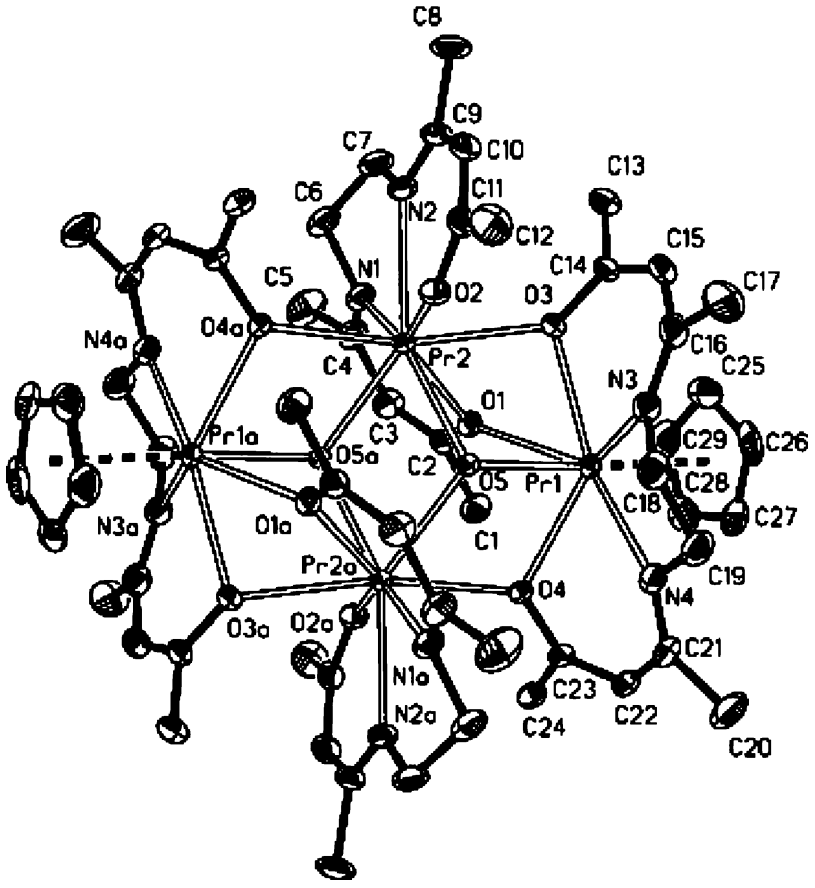

Fig. 15. Molecular structure of $[CpPr_2(acacen)_2(\mu\text{-}OH)]_2{\cdot}4THF$ (H_2acacen = bis(acetylacetone)ethylenediamine) [77].

$$2n\ NaCp^t + 2n\ LnCl_3 \xrightarrow[60\ ^\circ C]{THF} \{[Cp^tLn(THF)]_2(\mu_2\text{-}Cl)_2(\mu_3\text{-}Cl)_3Na(THF)\}_n$$

Ln = Nd, Sm, Gd, Yb

$Cp^t = Bu^tC_5H_4$

$$\{[Cp^tSm(THF)]_2(\mu_2\text{-}Cl)_2(\mu_3\text{-}Cl)_3Na(THF)\}_n + Na_2Se_5 \longrightarrow [Na(THF)_6]_2[Cp^t{}_6Sm_6(\mu_6\text{-}Se)(\mu\text{-}Se_2)_6]$$

Scheme 17.

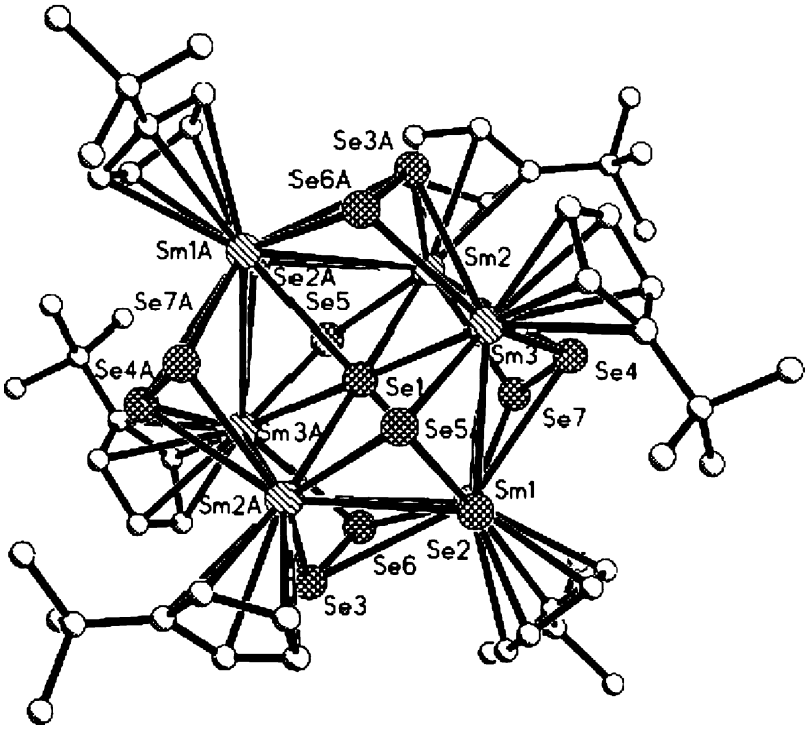

Fig. 16. Molecular structure of the dianion of $[Na(THF)_6]_2[Cp'_6Sm_6(\mu_6\text{-}Se)(\mu\text{-}Se_2)_6]$ [79].

$Tl(C_5H_4PPh_2)$ in THF at ambient temperature followed by direct treatment with $K(Tp^{Me2})$. According to the single-crystal X-ray analysis, the coordination geometry of the samarium atom is best described as distorted tetrahedral with the apexes occupied by four different ligands: Tp^{Me2}, $C_4H_4PPh_2$, I^- and THF. Variable temperature ^1H NMR spectroscopic investigation confirmed that the chiral, asymmetric structure is maintained in solution at low temperatures [81].

The reaction of the linked cyclopentadienyl-anilido ytterbium(II) complex $[Me_2Si(C_5Me_4)(NPh)]Yb(THF)_3$ has been studied. It yields the binuclear ytterbium(III) complex $[Me_2Si(C_5Me_4)(NPh)]$ $Yb(THF)(\mu\text{-}\eta^2\text{:}\eta^3\text{-}Ph_2N_2)Yb[Me_2Si(C_5$-

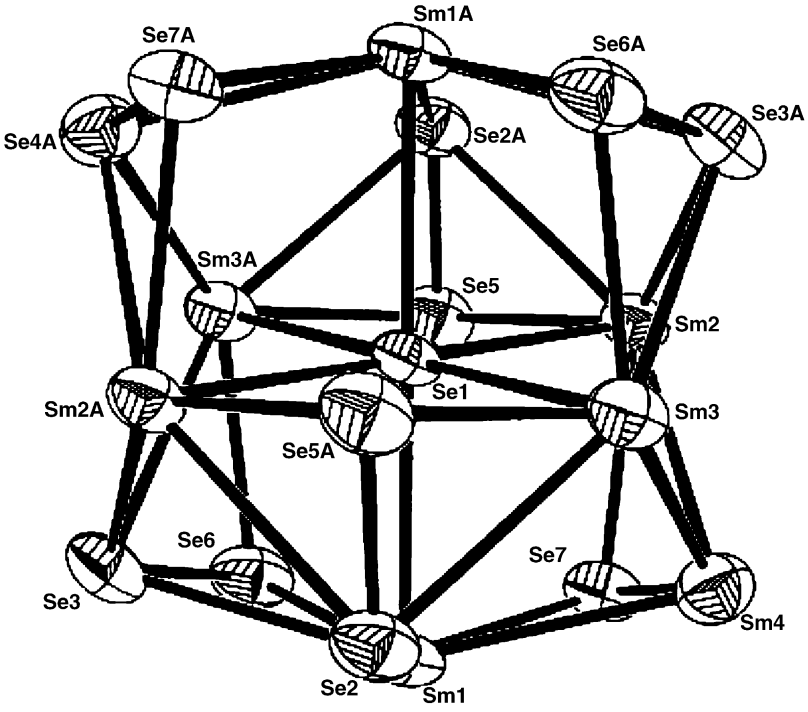

Fig. 17. Structure of the central $Se_{13}Sm_6$ core in the dianion of $[Na(THF)_6]_2[Cp'_6Sm_6(\mu_6\text{-}Se)(\mu\text{-}Se_2)_6]$ [79].

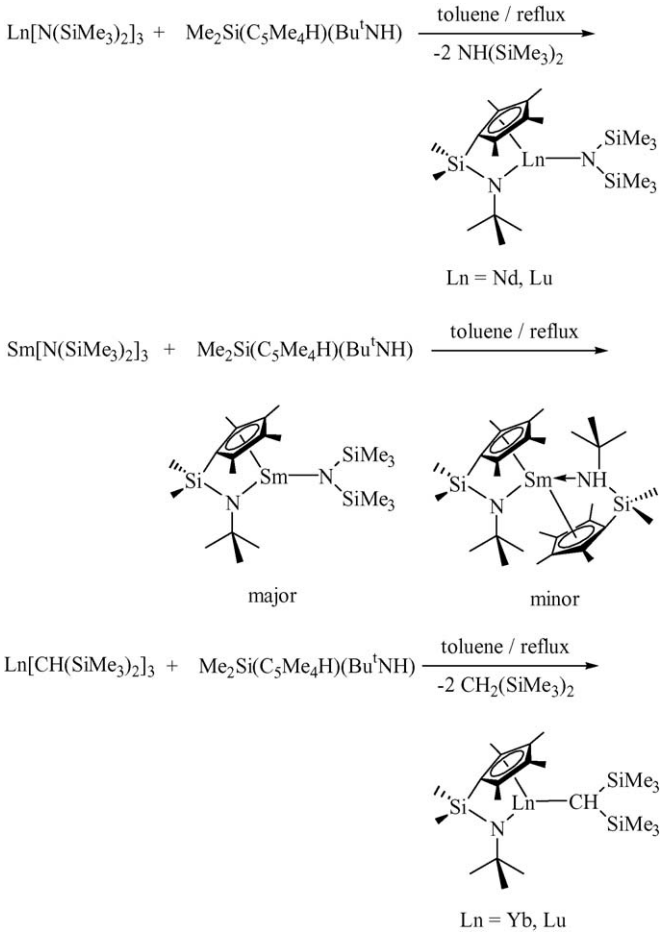

Scheme 18.

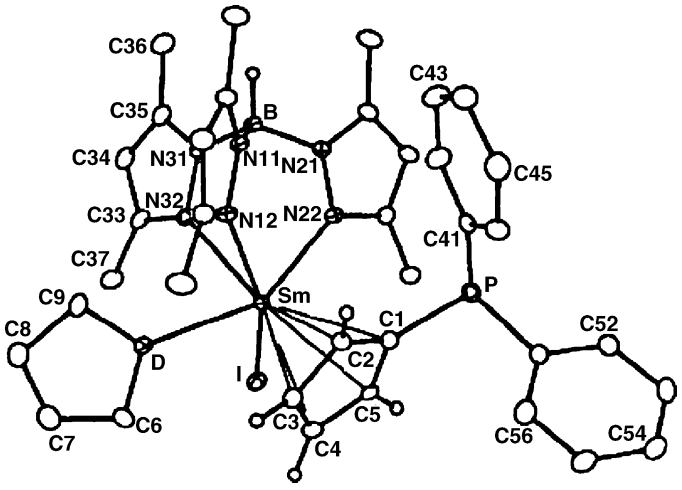

Fig. 18. Molecular structure of $(C_4H_4PPh_2)Sm(Tp^{Me2})(I)(THF)$ [81].

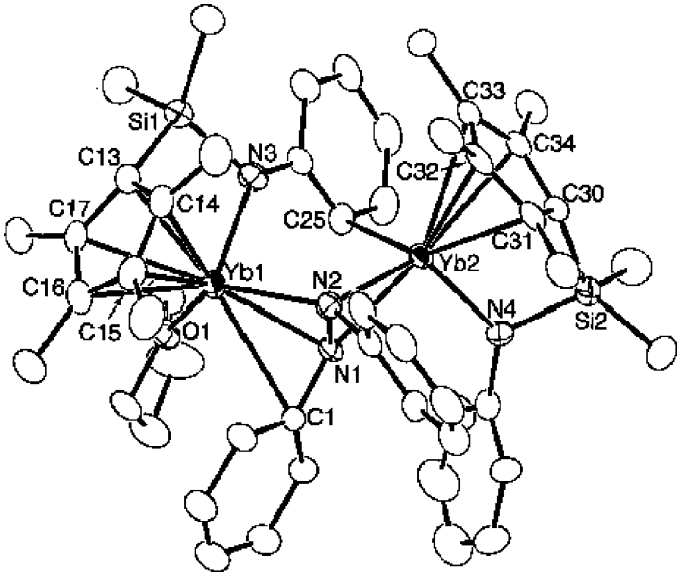

Fig. 19. Molecular structure of $[Me_2Si(C_5Me_4)(NPh)]Yb(THF)(\mu\text{-}\eta^2{:}\eta^3\text{-}Ph_2N_2)Yb[Me_2Si(C_5Me_4)(NPh)]$ [62].

$Me_4)(NPh)]$ (Scheme 19, Fig. 19), which contains a *cis*-oriented azobenzene dianion unit bonding in an η^3-fashion to one Yb atom and in an η^2-fashion to the other Yb atom [62].

Similar reaction of $[Me_2Si(C_5Me_4)(NPh)]Yb(THF)_3$ with 1 equiv. of fluorenone according to Scheme 20 gave the corresponding Yb(III) ketyl complex $[Me_2Si(C_5Me_4)(NPh)]Yb(THF)_2(OC_{13}H_8)$ (Fig. 20) in 75% isolated yield. Treatment of this mononuclear complex with hexane/diethyl ether led to formation of the binuclear pinacolate complex $\{[Me_2Si(C_5Me_4)(NPh)]Yb(THF)\}_2(\mu\text{-}O_2C_{26}H_{16})$ (Fig. 21). Dissolving the latter in THF cleaved the central C–C bond of the pinacolate unit and regenerated $[Me_2Si(C_5Me_4)(NPh)]Yb(THF)_2(OC_{13}H_8)$ quantitatively [62].

Pendant-arm amido-cyclopentadienyl ligands have also been shown to be useful in the stabilization of highly reactive mono(cyclopentadienyl)lanthanide alkyl and hydrido complexes. When the tris[(trimethylsilyl)methyl] complexes of lutetium and ytterbium, $Ln(CH_2SiMe_3)_3(THF)_2$ were treated in pentane solution with 1 equiv. of $(C_5Me_4H)SiMe_2NHCMe_2R$ (R = Me, Et) at 0 °C, the new complexes $(\eta^5{:}\eta^1\text{-}$

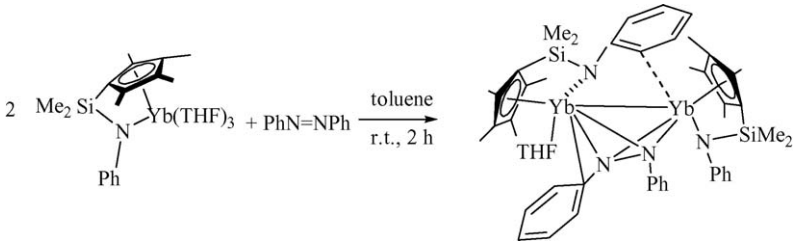

Scheme 19.

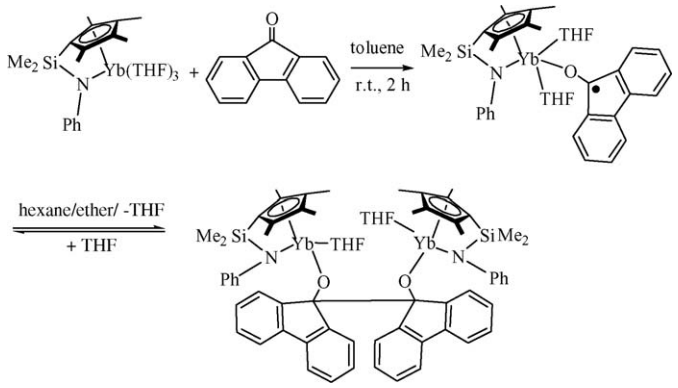

Scheme 20.

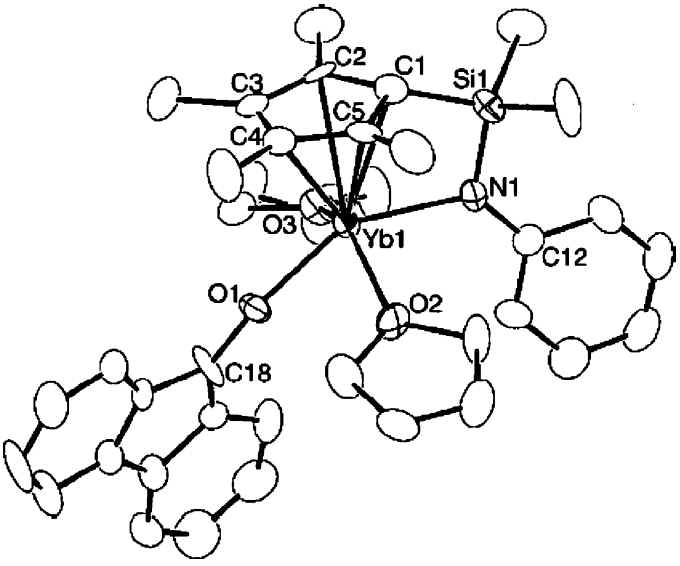

Fig. 20. Molecular structure of $[Me_2Si(C_5Me_4)(NPh)]Yb(THF)_2(OC_{13}H_8)$ [62].

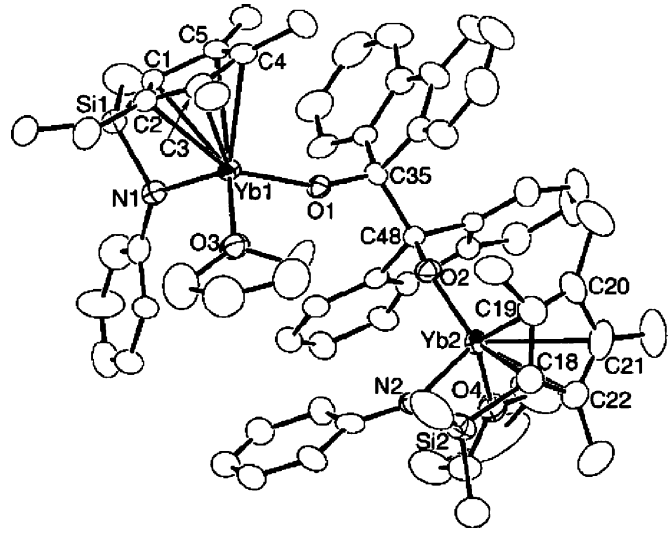

Fig. 21. Molecular structure of $\{[Me_2Si(C_5Me_4)(NPh)]Yb(THF)\}_2(\mu\text{-}O_2C_{26}H_{16})$ [62].

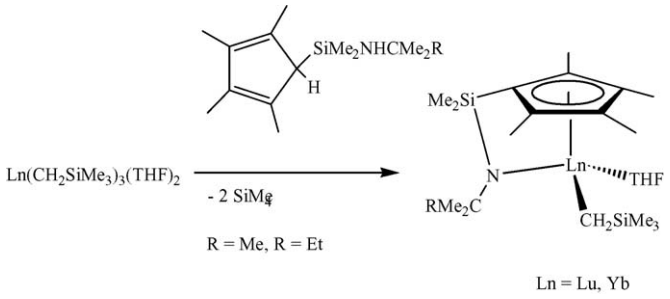

Scheme 21.

$C_5Me_4SiMe_2NCMe_2R)Ln(CH_2SiMe_3)(THF)$ were formed (Scheme 21) [80].

The half-sandwich alkyl complex $(\eta^5{:}\eta^1\text{-}C_5Me_4SiMe_2NBu^t)Y(CH_2SiMe_3)(THF)$ reacts with furan and thiophene to give the metalation products $[Ln(\eta^5{:}\eta^1\text{-}C_5Me_4SiMe_2NBu^t)(\mu\text{-}2\text{-}C_4H_3X)]_2$ (X = O, S) (Scheme 22) which are sparingly soluble in hydrocarbons owing to the dimeric structure. Single crystal X-ray structure analysis of the 2-thienyl complex confirmed a six-membered core with bridging sulfur atoms and *trans*-disposed amido-tetramethylcyclopentadienyl ligands. In contrast to THF and pyridine, 1,2-dimethoxyethane (DME) was found to form isolable, crystalline adducts $(\eta^5{:}\eta^1\text{-}C_5Me_4SiMe_2NBu^t)Y(2\text{-}C_4H_3X)(DME)$. A structure determination of the 2-furyl derivative showed a four-legged piano stool configuration (Fig. 22) [82,83].

Both the lutetium and ytterbium alkyl complexes were subjected to hydrogenolysis with dihydrogen or with phenylsilane in pentane at room temperature to give the dimeric hydrides $[(\eta^5{:}\eta^1\text{-}C_5Me_4SiMe_2NCMe_2R)Ln(THF)(\mu\text{-}$

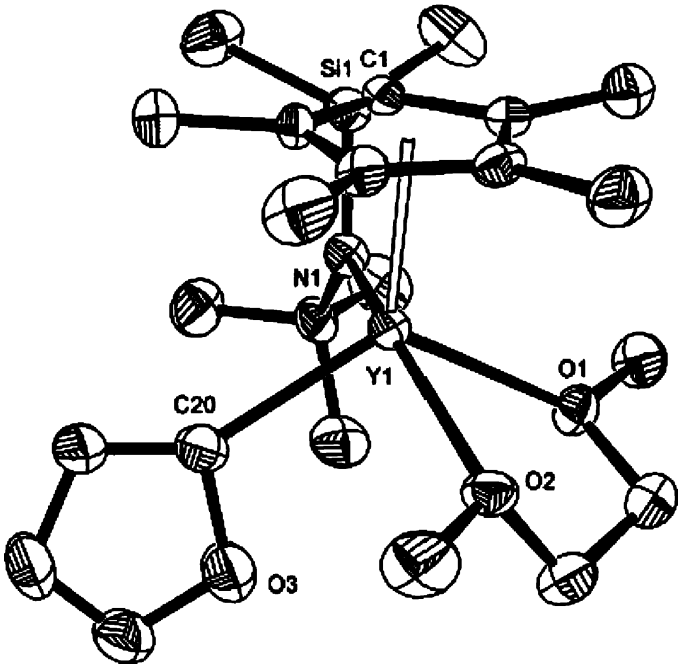

Fig. 22. Molecular structure of $(\eta^5{:}\eta^1\text{-}C_5Me_4SiMe_2NBu^t)Y(2\text{-}C_4H_3O)(DME)$ [83].

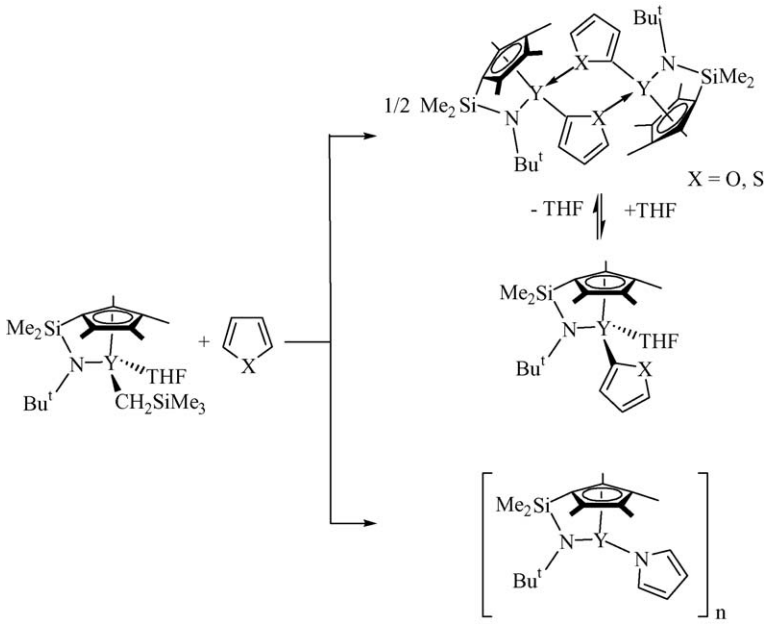

Scheme 22.

H)]$_2$ (Ln = Lu, Yb, Y) (Scheme 23). Because of the thermal instability of the alkyl complexes of lutetium and ytterbium, it proved advantageous to prepare the hydride complexes in a one-pot procedure without isolating the alkyl complexes [80].

The hydrido complex [(η^5:η^1-$C_5Me_4SiMe_2NBu^t$)Y(THF)(μ-H)]$_2$ smoothly reacts with stoichiometric amounts of olefinic substrates such as ethylene, α-olefins, butadiene, and styrenes to give the corresponding alkyl or allyl complexes, respectively (Scheme 24) [80].

A redox transmetalation reaction of the tetranuclear cubane-like cluster complex [{$C_5H_4CH_2CH(\eta^1$-O)OBu^n}Yb]$_4$ with Me_2Hg produced a monomeric σ-methyl complex of trivalent ytterbium, [$C_5H_4CH_2CH(\eta^1$-O)OBu^n]YbMe(THF) in nearly quantitative yield [61]. Related half-sandwich complexes have been synthesized utilizing the tridentate ligands [$C_5H_4CH_2CH(O)CH_2OBu^n$]$^{2-}$ [84].

Unexpected results have been obtained by investigating the chemistry of yttrium complexes containing the alkene-substituted tetramethylcyclopentadiene ligand $C_5Me_4Si(Me)_2CH_2CH{=}CH_2^-$ (Scheme 25). The neutral diene reacts with Y(CH_2SiMe_3)$_3$(THF)$_2$ to form a bright yellow mono(cyclopentadienyl) dialkyl derivative. While insertion of CO_2 produced the expected insertion product, thermolysis at 65 °C led to a dark red compound resulting from double metalation of the ligand and formation of a new type of trianionic cyclopentadienyl allyl ligand, [$Me_2Si(C_5Me_4)(C_3H_3)$]$^{3-}$ (Fig. 23) [85].

2.5.4. *Cp$_2$LnX compounds*

The crystal structures of $Cp_2YbX(THF)$ (X = Cl, Br) have been determined. The ligand arrangements around the formally eight-coordinate Yb atom are *pseudo*-tetrahedral. These two structure determinations completed the first series of $Cp_2LnX(L)$ (X = F, Cl, Br, I) structures covering all halogens for one lanthanide element [86]. The bis(butenylcyclopentadienyl)lanthanide chlorides ($C_5H_4CH_2CH_2CH{=}CH_2)_2LnCl(THF)_2$ (Ln = Sm, Y, Dy, Er) have been synthesized as air- and moisture-sensitive, free-flowing oils. No evidence of intramolecular coordination of the butenyl side-chain was observed [87]. Numerous bis(cyclopentadienyl)lanthanide complexes containing the 1-(but-3-enyl)-2,3,4,5-tetramethylcyclopentadienyl ligand have been synthesized and structurally characterized [88]. The reaction of $LnCl_3$ (Ln = Sm, Yb) with Li($C_5H_3Bu^t_2$-1,3) afforded the ($C_5H_3Bu^t_2$-1, 3)$_2$Ln(μ_2-Cl)$_2$Li(THF)$_2$ *ate*-complexes [89]. In [($C_5H_4Me)_2$Sm(μ-Cl)(THF)]$_2$ the Sm^{3+} ion is coordinated by two C_5H_4Me groups, two chloride ions and one O atom from THF to form a distorted trigonal-bipyramidal geometry [90].

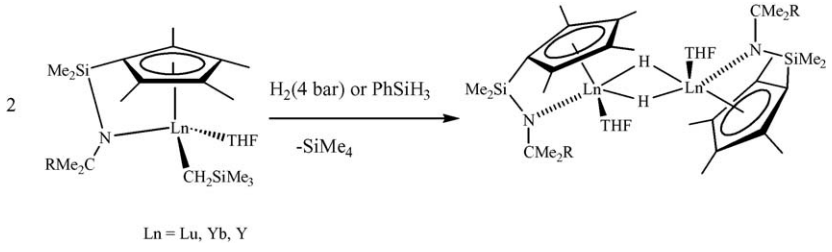

Scheme 23.

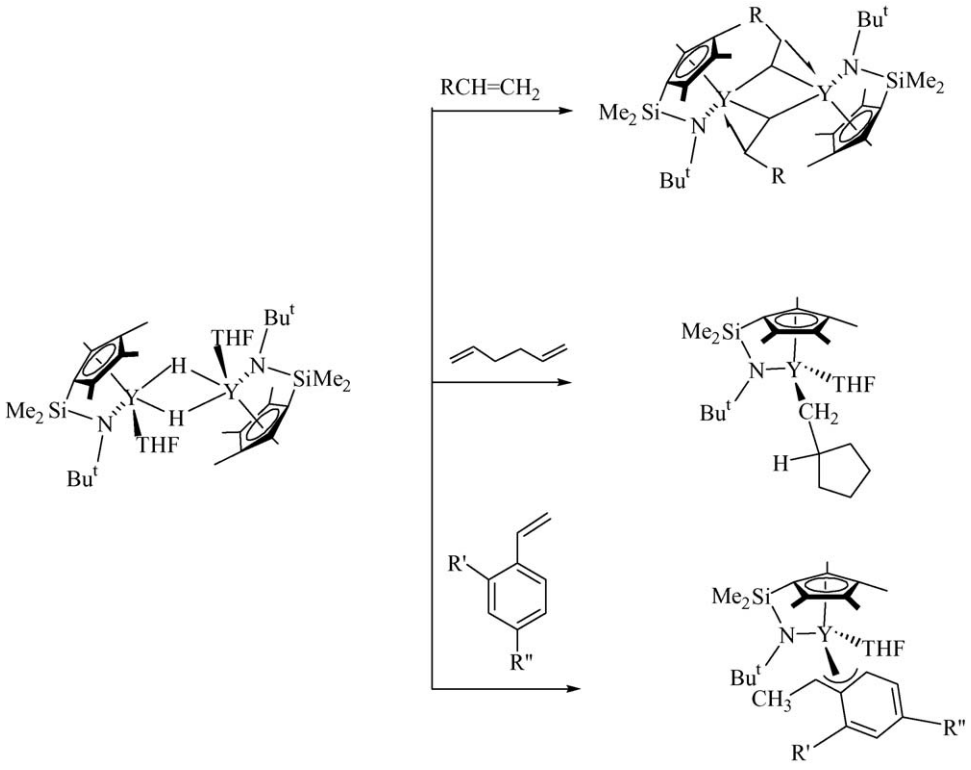

Scheme 24.

The cyanoethyl-substituted bis(cyclopentadienyl) samarium complex $Cp(C_5H_4CH_2CH_2CN)SmCl$ has been reported [91]. Solvent-free $[Cp''_2Tm(\mu\text{-}Cl)]_2$ was made from $TmI_2(THF)_2$ and Cp″MgCl [92]. The trichlorides of yttrium, samarium, and lutetium react with 2 equiv. of $K(C_5H_4SiEt_3)$ to form the dimeric compounds $[(C_5H_4SiEt_3)_2Ln(\mu\text{-}Cl)]_2$ (Ln = Y, Sm, Lu) [93]. Reaction of 2 equiv. of 1,3-dimesitylimidazolium chloride with Cp_3Yb in refluxing THF afforded the golden-orange salt [bis(l,3-dimesitylimidazolium)(μ-cyclopentadienide)][bis(cyclopentadienyl)dichloroytterbate(III)], $[Imid_2Cp][Cp_2YbCl_2]$. In the crystal structure the T-stacked cation is composed of two imidazolium fragments that are C–H···C(π) hydrogen bonded to the bridging cyclopentadienide anion (Fig. 24) [94].

Complexes of the type Cp_2LnCl have been isolated with the very bulky tetraisopropylcyclopentadienyl ligand. Even in this case incorporation of alkali metal halide leads to formation of *ate*-complexes (Scheme 26). Fig. 25 illustrates the molecular structure of the neodymium dimer $[(C_5H^i{}_4Pr_4)_2Nd(\mu\text{-}Cl)(\mu_3\text{-}Cl)Na(OEt_2)]_2$ [95].

The alkoxy-functionalized cyclopentadienyl ligand $C_5H_5CH_2CH_2C(Ar_F)_2OH$ (Ar_F = 3,5-$(CF_3)_2C_6H_3$) has been

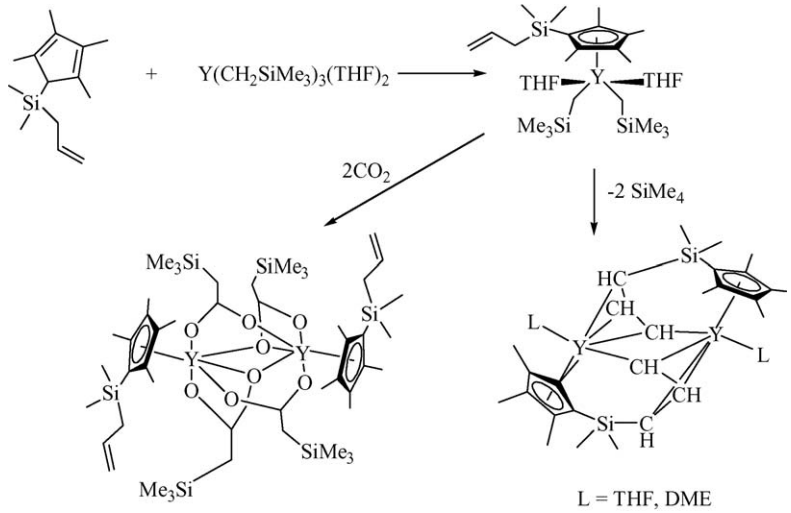

Scheme 25.

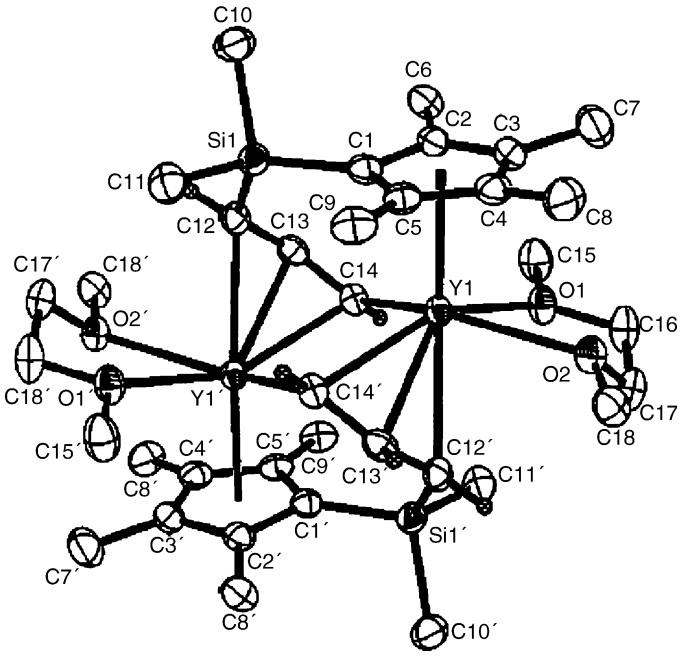

Fig. 23. Molecular structure of $\{[Me_2Si(C_5Me_4)(C_3H_3)]Y(DME)\}_2$ [85].

employed in the synthesis of the corresponding bis(cyclopentadienyl)yttrium complexes, including halide precursors as well as aryloxide, silylamide and alkyl derivatives [96]. A chloro-bridged dimeric bis(amino)-functionalized cyclopentadienylyttrium complex has been synthesized in high yield by the reaction of YCl_3 with 2 equiv. of $NaC_5H_4CH([CH_2]_2)_2NMe$ [97]. Bis(donor)-substituted monomeric $(C_5H_4CH_2CH_2NMe_2)_2TmI$ has been made from $TmI_3(THF)_3$ and $K(C_5H_4CH_2CH_2NMe_2)$ [92]. Monomeric $(C_5H_4CH_2CH_2PPh_2)_2LuCl$ was made from $LuCl_3(THF)_3$ and $Li(C_5H_4CH_2CH_2PPh_2)$. NMR studies revealed that in this complex both phosphino groups are coordinated to the lutetium center [98]. An interesting route leading to bis(cyclopentadienyl)samarium(III) alkoxides involves oxidation of samarium(II) precursors such as $(C_5HPr^i_4)_2Sm(THF)$ with di-*t*-butylperoxide [94].

Dimeric structures have been determined for the ytterbium benzoate complexes $[(C_5H_4Me)_2Yb(\mu\text{-}O_2CPh)]_2$ (orange-red needles) [99]. Complexes of the type $Cp_2Ln(PhCONHO)$ (Ln = Pr, Gd, Dy, Ho, Er, Tm, Yb) have been obtained by allowing the corresponding tris(cyclopentadienyl)lanthanides to react with benzohydroxamic acid [100]. A similar series of complexes, $Cp_2Ln(PhCONOPh)$ (Ln = Pr, Nd, Sm, Gd, Dy, Ho, Er, Yb) has been synthesized with the use of the *N*-phenylbenzohydroxamic acid ligand [101], and related compounds with Ln = La, Pr, Sm, Dy, and Yb have been made starting from piperonal dimethylacetal [102]. Dimerization of phenylisocyanate and formation of the binuclear complex $[\mu\text{-}(PhN)OCCO(NPh)][(MeC_5H_4)_2Sm(THF)]_2$ occurs when the divalent precursor $(C_5H_4Me)_2Sm(THF)$ is treated with PhNCO in a 1:1 molar ratio [103,104]. Monomeric complexes have

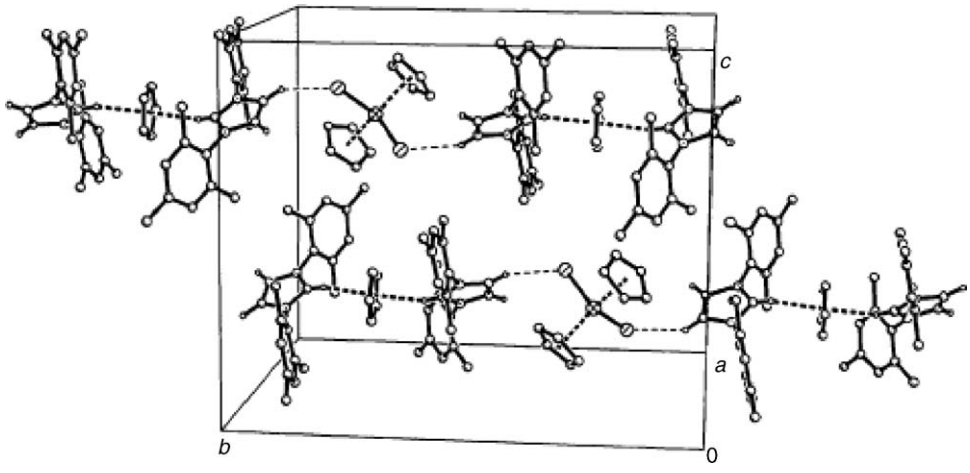

Fig. 24. Partial crystal packing diagram for $[Imid_2Cp][Cp_2YbCl_2]$ showing the cation–anion C–H···Cl interaction (most hydrogen atoms omitted for clarity) [94].

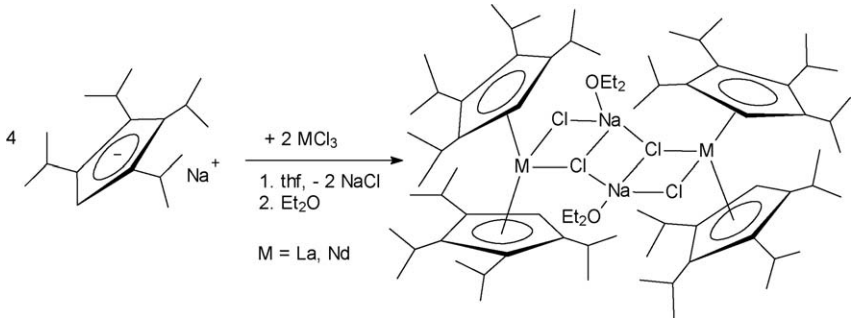

Scheme 26.

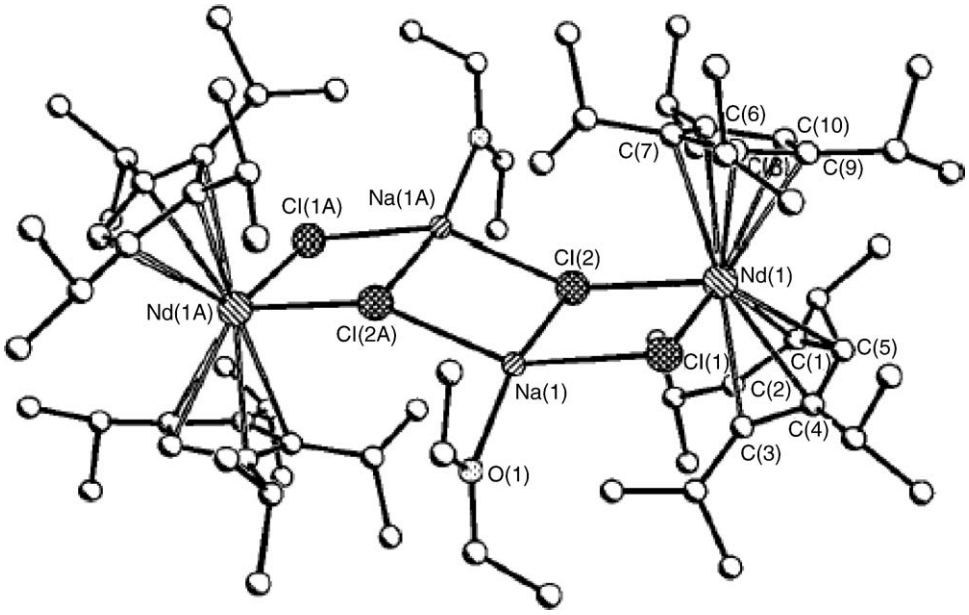

Fig. 25. Molecular structure of $[(C_5H^i{}_4Pr_4)_2Nd(\mu\text{-}Cl)(\mu_3\text{-}Cl)Na(OEt_2)]_2$ [95].

been obtained from reactions of $[(C_5H_4Me)_2Ln(\mu\text{-}Cl)]_2$ with the lithium salt of ε-caprolactam in toluene at 0 °C [103]. The reaction of a tris(cyclopentadienyl)lanthanide with the tridentate Schiff base *N*-1-(*ortho*-methoxyphenyl)salicylideneamine in THF at room temperature afforded the monomeric lanthanocene Schiff base complexes $Cp_2Ln(OC_{14}H_{13}NO)$ (Ln = Sm, Er, Dy, Y) (Scheme 27) [105].

The reaction of Cp_3Ln (Ln = Yb, Dy, Sm, Y) with an equimolar amount of 2-mercapto-benzothiazole (HSBT) in THF at room temperature yields the monomeric bis(cyclopentadienyl) complexes $Cp_2Ln(SBT)(THF)$ (Ln = Yb, Dy, Sm, Y) [106,107]. The crystal structural analysis showed that in $Cp_2Yb(SBT)(THF)$ and $Cp_2Dy(SBT)(THF)$ each lanthanide ion is coordinated by two cyclopentadienyl groups, one oxygen atom of THF, and one sulfur and one nitrogen atom from the chelating benzothiazole-2-thiolate ligand to form a distorted trigonal-bipyramidal coordination geometry. The Yb–S distance of 2.84 Å is longer than those found in related compounds, while the Yb–N distance of 2.39 Å is relatively short compared with analogous compounds. Presumably, the rather long Ln–S and the rather short Ln–N bond distance result from the fact that the benzothiazole-2-thiolate group has a resonance structure as shown in Scheme 28 where the negative charge is partially delocalized to the N atom. Closely related benzothiazole-2-thiolate complexes have also been prepared starting from the chloride-bridged precursor $[(C_5H_4SiMe_2Bu^t)_2Gd(\mu\text{-}Cl)]_2$ [108].

A similar series of complexes with Ln = Pr, Gd, Dy, Ho, Er, Tm, and Yb has been prepared with the anion of benzotriazole as ligand [109,110]. Metallocenes of yttrium and the lanthanides with bis(phosphinimino)methanides in the coordination sphere have been reported. Reaction of $[\{CH(PPh_2NSiMe_3)_2\}LnCl(\mu\text{-}Cl)]_2$ (Ln = Y, Sm, Er) with NaCp in a 1:4 molar ratio in THF afforded the corresponding metallocenes $Cp_2Ln[CH(PPh_2NSiMe_3)_2]$. The structures of these compounds have been investigated in solution and in the solid state. Single crystal X-ray structures showed that both imine groups and the central methine carbon are bonded to the lanthanide atom [111].

The reactivity of $(C_5H_4Me)_2Yb(NPh_2)(THF)$ (Ln = Y, Yb) has been studied, and the corresponding products resulting from heterocumulene insertion into the Ln–N bond have been isolated [112]. In a similar manner, treatment of Cp_2LnBu^n (Ln = Y, Dy, Er) with *N*,*N*′-di-*t*-butylcarbodiimide resulted in monoinsertion of carbodiimide into the Ln–C bond to yield the amidinate complexes $Cp_2Ln[Bu^tNC(Bu^n)NBu^t]$ [113], while insertion of PhNCO led to formation of $[(C_5H_4Me)_2Ln\{\mu\text{-}OC(R)NPh\}]_2$ (R = Bu^n, Ln = Sm, Dy, Er; R = α-naphthyl, Ln = Dy). Fig. 26 depicts the molecular structure of the erbium complex $Cp_2Er[Bu^tNC(Bu^n)NBu^t]$ [114].

Amine elimination reactions between homoleptic silylamide lanthanide complexes and an isopropylidene-bridged cyclopentadiene–fluorene system led to unusual

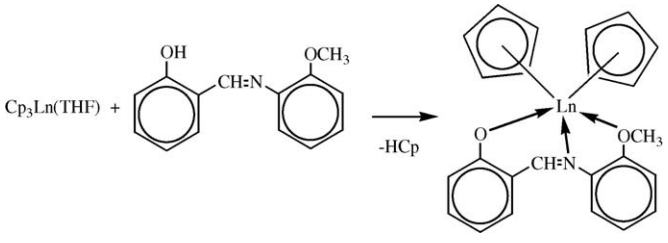

Scheme 27.

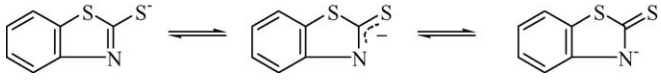

Scheme 28.

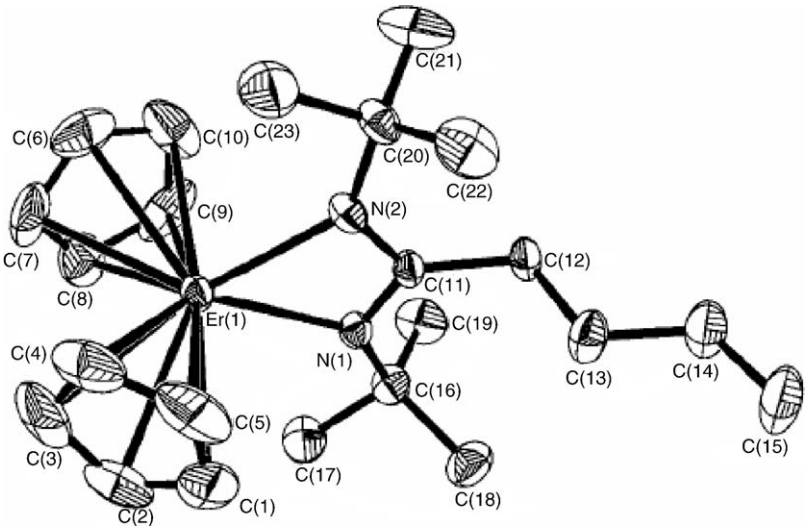

Fig. 26. Molecular structure of $Cp_2Er[Bu^tNC(Bu^n)NBu^t]$ [113].

bis(cyclopentadienyl) complexes in which the fluorene unit does not participate in coordination to the central lanthanide atom. A typical reaction sequence is outlined in Scheme 29. The molecular structure of the resulting yttrium silylamide complex is shown in Fig. 27 [115].

Insertion chemistry with PhNCO and PhNCS into a Ln–S bond has been reported for the thiolate-bridged dimeric neodymium complex $[(C_5H_4Me)_2Nd(\mu\text{-}SPh)(THF)]_2$ [116]. A series of bis[1,3-bis(trimethylsilyl)cyclopentadienyl]yttrium phosphide complexes has been synthesized and structurally

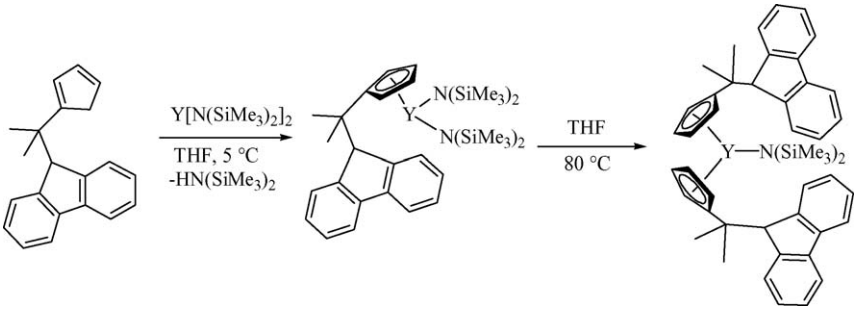

Scheme 29.

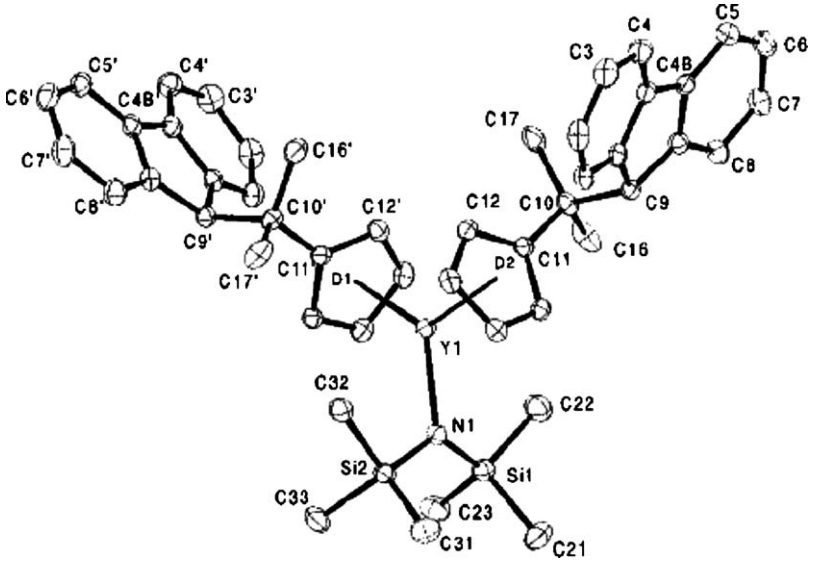

Fig. 27. Molecular structure of $(C_5H_4CMe_2FluH)_2Y[N(SiMe_3)_2]$ [115].

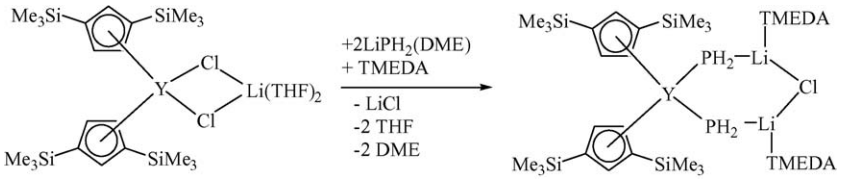

Scheme 30.

characterized. The chloro-bridges in $Cp''_2Y(\mu\text{-}Cl)Li(THF)_2$ ($Cp'' = C_5H_3(SiMe_3)_2$-1,3) can be selectively replaced by one or two triisopropylsilylphosphide substituents. The metathesis reaction of the yttrium precursor with $LiPH_2(DME)$ followed by treatment with TMEDA gave a colorless bis(phosphido)yttriate as shown in Scheme 30. The central YP_2Li_2Cl cycle is nearly planar with Y–P bond lengths of 2.849 Å (Fig. 28) [117].

In a similar manner, the metathesis reaction of [1,3-$(Me_3Si)_2C_5H_3]_2YCl$ with $KPHSiBu^t_3$ afforded monomeric $[C_5H_3(SiMe_3)_2$-1,3$]_2YPHSiBu^t_3$ as colorless crystals in 65% yield. The compound was structurally characterized by X-ray methods [37].

An unusual μ-peroxo organolanthanide complex $(\mu\text{-}O_2)[(C_5H_4C_5H_9)_2Yb(THF)]_2$ was serendipitously obtained from a reaction between YbI_2 and cyclopentylcyclopentydienyl sodium, $Na(C_5H_4C_5H_9)$, in the presence of trace amounts of oxygen. In the molecular structure of $(\mu\text{-}O_2)[(C_5H_4C_5H_9)_2Yb(THF)]_2$, the ytterbium atoms and the asymmetric O_2 unit defines a plane that contains a C_1 symmetry center (Fig. 29) [118].

The dimeric compounds $[(C_5H_4SiEt_3)_2Ln(\mu\text{-}Cl)]_2$ (Ln = Y, Sm, Lu) react with 1 equiv. of methyllithium to give the corresponding dimeric lanthanocene methyl complexes $[(C_5H_4SiEt_3)_2Ln(\mu\text{-}Me)]_2$. Monomeric methyl complexes of the type $Cp''_2LnMe(THF)$ (Ln = Sm, Lu, $Cp'' = C_5H_3(SiMe_3)_2$-1,3) were obtained by the reaction of $SmCl_3$ and $LuCl_3$, respectively, with 2 equiv. of KCp'' [93].

DFT(B3PW91) calculations have been used to propose models for C_5H_5 (Cp) in lanthanides at low computational cost. The H exchange reaction, $Cp_2LnH^* + H_2 \rightarrow Cp_2LnH + HH^*$, previously studied with C_5H_5 has been used as a benchmark [119].

2.5.5. Cp_3Ln compounds

The mean dipole-polarizability of the tris(cyclopentadienyl)lanthanides Cp_3Nd, Cp_3Sm, and Cp_3Er have been exactly determined by means of refractive index measurements in the vapor phase [57]. High yields of Cp_3Ln (Ln = Pr, Er, Yb) have been obtained from the reaction of the metallic lanthanides with $CpCuPPh_3$ [67].

A tris(amino)-functionalized cyclopentadienylyttrium complex (Fig. 30) has been synthesized in high yield by the reac-

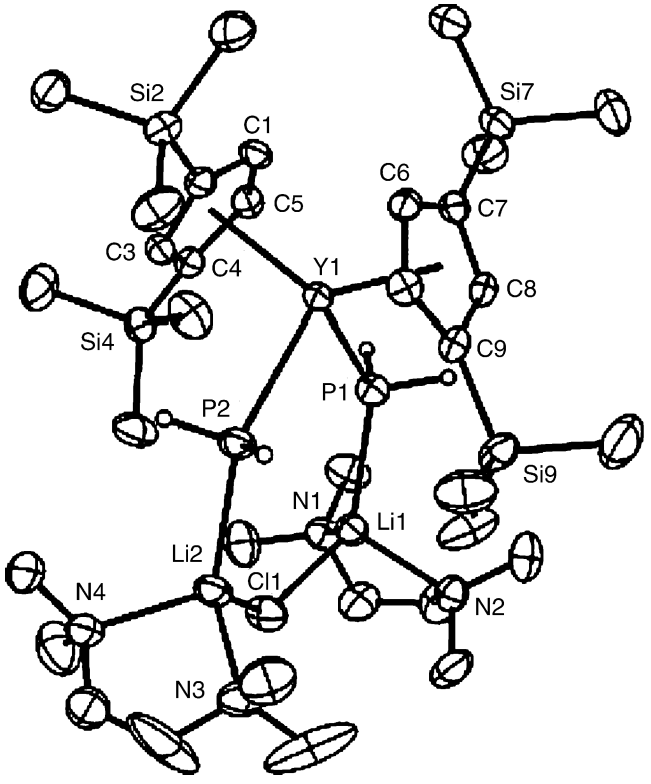

Fig. 28. Molecular structure of $[C_5H_3(SiMe_3)_2$-1,3$]_2Y[Cl\{Li(TMEDA)PH_2\}_2]$ [117].

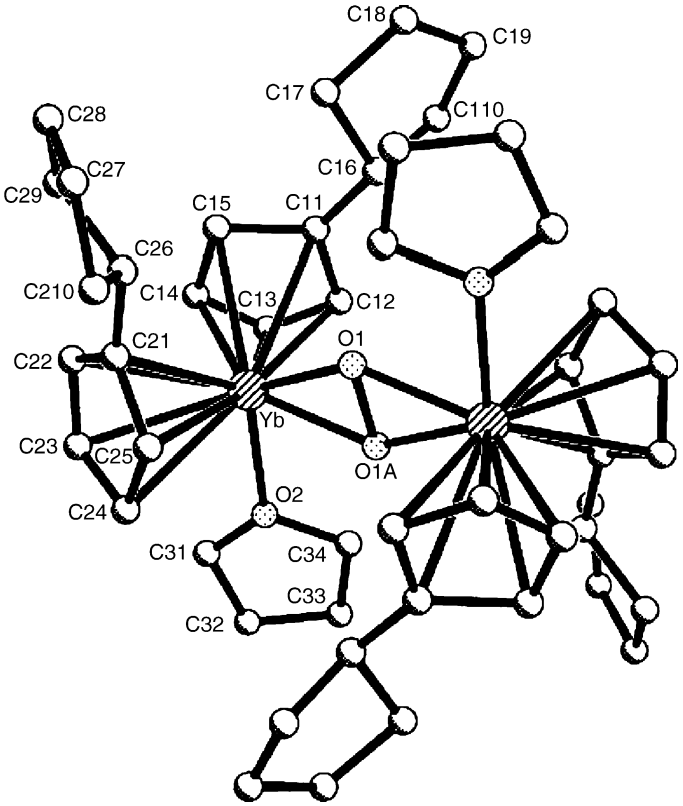

Fig. 29. Molecular structure of $(\mu\text{-}O_2)[(C_5H_4C_5H_9)_2Yb(THF)]_2$ [118].

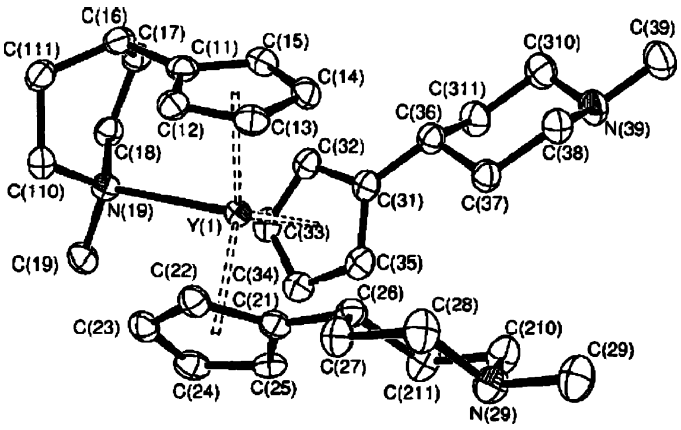

Fig. 30. Molecular structure of $Y[C_5H_4\{(CH_2)_2\}_2NMe]_3$ [97].

tion of YCl_3 with 3 equiv. of $Na[C_5H_4CH\{(CH_2)_2\}_2NMe]$. The three amino-functionalized cyclopentadienyl units in $Y[C_5H_4CH\{(CH_2)_2\}_2NMe]_3$ (Fig. 30) are fluxional at room temperature, giving thus a rare example of stabilization of an yttrium center without the use of extraneous ligands [97].

2.5.6. Cp_3LnL and Cp_3LnL_2 compounds

Absorption and magnetic circular dichroism spectra have been measured for the THF adduct $Cp_3Tm(THF)$ [120]. The crystal structure of $(C_5H_4Me)_3Sm(THF)$ has been determined [121]. Synthesis and characterization of the tris(cyclopentylcyclopentadienyl)lanthanide complexes $(C_5H_4C_5H_9)_3Nd(\mu\text{-}Br)Li(THF)_3$ and $(C_5H_4C_5H_9)_3Sm(THF)$ have been reported [122]. Other Cp_3Ln adducts which have been investigated include those with (S)-(−)-nicotine (Scheme 31) [123].

2.5.7. Pentamethylcyclopentadienyl compounds

2.5.7.1. Cp^*MX compounds. Red $Cp^*Yb[N(SiMe_3)_2](THF)_2$ can be generated from $KN(SiMe_3)_2$ and $[Cp^*Yb(\mu\text{-}I)(THF)_2]_2$ in THF (79% yield) and crystallizes from toluene with a distorted piano stool geometry (Fig. 31) [124].

2.5.7.2. Cp^*_2M compounds. In a theoretical study, relativistic, gradient-corrected density functional theory was used to establish the equilibrium geometric structures of Cp^*_2Yb. The molecule is significantly bent with a Cp^*–Yb–Cp^* angle of 160°. The bent structure is 5 kJ/mol more stable than the linear. The agreement between the calculated structure of Cp^*_2Yb and that detected experimentally in the gas phase is excellent. The origins of the deviation from linearity have been discussed in detail and placed in the context of previous, contrasting explanations for bending in metallocenes. Evidence was found for both valence

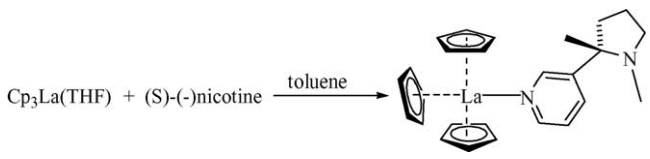

Scheme 31.

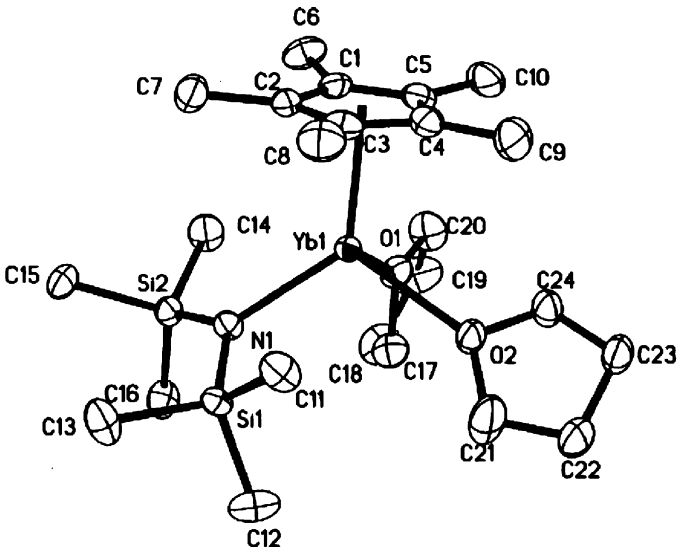

Fig. 31. $Cp^*Yb[N(SiMe_3)_2](THF)_2$ [124].

and core metal electron participation in the bending process. Previous implications that the Cp^*_2 moiety should of itself adopt a bent geometry were not supported. The metal–ligand bonding Cp^*_2Yb is predominantly ionic, with small amounts of *d* and (to a lesser extent) *f* orbital covalency [125].

Coordination of carbon monoxide and isocyanides to Cp^*_2Yb and related divalent ytterbocenes have been studied in detail. In the course of these investigations, the crystal structures of $Cp^*_2Yb(2,6\text{-}Me_2C_6H_3NC)_2$ has been determined [71].

The first dihydrido lanthanide(III) complex was prepared according to Scheme 32. The orange-red crystalline product was isolated in 42% yield and structurally characterized by X-ray diffraction (Fig. 32). The six Sm atoms in this unusual compound constitute a trigonal prism whose three squares are each capped by one K atom. There are 15 hydrido ligands in this molecule, one being body-centered in a μ_6-H-Sm_6 fashion and others each capping a metal triangle in either μ_3-H-Sm_3 or μ_3-H-Sm_2K form. The whole molecule has crystallographic D_{3h} symmetry. One three-fold axis passes through the Sm_3-μ_3-capped and the Sm_6-μ_6-centered H atoms. Perpendicular to this three-fold axis exist three two-fold axes, each passing through both the μ_6-centered H and one K atoms and bisecting a Sm···Sm prism edge [126].

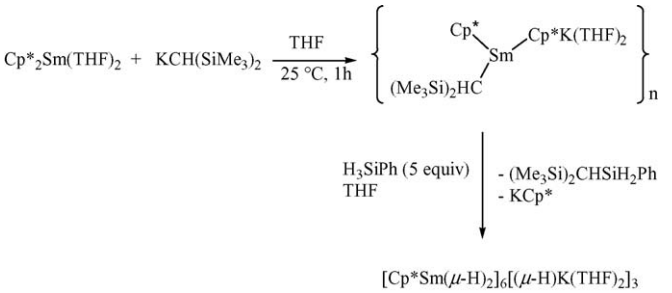

Scheme 32.

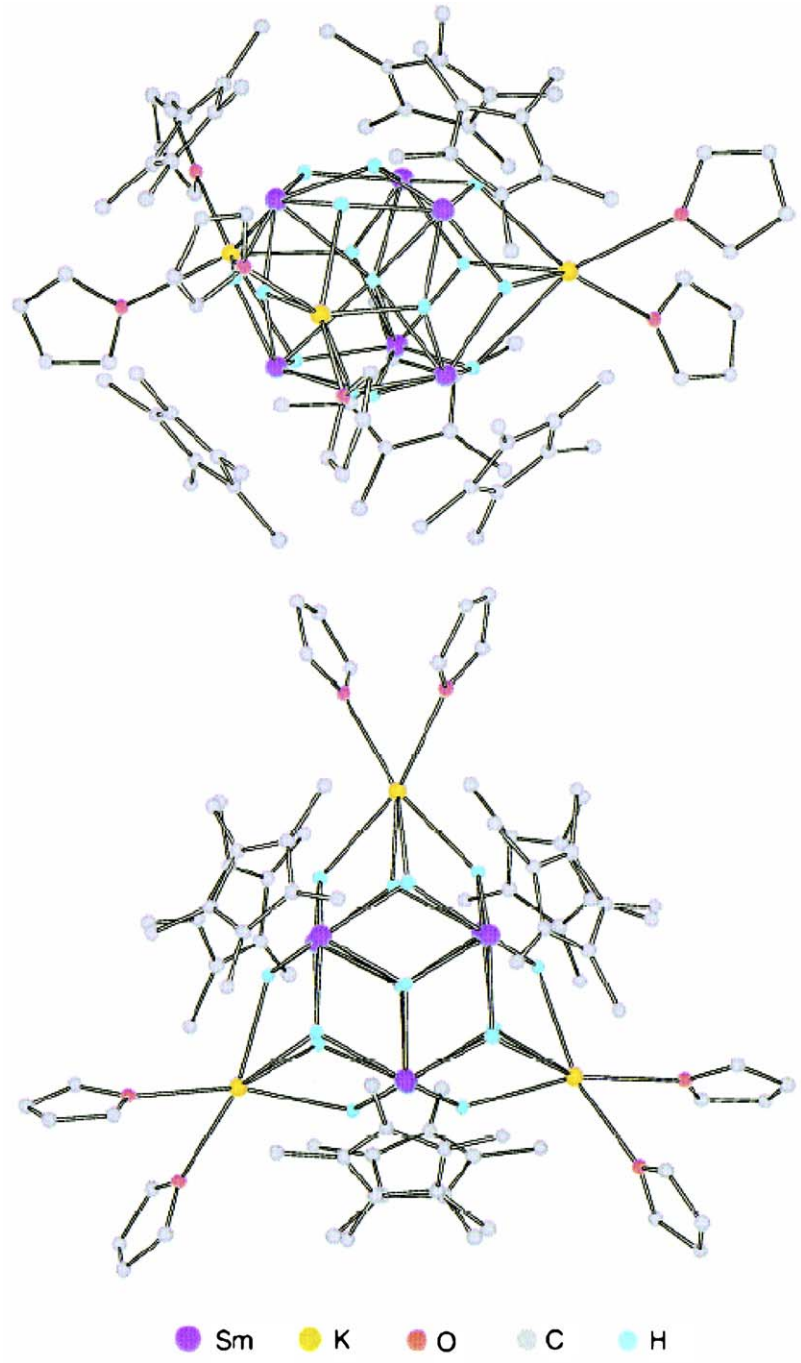

Fig. 32. Molecular structure of $[Cp^*Sm(\mu\text{-}H)_2]_6[(\mu\text{-}H)K(THF)_2]_3$. Top: general view. Bottom: view along the three-fold axis [126].

2.5.7.3. Mono(pentamethylcyclopentadienyl)lanthanide(III) compounds. Controlled hydrolysis of the divalent organosamarium complex $Cp^*_2Sm(THF)_2$ formed the hexametallic organosamarium oxide hydroxide cluster $[Cp^*Sm]_6O_9H_6$ as brown crystals in 40% yield. The compound has a solid-state structure consisting of a distorted octahedral array of six Cp^*Sm^{2+} units connected by eight triply bridging oxygens and a central oxygen (Fig. 33) [127].

The utility of the chloride precursor $[(salen')Y(\mu\text{-}Cl)(THF)]_2$ (salen′ = *N*,*N*′-bis(3,5-di-*t*-butylsalicylidene)ethylenediamine) in preparing organometallic derivatives of this ancillary ligand has been demonstrated. The mono(pentamethylcyclopentadienyl) derivative could be prepared by reaction with KCp^*. The yellow solid was isolated in 75% yield, and its structure was verified by an X-ray analysis [128]. The mono(pentamethylcyclopentadienyl)yttrium bis(amide) complex $Cp^*Y[N(SiHMe_2)_2]_2$ is accessible as an unsolvated, monomeric species by reacting $Y[N(SiHMe_2)_2]_3$ with Cp^*H (40% yield) [129].

The synthesis of a mono(pentamethylcyclopentadienyl)neodymium allyl complex, green $Cp^*Nd(\eta^3\text{-}C_3H_5)_2$(dioxane), has been achieved by protonation of $Nd(\eta^3\text{-}C_3H_5)_2$(dioxane) with

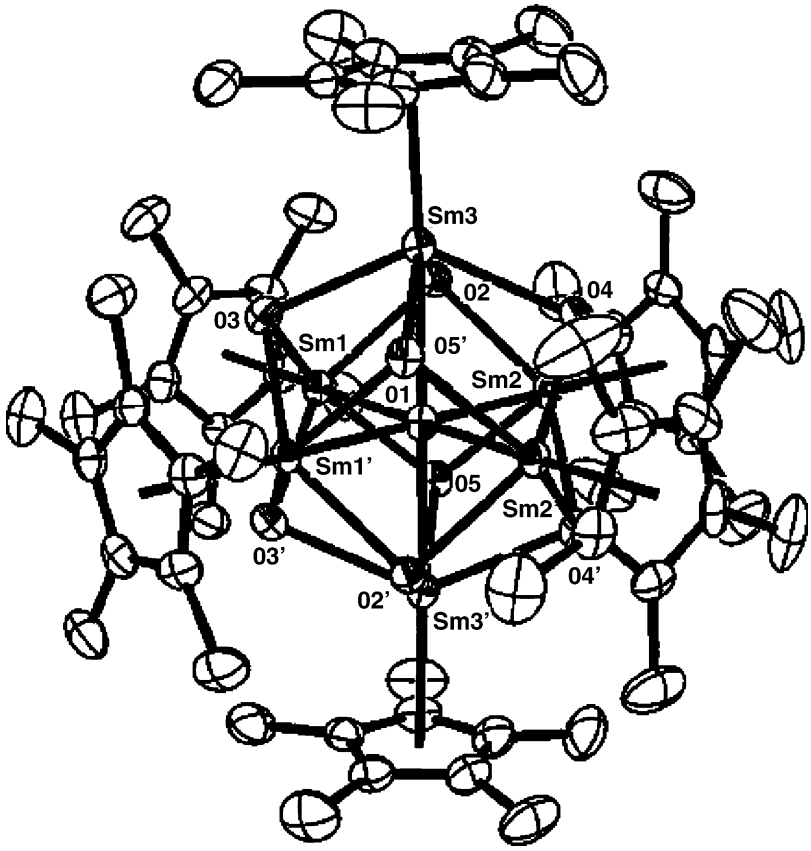

Fig. 33. Molecular structure of $[Cp^*Sm]_6O_9H_6$ [127].

pentamethylcyclopentadiene. The ease of this protolytic reaction is due to the predominantly ionic nature of the tris(allyl) precursor [60].

2.5.7.4. Bis(pentamethylcyclopentadienyl)lanthanide(III) compounds. To investigate the potential role of Sm–Ph species as intermediates in the samarium-catalyzed redistribution of $PhSiH_3$ to Ph_2SiH_2 and SiH_4, the samarium phenyl complex $[Cp^*_2SmPh]_2$ was prepared by oxidation of Cp^*_2Sm with $HgPh_2$. $[Cp^*_2SmPh]_2$ thermally decomposes to yield benzene and the phenylene-bridged disamarium complex $Cp^*_2Sm(\mu\text{-}1,4\text{-}C_6H_4)SmCp^*_2$ (Fig. 34). This decomposition reaction appears to proceed through dissociation of $[Cp^*_2SmPh]_2$ into monomeric Cp^*_2SmPh species which then react with unimolecular and bimolecular pathways, involving rate-limiting Cp^* metalation and direct C–H activation (Scheme 33) [130].

The unsolvated bimetallic yttrium complex $Cp^*_2Y(\mu\text{-}Cl)YCp^*_2Cl$ has been utilized as a convenient platform upon which to compare the coordination chemistry of oxygen-donor

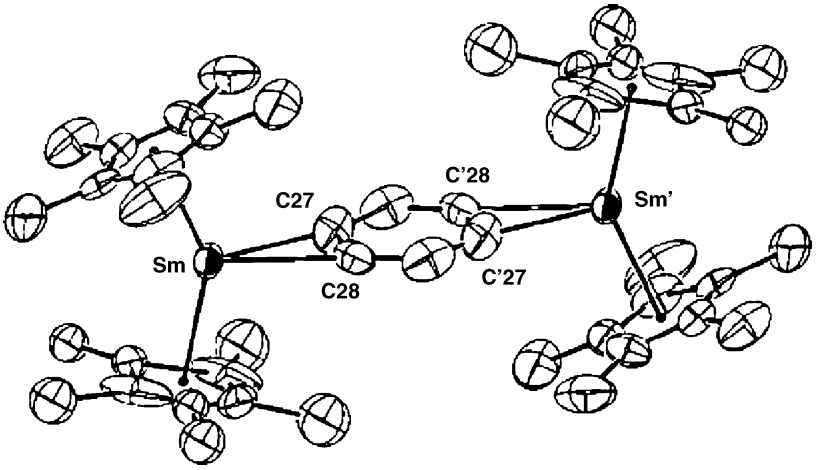

Fig. 34. Molecular structure of $Cp^*_2Sm(\mu\text{-}1,4\text{-}C_6H_4)SmCp^*_2$ [130].

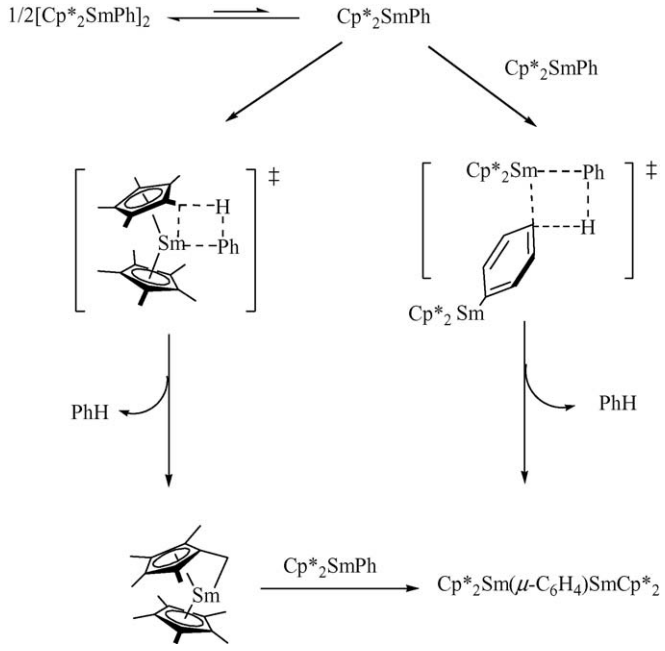

Scheme 33.

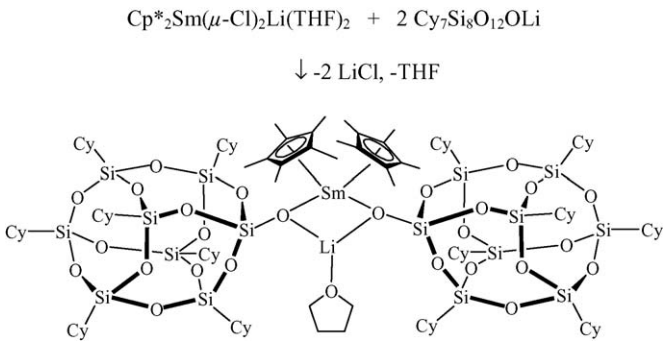

Scheme 34.

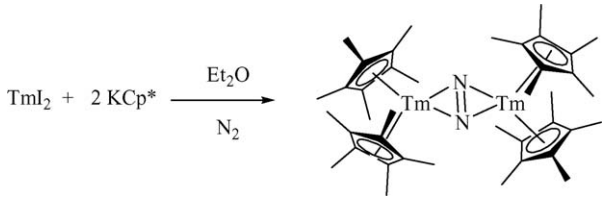

Scheme 35.

ligands and monomers with Lewis acidic metal ions. Reactions of $Cp^*_2Y(\mu\text{-}Cl)YCp^*_2Cl$ with 2 equiv. of oxygen-containing substrates formed the monomeric complexes $Cp^*_2YCl(L)$ (L = THF, benzophenone, methyl methacrylate, ε-caprolactone, HMPA, ε-caprolactam, 1-methyl-2-pyrrolidone, and *N*,*N*′-dimethylpropylenurea). Each of these readily crystallize, which allowed comparison of the Y–O interaction in the solid state [131].

$Cp^*_2Tm(III)$ complexes have been isolated from reactions of $TmI_2(THF)_2$ with KCp^* [92]. Yellow $Cp^*_2Sm[\mu\text{-}Cy_7Si_8O_{12}O_2]_2$ (Cy = *c*-C_6H_{11}), the first organolanthanide silsesquioxane complex, has been obtained in 68% yield by treatment of the *ate*-complex $Cp''_2Sm(\mu\text{-}Cl)_2Li(THF)_2$ with $Cy_7Si_8O_{12}OLi$ in a molar ratio of 1:2. In this complex samarium and lithium are bridged by two silsesquioxane silanolate ligands (Scheme 34, Fig. 35) [132].

Facile dinitrogen reduction via organometallic Tm(II) chemistry has been reported. TmI_2, prepared directly from Tm and I_2, reacts with KCp^* in Et_2O under nitrogen to form a white precipitate and a reddish-orange solution from which $(\mu\text{-}N_2)[TmCp^*_2]_2$ could be crystallized in 55% yield (Scheme 35). Fig. 36 shows the molecular structure of $(\mu\text{-}N_2)[Tm\{C_5H_3(SiMe_3)_2\text{-}1,3\}_2]_2$, which was made analogously.

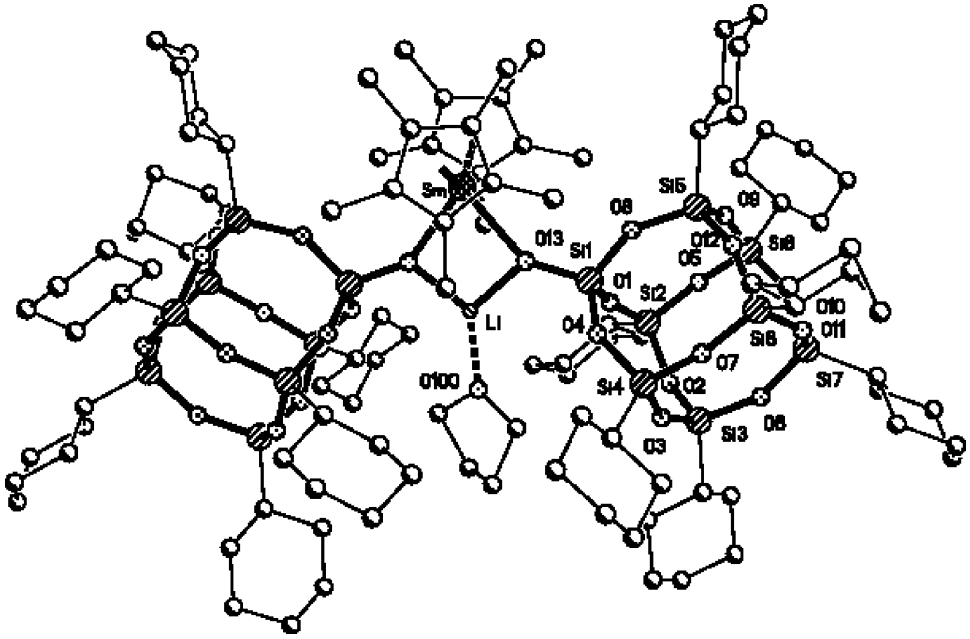

Fig. 35. Molecular structure of $Cp^*_2Sm[\mu\text{-}Cy_7Si_8O_{12}O]_2$ (Cy = *c*-C_6H_{11}) [132].

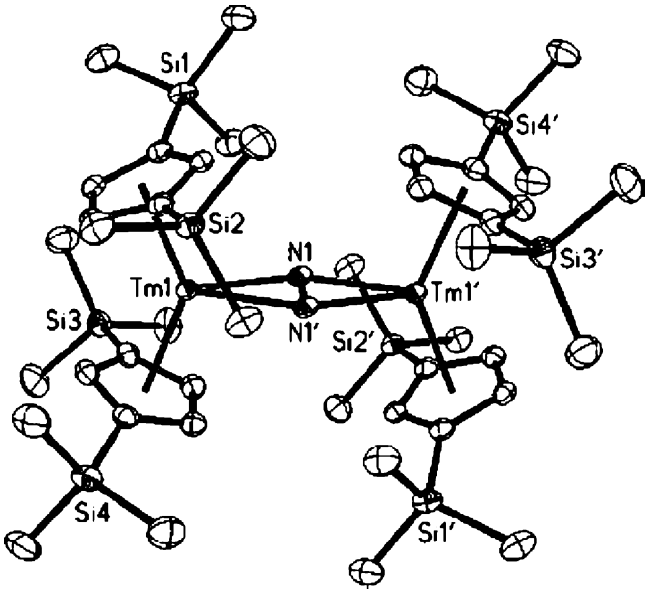

Fig. 36. Molecular structure of (μ-N_2)[Tm{$C_5H_3(SiMe_3)_2$-l,3}$_2$]$_2$ [133].

The two bent metallocene units complex the dinitrogen such that the two Tm centers and the two nitrogen atoms are coplanar. The N–N distance is 1.259(4) Å [133].

Notably, a control reaction of TmI_2 with KCp^* in Et_2O under argon proceeded differently. It formed a purple solution that changed color to orange when nitrogen was added. In the absence of nitrogen, the purple solution slowly changed to yellow-orange over a period of hours. From this solution yellow crystals of $Cp^*_2Tm(\mu\text{-}OEt)_2TmCp^*(\mu\text{-}O)TmCp^*_2$ could be isolated, which resulted from diethyl ether cleavage (Scheme 36) [133].

Adduct formation between $Cp^*_2Yb(THF)_2$ with 2,2′-bipyridine and 1,10-phenanthroline [134] as well as various nitrogen heterocycles involving diazadiene systems [135] has been studied in detail. In all cases deeply colored adducts of the type $Cp^*_2Yb(L)$ were formed (1:1 adducts with 2,2′-bipyridyl, 1,10-phenanthroline, pyrazine, quinoxaline, 1,5- and 1,8-naphthyridine, phthalazine, azobenzene, and 4,4′-bipyridine; 1:2 adducts with phenazine, 2,2′-azopyridine, 2,2′-bipyrimidine, and 2,3-bis(2-pyridino)quinoxaline), which all have to be formulated as $Cp^*_2YbIII(L\cdot^-)$ ($L\cdot^-$ = radical anion) [136]. The potassium salt of the 2,3-dimethylindolide anion (=DMI), $[K(DMI)(THF)]_n$, reacts with $Cp^*_2Ln(\mu\text{-}Cl)_2K(THF)_2$ (Ln = Sm, Y) to form unsolvated amide complexes $Cp^*_2Ln(DMI)$, in which DMI attaches primarily through nitrogen, although the edge of the arene ring is oriented toward the metals at long distances [136]. Lanthanidocene silylamide complexes of the type $Cp'_2Ln[N(SiHMe_2)_2]$ ($Cp' = Cp^*$, C_5HMe_4, C_5HPh_4) have been prepared by allowing the precursors $Y[N(SiHMe_2)_2]_3(THF)_2$ to react with the highly substituted cyclopentadiene derivatives Cp^*H, $C_5H_2Me_4$, and $C_5H_2Ph_4$ [129]. Several samarium(II) and ytterbium(II) carbene complexes have been synthesized analogously [137]. The dissociation of the dimer $[Cp^*_2Y(\mu\text{-}H)]_2$ to the Cp^*_2YH monomer is an important process in the reactions of the dimer with alkenes. The kinetics and formation of yttrium alkyl complexes from $[Cp^*_2Y(\mu\text{-}H)]_2$ and alkenes have been investigated (Scheme 37) [138].

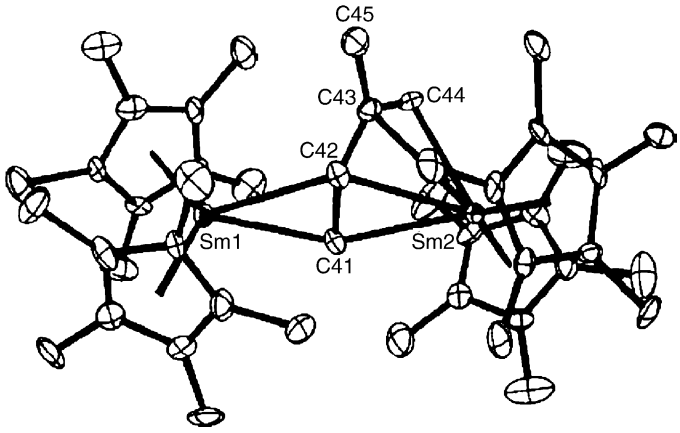

Fig. 37. Molecular structure of [μ-η^2:η^4-$CH_2CHC(Me)CH_2$][Cp^*_2Sm]$_2$ [139].

The interaction of the substituted diene monomers isoprene and myrcene with Cp^*_2Sm has been studied. In both cases binuclear complexes with bridging diene ligands were obtained. Scheme 38 illustrates the formation of the isoprene derivative as an example, while Fig. 37 depicts its molecular structure [139].

Activation of the Si–C bond of $C_6F_5SiH_3$ with $[Cp^*_2Lu(\mu\text{-}H)]_2$ yielded the lutetium aryl complex $Cp^*_2LuC_6F_5$ and oligosilanes. In contrast, the reaction of $[Cp^*_2Lu(\mu\text{-}H)]_2$ with *o*-$MeOC_6H_4SiH_3$ resulted in the formation of dihydrogen and a neutral lutetium silyl complex as shown in Scheme 39 [140].

2.5.7.5. Tris(pentamethylcyclopentadienyl)lanthanide(III) compounds. The recently discovered tris(pentamethylcyclopentadienyl)lanthanides and their fascinating chemistry have been summarized in several review articles by Evans [6–8].

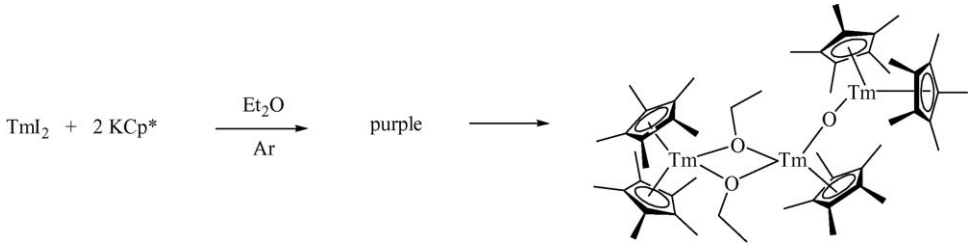

Scheme 36.

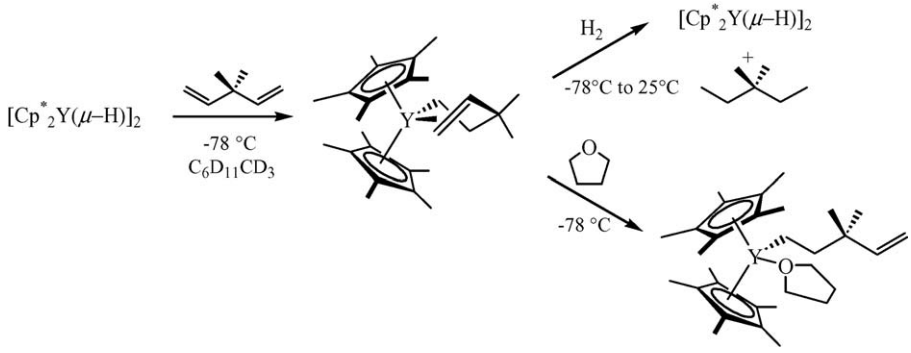

Scheme 37.

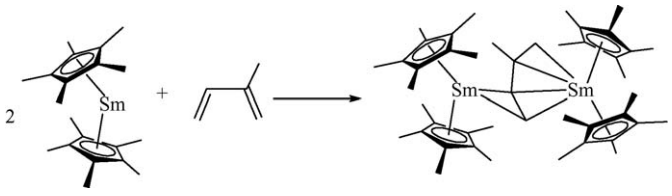

Scheme 38.

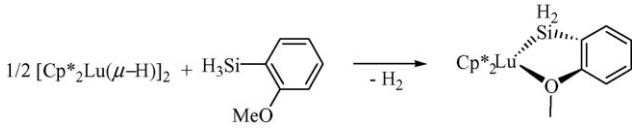

Scheme 39.

A four-step procedure to synthesize Cp^*_3La has been developed. Its molecular structure is illustrated in Fig. 38. The same synthetic route could also be successfully applied to the preparation of the highly crowded tris(peralkylcyclopentadienyl) lanthanum complexes $(C_5Me_4Et)_3La$, $(C_5Me_4Pr^i)_3La$, and $(C_5Me_4SiMe_3)_3La$, which have all been structurally characterized by X-ray analyses [141].

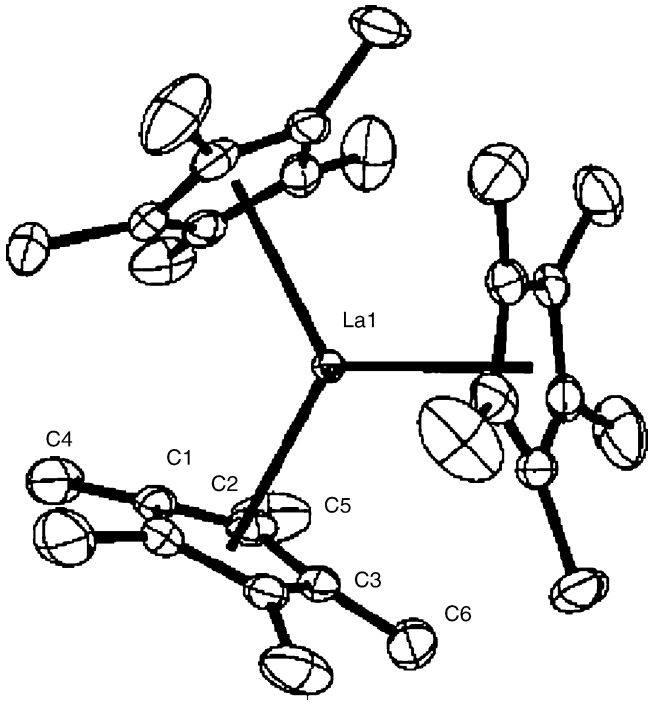

Fig. 38. Molecular structure of Cp^*_3La [141].

2.5.8. Compounds with ring-bridged cyclopentadienyl ligands

2.5.8.1. Lanthanide(II) compounds. *ansa*-Metallocenes of the formula $(\eta^5{:}\eta^5\text{-}C_{24}H_{16})Ln(THF)_2$ (Ln = Sm, Yb) were prepared in 80–90% yields by the in situ reactions of 2 equiv. of potassium acenaphthylenide, $KC_{12}H_8$, with LnI_2 or by reacting the naphthalene complexes of Sm and Yb with acenaphthylene (Scheme 40) [142,143].

The same compounds are also readily accessible via reductive coupling of acenaphthylene with activated ytterbium or samarium as depicted in Scheme 41. The molecular structure of the ytterbium derivative is shown in Fig. 39 [144].

The powerful reducing agent thulium(II) diiodide reacts directly with acenaphthylene in THF solution to give orange crystals of *ansa*-$[(\eta^5\text{-}C_{12}H_8)_2]TmI(THF)$ in 82% yield (Scheme 42, Fig. 40) [145].

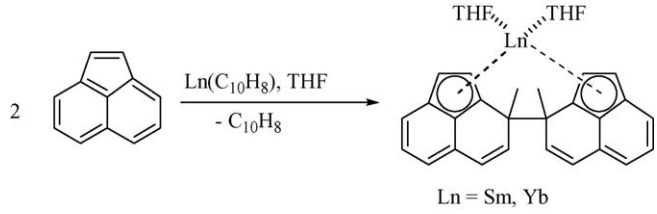

Scheme 40.

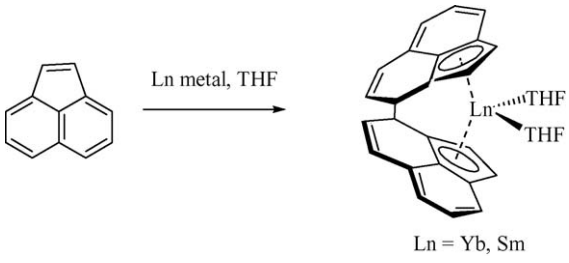

Scheme 41.

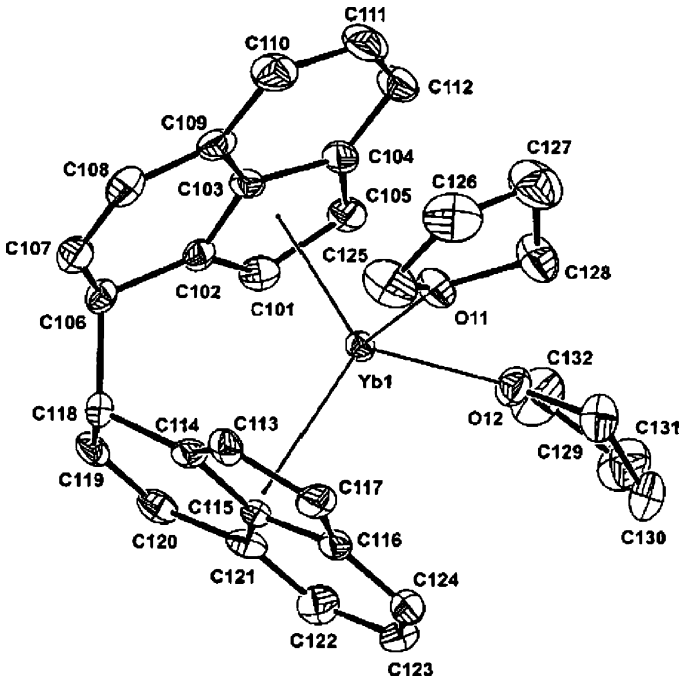

Fig. 39. Molecular structure of *ansa*-[(η^5-$C_{12}H_8$)$_2$]Yb(THF)$_2$ [144].

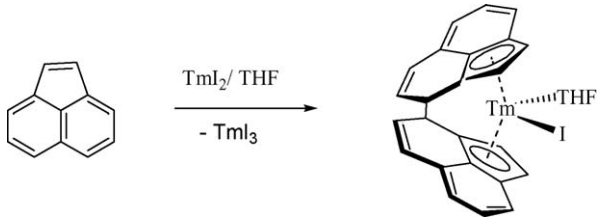

Scheme 42.

2.5.8.2. Lanthanide(III) compounds. *ansa*-Metallocenes of the formula (η^5:η^5-$C_{24}H_{16}$)LnI(THF) (Ln = Dy, Er, Tm, Lu) were prepared in 50–90% yields by the in situ reactions of 2 equiv. of potassium acenaphthylenide, $KC_{12}H_8$, with LnI_3 [142,143]. Catalytically active (isoprene polymerization) non-hindered *ansa*-dicyclopentadienylallyl complexes of samarium have been synthesized either starting from the magnesium salt of the ligand or by dimerization of 6,6-dimethylfulvene in the presence of samarium followed by oxidation (Scheme 43) [146].

Sterically congested dimethylsilylene-bis(cyclopentadienyl) ligands containing four bulky substituents have been employed in the synthesis of *ansa*-neodymocenes as illustrated in Scheme 44 [147,148].

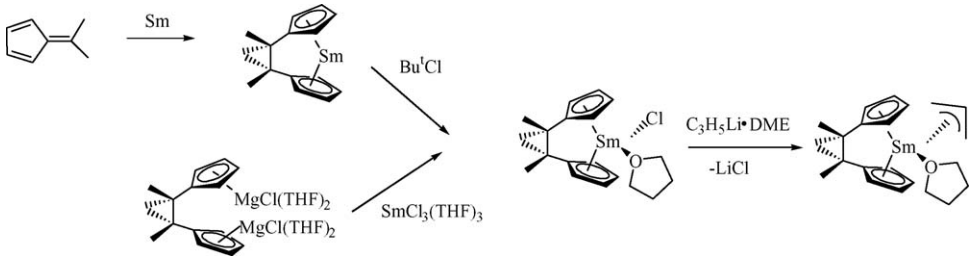

Scheme 43.

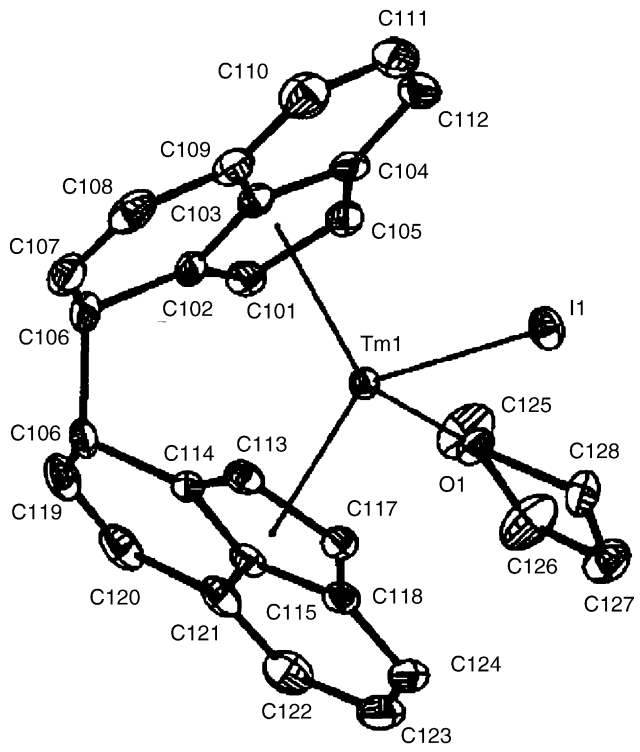

Fig. 40. Molecular structure of *ansa*-[(η^5-$C_{12}H_8$)$_2$]TmI(THF) [145].

Five homologues of the new *ansa*-lanthanidocene series [LnL(μ-OTf)]$_2$ with Ln = Y, Pr, Nd, Sm, Yb have been prepared from Ln(OTf)$_3$ (OTf = trifluoromethanesulfonate) and Na_2L, where L designates two cyclopentadienyl rings tethered by a 2,6-bis(methylene)pyridyl unit [149].

2.5.9. Indenyl and fluorenyl compounds

2.5.9.1. Lanthanide(II) compounds. Ruby-red (C_9H_7)YbI(DME)$_2$ has been prepared in 76% yield according to Scheme 45 as the first indenyl half-sandwich complex of divalent ytterbium. The complex is a monomer in the solid state and stable in DME solution [150].

Fluorenyl complexes of divalent ytterbium ($C_{13}H_9$)$_2$Yb(L)$_n$ (L = THF, n = 2; L = DME, n = 1) have been prepared by reaction of YbI_2(THF)$_2$ with 2 equiv. of $KC_{13}H_9$ as well as by reaction of ($C_{10}H_8$)Yb(THF)$_2$ with fluorene in THF (Scheme 46) [151].

Oxidation of ($C_{13}H_9$)$_2$Yb(THF)$_2$ with $Bu^tN{=}CHCH{=}NBu^t$ (DAD) resulted in formation of ($C_{13}H_9$)$_2$Yb(DAD), which was isolated as deep-green crystals in virtually quantitative yield (98%) (Scheme 47) [151].

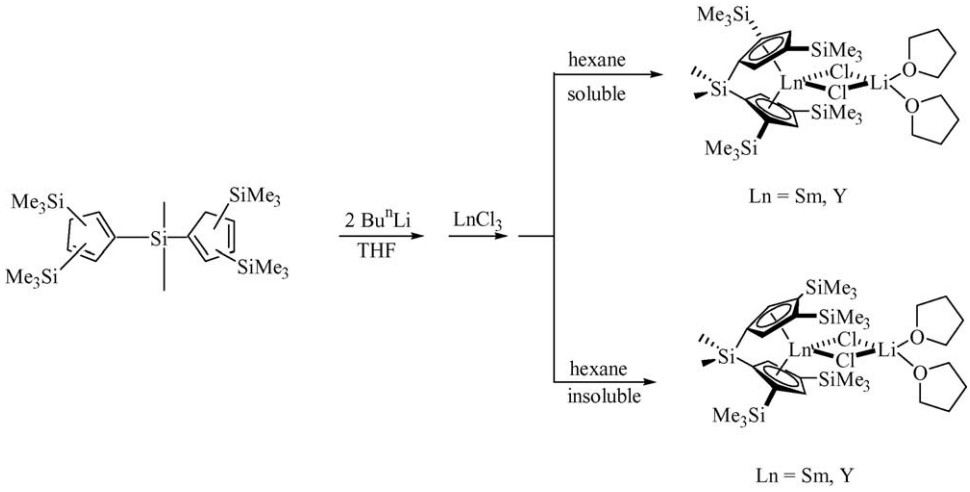

Scheme 44.

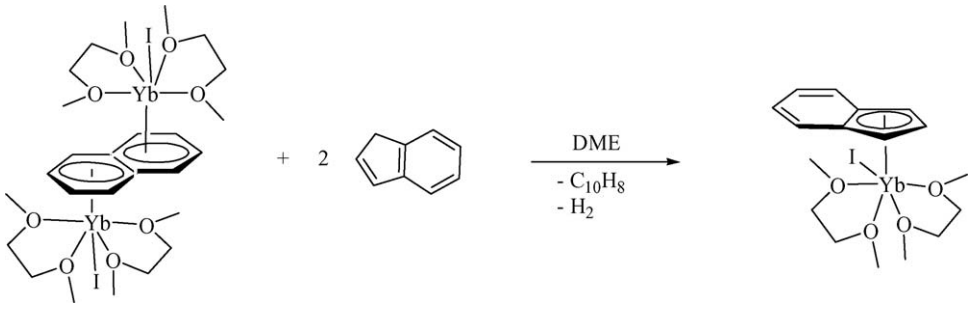

Scheme 45.

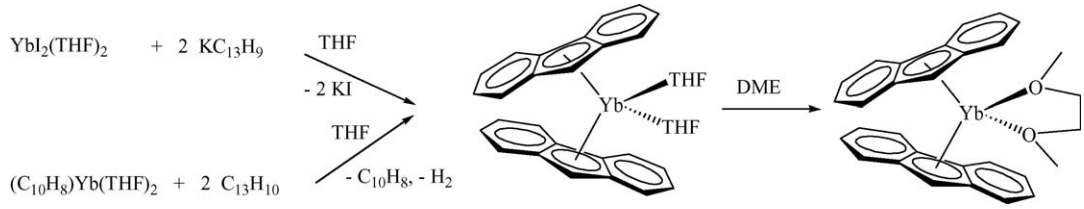

Scheme 46.

The first mixed-ligand sandwich complex of a divalent lanthanide metal, yellow $(C_{13}H_9)Cp^*Yb(DME)$ was synthesized in a one-pot reaction of $(\mu\text{-}C_{10}H_8)[YbI(DME)_2]_2$ with Cp^*H and $KC_{13}H_9$ in DME (Scheme 48, Fig. 41) [151].

The substituted indenyl ytterbium(II) complex $(C_9H_6C_5H_9)_2Yb(THF)_2$ was made by reaction of YbI_2 with 2 equiv. of 1-cyclopentylindenyl lithium, $Li(C_9H_6C_5H_9)$ [118]. Complexes of the type $(C_9H_6C_5H_9)_2Ln(THF)_n$ (Ln = Sm, $n = 1$, black crystals; Ln = Yb, $n = 2$, purple crystals) were also prepared by the reaction between $K(C_9H_6C_5H_9)$ and anhydrous $LnCl_3$ (Ln = Sm, Yb) in a molar ratio of 2:1 in THF and subsequent treatment with Na–K alloy [152].

2.5.9.2. Lanthanide(III) compounds. Complexes of the types $(C_9H_7)_2LnCl(THF)$ and $[(C_9H_7)_2Ln(\mu\text{-}H)]_2{\cdot}4THF{\cdot}NaCl$ have been reported for Ln = Sm, Gd, and Dy [153]. Reaction of anhydrous lanthanide trichlorides with tetrahydrofurfurylindenyl lithium in THF afforded

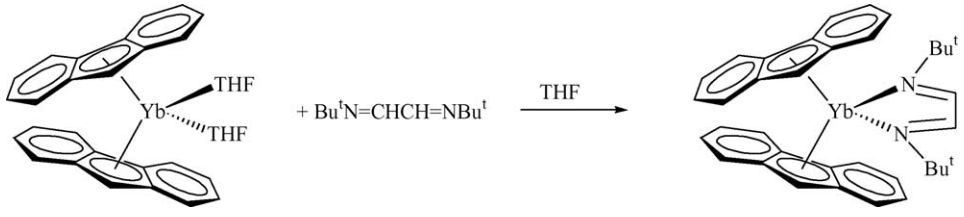

Scheme 47.

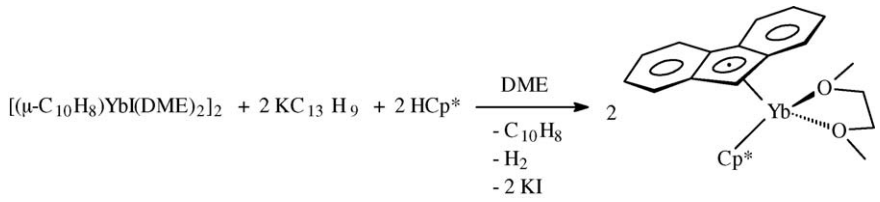

Scheme 48.

bis(tetrahydrofurfurylindenyl)lanthanocene chloride complexes $(C_4H_7OCH_2C_9H_6)_2LnCl$ (Ln = Nd, Sm, Dy, Ho, Er, Yb). The crystal structures of all six complexes have been determined. They are all unsolvated nine-coordinated monomeric complexes with a *trans* arrangement of both the sidearm and indenyl rings in the solid state [154]. Lewis base adducts of tris(indenyl)lanthanide with (S)-(−)-nicotine and various substituted pyridine ligands have been investigated [123].

2.5.9.3. ansa-Indenyl and fluorenyl compounds. The synthesis, structural characterization and catalytic behavior of one-atom bridged fluorenyl cyclopentadienyl lanthanocene complexes with C_s- or C_1-symmetry have been reviewed by Qian et al. [21]. A series of chiral 1,1′-(3-oxapentamethylene)-bridged bis(indenyl) *ansa*-lanthanidocenes have been synthesized with high stereoselectivity. The synthetic routes are illustrated in Scheme 49 [155].

ansa-$[Me_2Si(C_{13}H_9)_2]Yb(THF)$ and *ansa*-$[Me_2Si(C_{13}H_9)_2]Sm(THF)_4$ have been obtained in 75–85% yield by treatment of the appropriate lanthanide diiodides with $K_2[Me_2Si(C_{13}H_9)_2]$ in THF according to Scheme 50 [151].

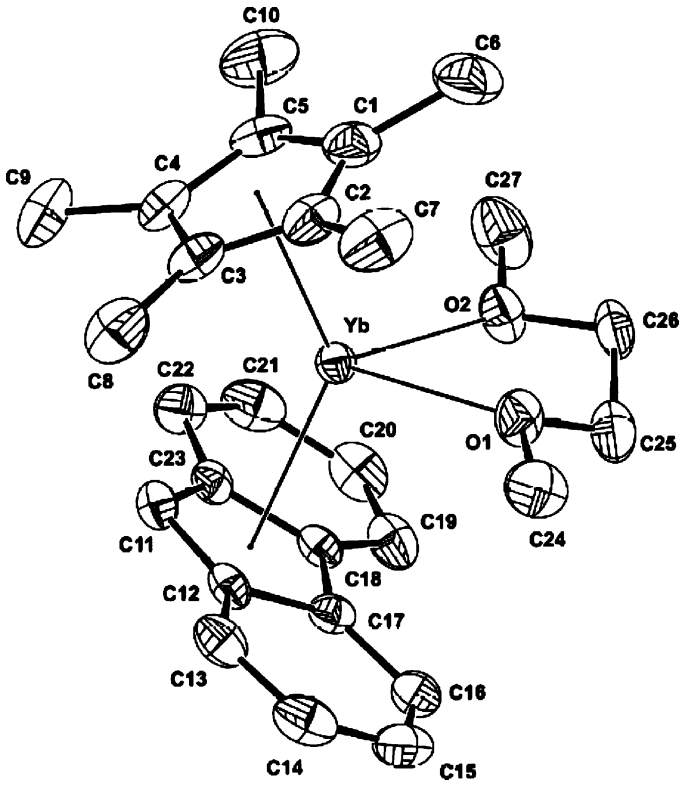

Fig. 41. Molecular structure of $(C_{13}H_9)Cp^*Yb(DME)$ [151].

The silyl-bridged organolanthanide complexes $[Me_2Si(Flu)_2]LnCl$ (Ln = La, Pr, Nd, Sm, Yb) were synthesized by the reaction of $LnCl_3$ with $Li_2[Me_2Si(Flu)_2]$ in THF [156]. The series $[MePhSi(Flu)_2]LnCl$ (Ln = La, Pr, Nd, Sm, Dy, Yb) was made analogously (Scheme 51) [157]. The one-carbon atom bridged amide complex $[Ph_2C(Flu)(C_5H_4)]LuN(SiMe_3)_2$ has been synthesized analogously by reaction of its chloride precursor with $LiN(SiMe_3)_2$ in toluene. An X-ray structural analysis showed an intramolecular $^{\beta}$Si–C agostic interaction with Lu (Fig. 42) [158].

A dinuclear anionic lanthanocene compound containing an *ansa*-fluorenyl ligand has been obtained by reaction of $Nd(BH_4)_3(THF)_3$ with $K_2[Ph_2C(Flu)(C_5H_4)]$ in THF solution (Scheme 52, Fig. 43). The crystallographically characterized product contains a dioxane ligand bridging the two potassium cations [159] (Fig. 44).

2.6. Organolanthanide complexes with cyclopentadienyl-like ligands

An excellent comprehensive review of heterocyclopentadienyl complexes of the Group 3 and lanthanide metals has been published in 2001 by Nief [160]. It covers complexes of monocyclic pyrrolyl, phospholyl, and arsolyl ligands, ring-fused pyrrolyl and phospholyl ligands, pyrazolyl, triphospholyl, and stibadiphospholyl ligands, as well as those containing bridged pyrrolyl ligands (dipyrrolyl complexes and macrocyclic tetrapyrrolyl complexes). Almost all compounds of the latter two classes display σ,π-complexation of the pyrrolyl rings to the lanthanide centers and should thus be considered true organometallic compounds.

2.6.1. Compounds with heteroatom five-membered ring ligands

Reactions of $SmI_2(THF)_2$ and $YbI_2(THF)_2$ with the alkali-metal salts of 2,5-dimethylpyrrole, or the reaction of $SmCl_3(THF)_3$ and $YbCl_3(THF)_3$ with the same ligands followed by reduction with the appropriate alkali metals, led to the formation of divalent mono- and polynuclear complexes. Structural analyses of these complexes indicated that the bonding mode adopted by the ligand depends on the nature of the alkali-metal cation retained in the structure [161]. Dipyrrolide dianions were formed by a transient divalent Tm complex via fragmentation of the $(Et_8$-calix[4]tetrapyrrole$)[K(DME)]_4$ ligand during the reaction with $TmI_2(DME)_3$ [162]. The related reaction of $YbI_2(THF)_2$ with diphenyldipyrrolylmethanide leads to a complex reaction from which a dark red octameric ytterbium(II) macrocyclic complex, [(diphenyldipyrromethanediyl)Yb]$_8$,

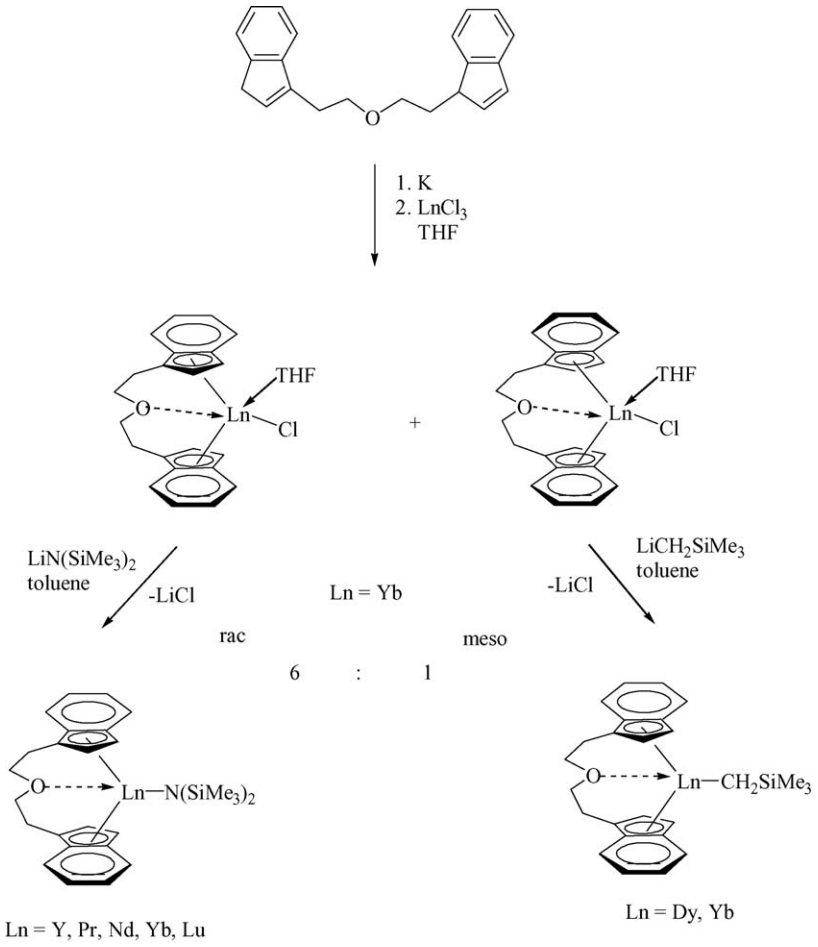

Scheme 49.

was obtained as a major product. A tetrameric cyclic Yb(II)-oxo complex $[K(THF)_3]_2(\mu\text{-}O)[(diphenyldipyrrolylmethanediyl)Yb]_4(THF)_2$ arising from solvent deoxygenation, and a monomeric Yb(III) complex $[K(THF)]_3$ Yb(diphenyldipyrrolylmethanediyl)$_3$ were also isolated as by-products of this complex reaction. All three products have been unambiguously characterized by X-ray structural analyses (Scheme 53, Figs. 45–47) [163].

Treatment of thulium diiodide with substituted phospholide and arsolide salts afforded stable bis(phospholyl)- and bis(arsolyl)thulium(II) complexes (Scheme 54) as green solids, that were characterized by multinuclear NMR and X-ray crystal structures. The latter clearly revealed the beneficial effects of the steric and electronic properties of crowded phospholyl and arsolyl ligands for the stabilization of divalent thulium [164].

Bis(pentamethylcyclopentadienyl) phospholyl and arsolyl samarium(III) complexes have been synthesized from decamethyl samarocene via two different synthetic routes, which are illustrated in Scheme 55 (Fig. 48) and Scheme 56 [164].

The molecular structure of $[K(18\text{-crown-}6)(THF)_2][(C_4Me_4P)_2Nd(BH_4)_2]$ has been determined by X-ray diffraction analysis [165].

2.6.2. Compounds with carboranyl ligands

The reaction between 1,1-$(SiMe_3)_2$-*closo*-1,2-$C_2B_4H_4$, $ErCl_3$, and K in a 2:1:4 molar ratio, in the absence of an outside

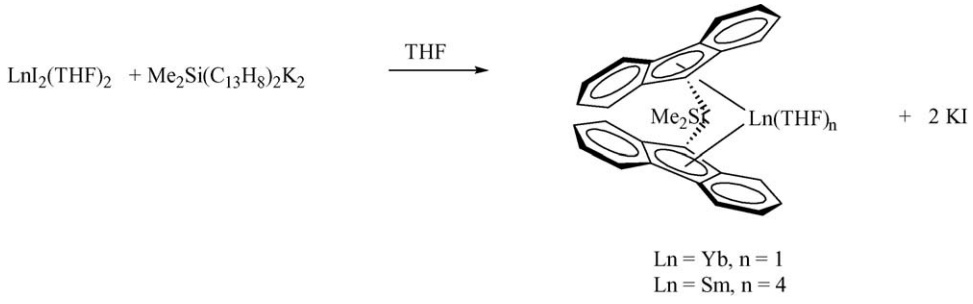

Scheme 50.

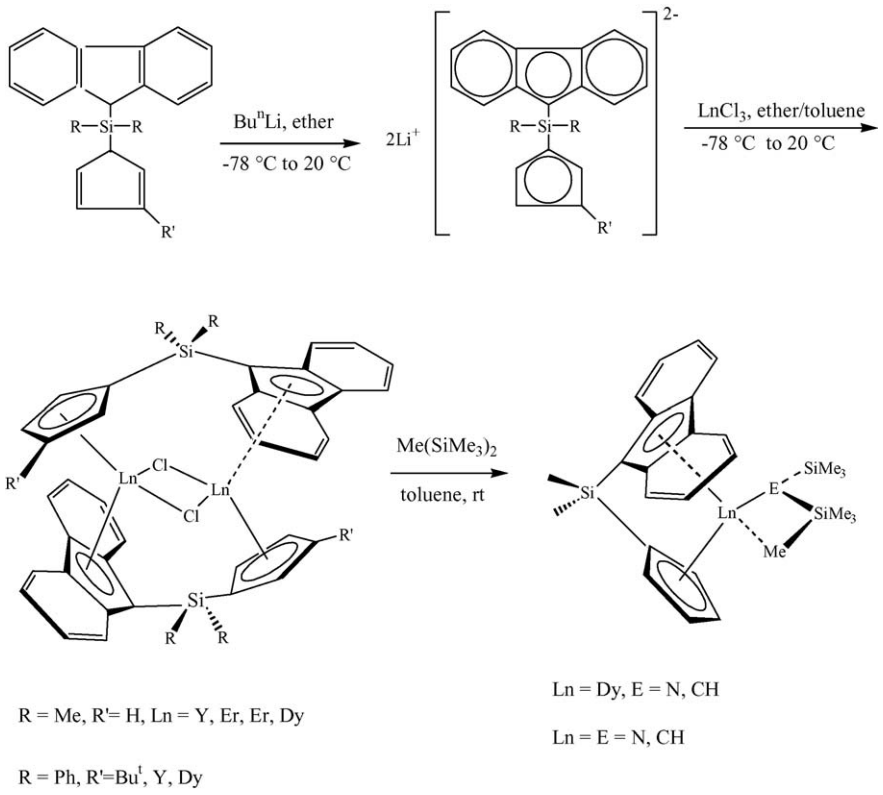

Scheme 51.

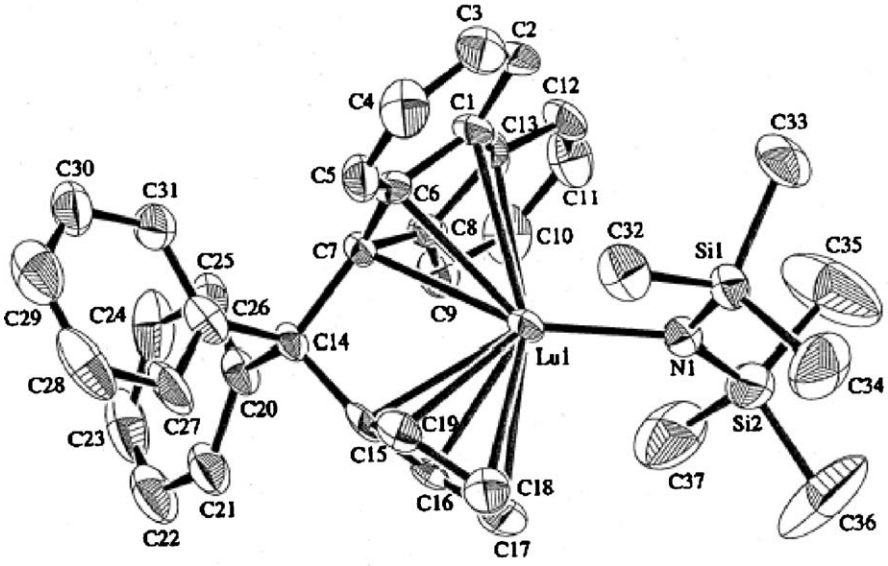

Fig. 42. Molecular structure of $[Ph_2C(Flu)(C_5H_4)]LuN(SiMe_3)_2$ [158].

$$Nd(BH_4)_3(THF)_3 + K_2[FluCPh_2(C_5H_4)]] \xrightarrow[18\text{-crown-6}]{\text{dioxane}} (\mu\text{-}C_4H_8O_2)[K(18\text{-crown-6})\{FluCPh_2(C_5H_4)Nd(BH_4)_2\}]_2$$

Scheme 52.

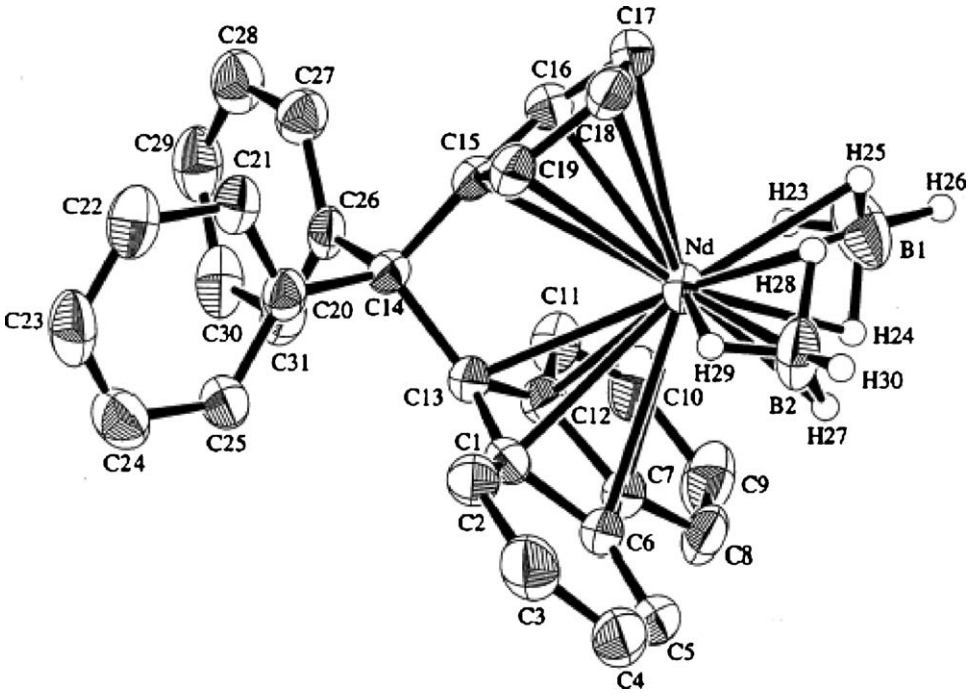

Fig. 43. Molecular structure of the $[Ph_2C(Flu)(C_5H_4)]Nd(BH_4)_2^-$ anion [159].

electron-transfer agent, produced the erbacarborane sandwich 2,2′,4,4′-$(SiMe_3)_4$-3,6′-[μ-H)$_2$K$(THF)_2$]-l,l′-*commo*-Er(η^5-2,4-$C_2B_4H_4)_2$ as light orange crystals in 82% yield. All experimental observations were consistent with a process in which the erbium metal is acting as both the capping group and an electron-transfer agent [166]. In a similar manner, the reaction of *closo-exo*-5,6-Na$(THF)_2$-1-Na$(THF)_2$-2,4-$(SiMe_3)_2$-2,4-$C_2B_4H_4$ and anhydrous $LnCl_3$ in a molar ratio of 3:1 in dry benzene at 60 °C produced novel lanthanocene analogues of metallacarborane complexes of the formula $[Na_3]$ [1,1′-[5,6-(μ-H)$_2$-*nido*-2,4-$(SiMe_3)_2$-2,4-$C_2B_4H_4$]-2,2′,4,4′-$(SiMe_3)_4$-1,1′-*commo*-Ln-(η^5-2,4-$C_2B_4H_4)_2$] (Ln = Er, Dy) as yellow crystalline solids in 82 and 78% yields, respectively, thus establishing a new structural pattern for lanthanacarboranes. Fig. 49 gives a perspective view of the erbium derivative [167].

The analogous reaction of *closo-exo*-5,6-Na$(THF)_2$-1-Na$(THF)_2$-2,4-$(SiMe_3)_2$-2,4-$C_2B_4H_4$ with anhydrous $LuCl_3$ in a molar ratio of 2:1 in dry benzene at 60 °C produce the first full-sandwich lutetiacarborane complex, 2,2′,4,4′-$(SiMe_3)_4$-3,5′,6′-[(μ-H)$_3$Na$(THF)_2$]-1,1′-*commo*-Ln-(η^5-2,4-$C_2B_4H_4)_2$ as an off-white crystalline solid in 88% yield [168].

In a comparative study closely related chemistry has been investigated using the tetramethylcyclopentadienyl-substituted carborane ligand $Me_2Si(C_5Me_4H)(C_2B_{10}H_{11})$. Reaction of $(C_5Me_4H)SiMe_2Cl$ with 1 equiv. of $Li_2C_2B_{10}H_{11}$ gave a monoanionic salt, which could be converted into the dianionic salt by treatment with Bu^{n}Li (Scheme 57). Both lithium salts have been employed in the preparation of organolanthanide complexes containing these ligands. As a representative example, the molecular structure of the "ate"-complex [η^5-$Me_2Si(C_5Me_4)(C_2B_{10}H_{11})$]$_2$Nd(μ-Cl)$_2Li(OEt_2)$(THF) is illustrated in Fig. 50. In this complex only the tetramethylcyclopentadienyl-rings are coordinated to neodymium [169].

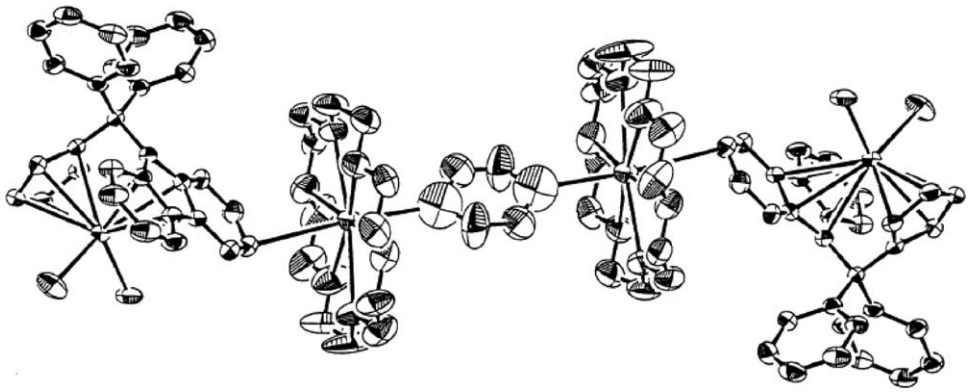

Fig. 44. Molecular structure of (μ-$C_4H_8O_2$)[K(18-crown-6){$FluCPh_2(C_5H_4)Nd(BH_4)_2$}]$_2$ [159].

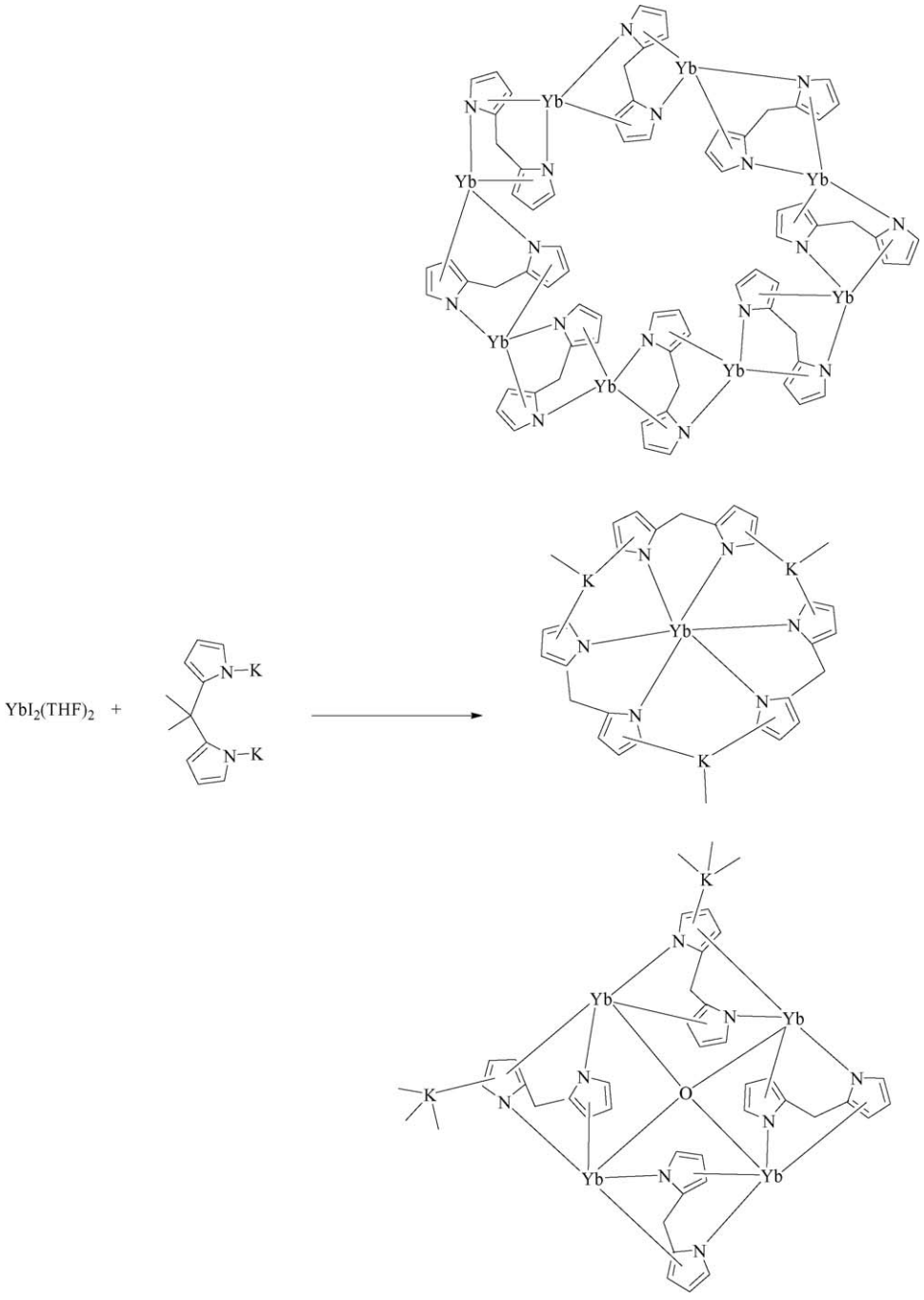

Scheme 53.

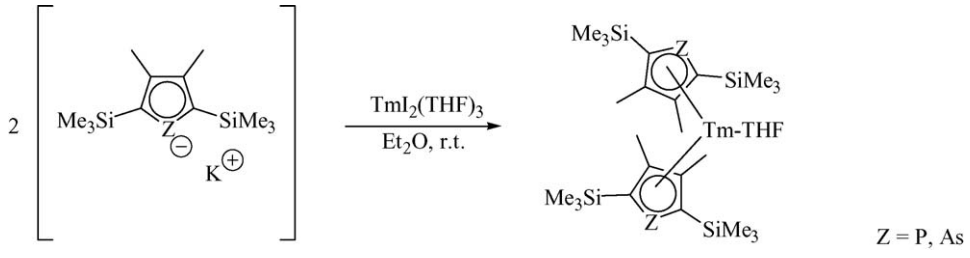

Scheme 54.

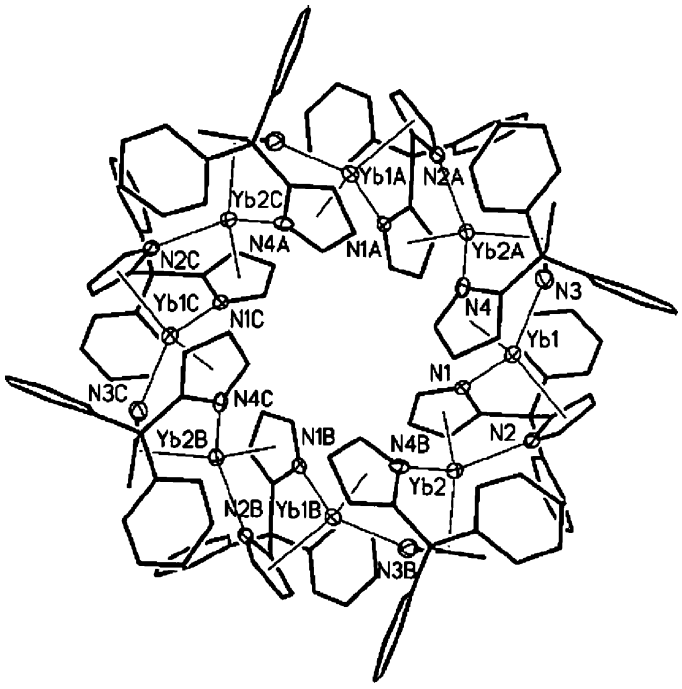

Fig. 45. Molecular structure of [(diphenyldipyrromethanediyl)Yb]$_8$ [163].

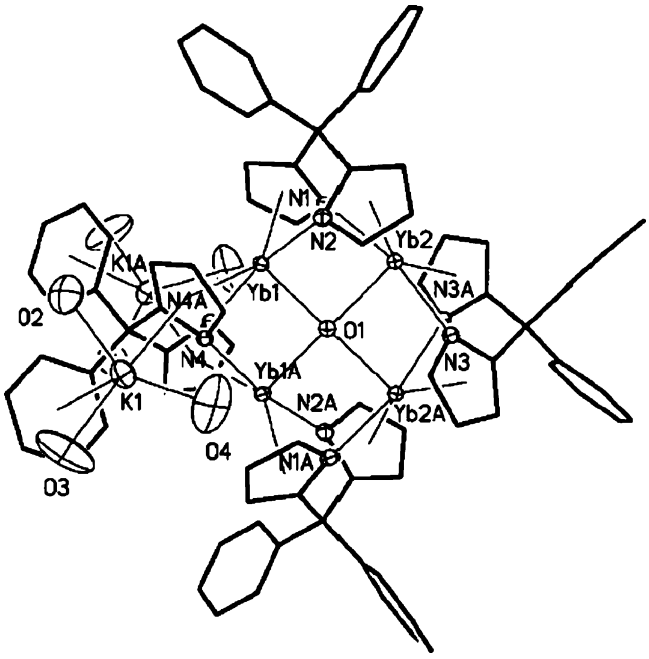

Fig. 47. Molecular structure of [K(THF)$_3$]$_2$(μ-O)[(diphenyldipyrrolylmethanediyl)Yb]$_4$(THF)$_2$ [163].

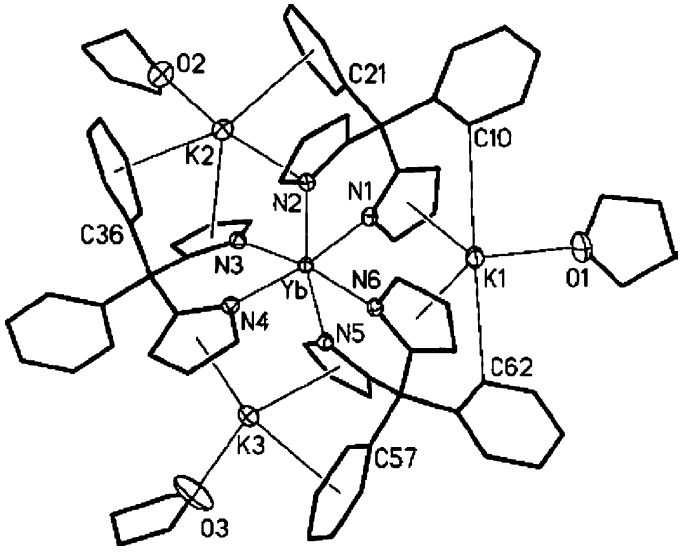

Fig. 46. Molecular structure of [K(THF)]$_3$Yb(diphenyldipyrrolylmethanediyl)$_3$ [163].

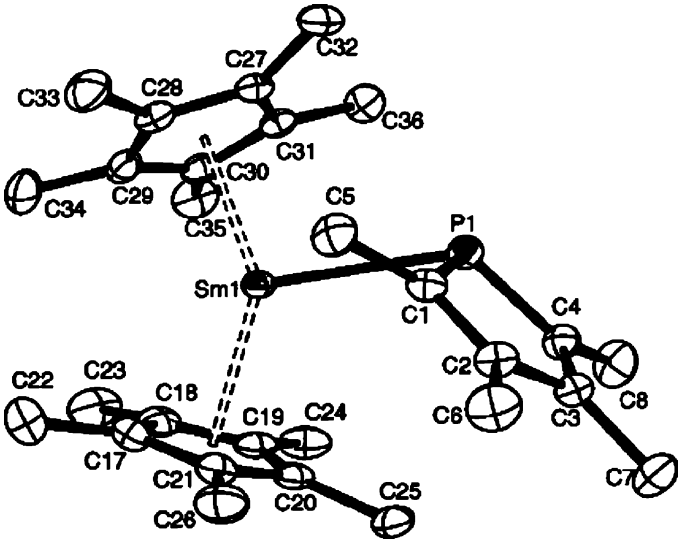

Fig. 48. Molecular structure of Cp*$_2$Sm(C$_4$Me$_4$P) [164].

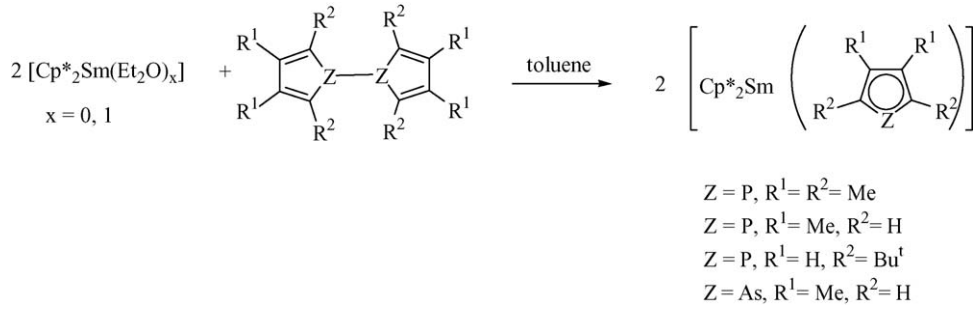

Scheme 55.

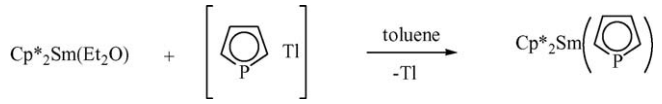

Scheme 56.

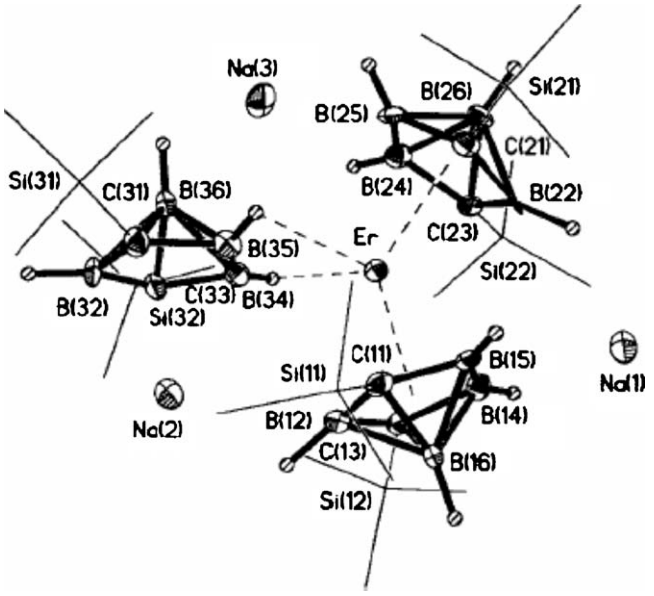

Fig. 49. Molecular structure of $[Na_3][1,1'\text{-}[5,6\text{-}(\mu\text{-}H)_2\text{-}nido\text{-}2,4\text{-}(SiMe_3)_2\text{-}2,4\text{-}C_2B_4H_4]\text{-}2,2',4,4'\text{-}(SiMe_3)_4\text{-}1,1'\text{-}commo\text{-}Er\text{-}(\eta^5\text{-}2,4\text{-}C_2B_4H_4)_2]$ [167].

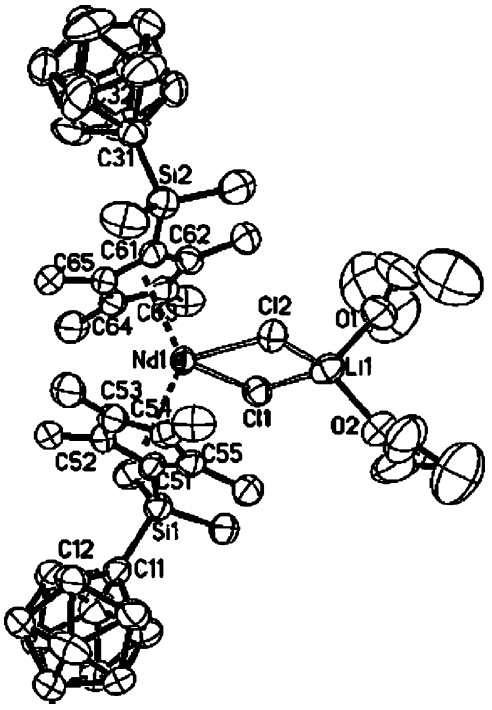

Fig. 50. Molecular structure of $[\eta^5\text{-}Me_2Si(C_5Me_4)(C_2B_{10}H_{11})]_2NdC(\mu\text{-}Cl)_2Li(OEt_2)(THF)$ [169].

Various lanthanacarboranes incorporating so-called "carbons-adjacent" *nido*- and *arachno*-carborane anions of the C_2B_{10} system have also been synthesized and structurally characterized [170]. An interesting variation of the indenyl/carborane ligand system is the introduction of additional donor-functionalized side-chains. New metallacarboranes bearing a $(nido\text{-}RC_2B_{10}H_{10})_2^{4-}$ ligand, $[Li(THF)_4][\{\eta^5{:}\eta^1{:}\eta^6\text{-}Me_2Si(C_9H_5CH_2CH_2G)(C_2B_{10}H_{10})Sm\}_2(\mu\text{-}Cl)]$ (G = NMe_2, OMe), have been prepared and structurally characterized by treatment of $SmI_2(THF)_x$ with 1 equiv. of $[Me_2Si(C_9H_5CH_2CH_2G)(C_2B_{10}H_{10})]Li_2(OEt_2)_2{\cdot}LiCl$ in THF via unexpected samarium-mediated ligand coupling reactions (Scheme 58). The molecular structure of the anion in $[Li(THF)_4][\{\eta^5{:}\eta^1{:}\eta^6\text{-}Me_2Si(C_9H_5CH_2CH_2NMe_2)(C_2B_{10}H_{10})Sm\}_2(\mu\text{-}Cl)]$ is shown in Fig. 51 [171].

Numerous organolanthanide complexes derived from the new versatile boron-bridged ligand $Pr^i{}_2NB(C_9H_7)(C_2B_{10}H_{11})$. Fig. 52 shows a the molecular structure of a representative example, i.e. the complex anion in the green ytterbium species *meso*-$[Li(DME)_3][\{\eta^5{:}\sigma^1\text{-}{}^iPr_2NB(C_9H_6)(C_2B_{10}H_{10})\}_2Yb]$ [172].

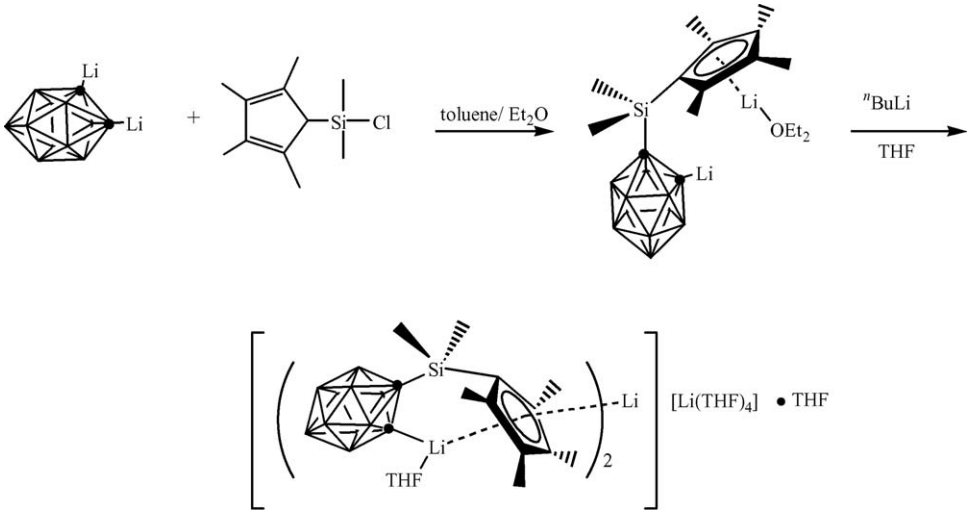

Scheme 57.

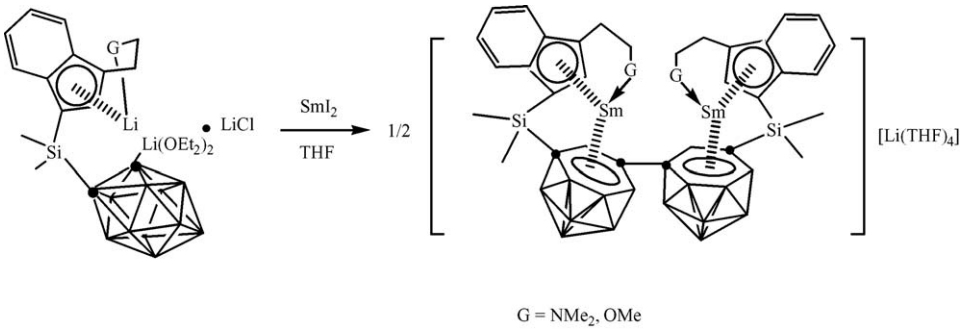

Scheme 58.

A series of bis(cyclopentadienyl)lanthanide complexes containing bridging 1,2-dicarba-*closo*-dodecaborane-1,2-dichalcogenolate ligands has been synthesized and structurally characterized. Scheme 59 illustrates the preparation of the starting materials as well as the products. The dimeric carborane precursors are accessible via insertion of elemental chalcogen E (E = S, Se) into the Li–C bonds of dilithium *o*-carborane in THF solution. The central Ln_2E_2 four-membered ring in the products is not planar. As a typical representative, the molecular structure of the anionic moiety in the Nd/Se derivative $[Li(THF)_4][(\eta^5\text{-}^t BuC_5H_4)_2NdSe_2C_2B_{10}H_{10}]_2$is shown in Fig. 53 [173,174].

2.7. Lanthanide arene complexes

The synthesis, arrangement, and reactivity of arene-lanthanide compounds have recently been comprehensively reviewed by Bochkarev [3]. The nature of the metal–ligand bond in trivalent neodymium complexes with neutral π-donor ligands, including benzene, has been the subject of a theoretical study [175]. Mono- and bis-adducts of benzene of the type $Ln(C_6H_6)_{1,2}^+$ (Ln = Sc, Y, Ln) have been generated in the gas phase, and their reactivities toward molecular oxygen have been measured using an inductively coupled plasma/selected-ion flow tube tandem mass spectrometer [176]. Theoretical calculations have been carried out on the binding between Sc^+ and phenol [177] as well as of ScX_n (X = Cl, Br; x = 1–3) with benzene [84].

Recrystallization of the linked cyclopentadienyl-anilido ytterbium(II) complex $[Me_2Si(C_5Me_4)(NPh)]Yb(THF)_3$ from toluene/hexane yielded the less solvated complex $[\{Me_2Si(C_5Me_4)(NPh)\}Ln(THF)]_2$ as brown crystals in 91% yield. The compound forms a dimeric structure through an intermolecular Yb–Ph π-interaction (Scheme 60, Fig. 54) [62].

Reaction of a freshly prepared solution of lithium anthracenide, $Li(C_{14}H_{10})$, in DME to a suspension of TmI_2 (1:1 molar ratio) produced a dark red-brown solution from which red crystals of $(\eta^2\text{-}C_{14}H_{10})TmI(DME)_2$ (Fig. 55) could be isolated in about 80% yield [145].

The formation of highly colored yttrium arene complexes with macrocyclic ancillary ligands has been reported [178]. The compound $[\{P_2N_2\}Y(\mu\text{-}C1)]_2$ ($\{P_2N_2\} = [PhP(CH_2SiMe_2NSiMe_2CH_2)_2PPh]^{2-}$) reacts with phenyllithium to give a dark blue product comprising the empirical formula $\{P_2N_2\}Y(C_6H_5)$. The same product was obtained in a C–H activation reaction between $\{P_2N_2\}YCH(SiMe_3)_2$ and benzene. An X-ray structure

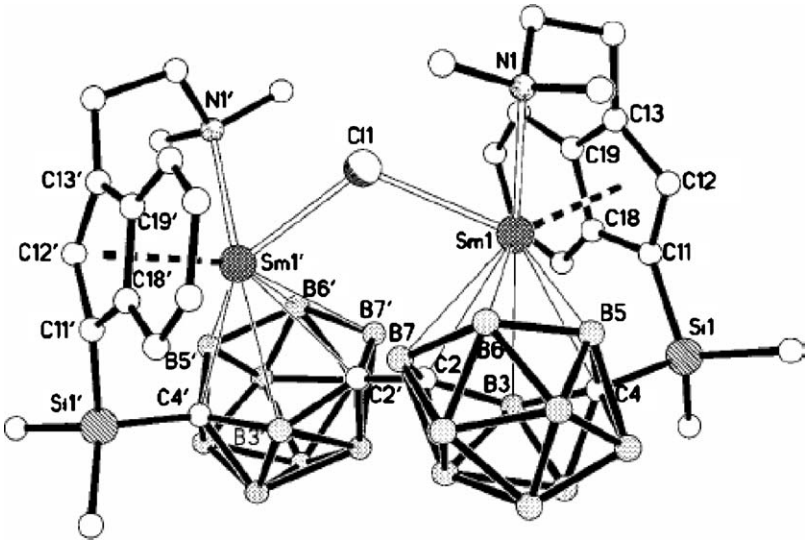

Fig. 51. Molecular structure of the $[\{\eta^5\text{:}\eta^1\text{:}\eta^6\text{-}Me_2Si(C_9H_5CH_2CH_2NMe_2)(C_2B_{10}H_{10})Sm\}_2(\mu\text{-}Cl)]^-$ anion [171].

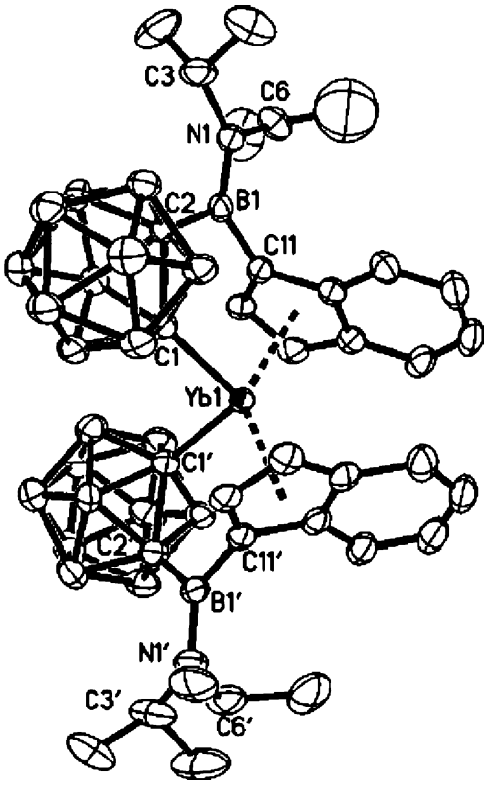

Fig. 52. Molecular structure of the $[\{\eta^5{:}\sigma^1\text{-}^{i}Pr_2NB(C_9H_6)(C_2B_{10}H_{10})\}_2Yb]^-$ anion [172].

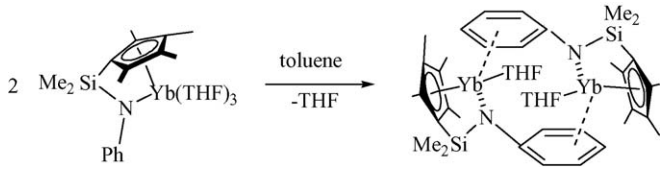

Scheme 60.

determination of the isolated deep blue crystals revealed the presence of an unusual dimeric complexes of the composition $(\mu\text{-}\eta^6{:}\eta^6\text{-}C_6H_5C_6H_5)[\{P_2N_2\}Y]_2$ as depicted in Scheme 61.

The compound $(\mu\text{-}\eta^6{:}\eta^6\text{-}C_6H_5C_6H_5)[\{P_2N_2\}Y]_2$ is a dinuclear complex with a biphenyl dianion bridging two $\{P_2N_2\}Y$ fragments with each of these units bound in an η^6-fashion to the opposite faces of the biphenyl moiety. While the same type of dark blue compound could be generated using *m*-tolyllithium, the reaction of $[\{P_2N_2\}Y(\mu\text{-}C1)]_2$ with *p*-tolyllithium had a different outcome affording a dark brown crystalline product. In this case an X-ray diffraction study showed again the presence of a dinuclear complex containing a bridging bi-*p*-tolyl ligand. However, in this case the two $\{P_2N_2\}Y$ fragments are sandwiching one tolyl group leaving the second uncoordinated (Fig. 56) [178].

Reaction of 3 equiv. of 2,6-diisopropylaniline with $Sm[N(SiMe_3)_2]_3$ afforded the dimeric species $[Sm(NHAr)_3]_2$ (Scheme 62). X-ray crystallography revealed that each metal center engages in an η^6-arene interaction with the aryl ring of an amide ligand attached to an adjacent samarium (Fig. 57) [179].

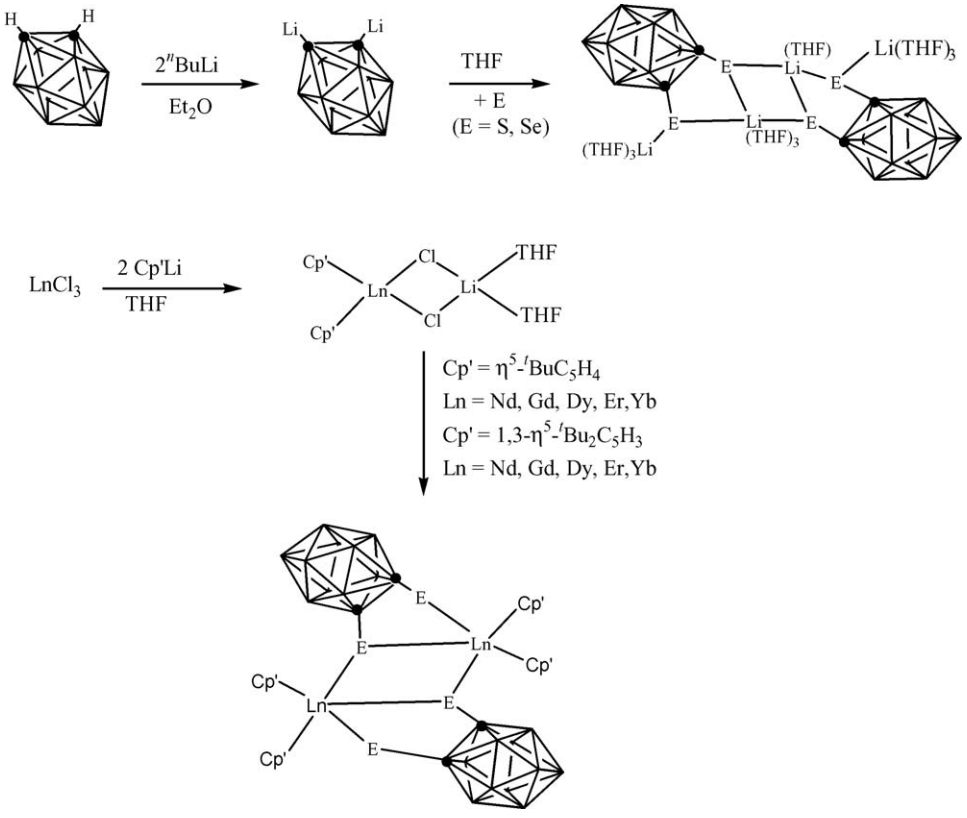

Scheme 59.

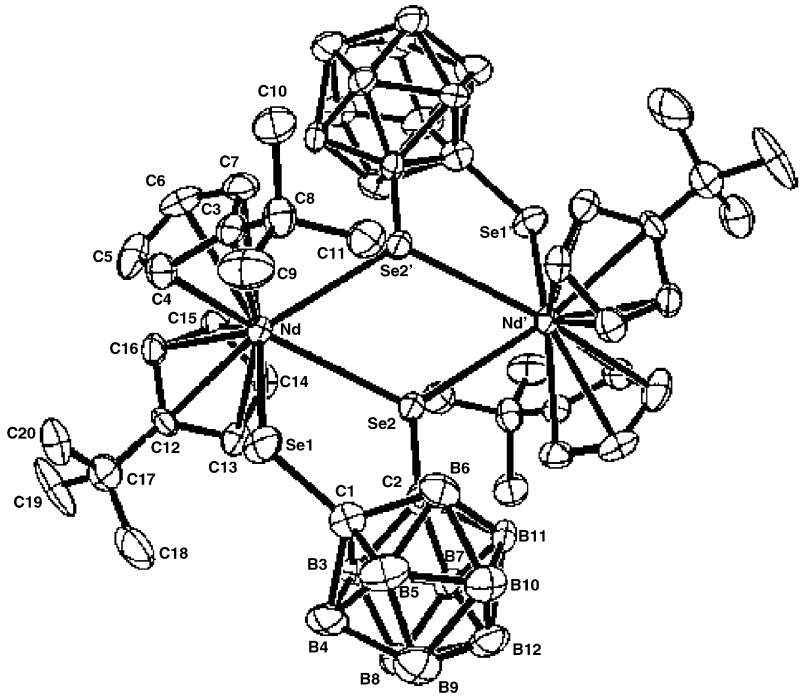

Fig. 53. Molecular structure of the $[(\eta^5\text{-}^t\text{BuC}_5\text{H}_4)_2\text{NdSe}_2\text{C}_2\text{B}_{10}\text{H}_{10}]_2^-$ anion [174].

The chemistry of boratabenzene Group 3 complexes has been extended to yttrium as well as differently substituted boratabenzene ligands. The reaction of yttrium trichloride with lithium 1-methylboratabenzene (1:2) in toluene (110 °C, 3 days) afforded the donor-free dinuclear sandwich complex $[(C_5H_5BMe)_2Y(\mu\text{-}Cl)]_2$ in 85% yield as pale yellow crystals. By means of single crystal and powder diffraction methods, three conformational polymorphs of this complex were characterized in the solid state [180].

2.8. Lanthanide cyclooctatetraenyl compounds

The use of neodymium borohydride complexes as precursors for (COT)lanthanide complexes has been reviewed by Ephritikhine et al. A comparison has been made to the corresponding uranium chemistry [181].

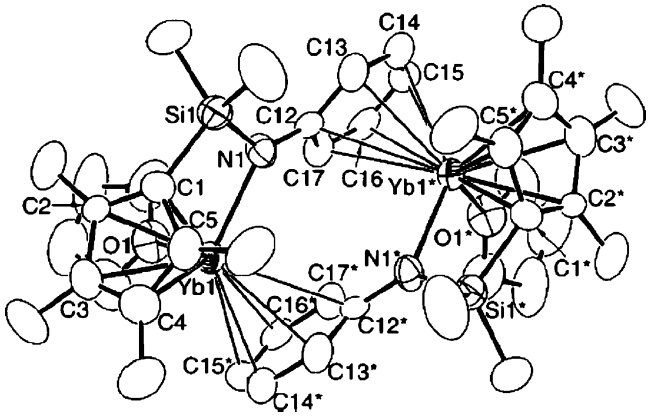

Fig. 54. Molecular structure of $[\{Me_2Si(C_5Me_4)(NPh)\}Ln(THF)]_2$ [62].

2.8.1. Cyclooctatetraenyl lanthanide(II) compounds

Inverse sandwich complexes containing a COT ligand bridging lanthanide bis(silylamide) units have been reported for divalent samarium and ytterbium. Blue-green $(\mu\text{-COT})[Sm\{N(SiMe_3)_2\}(THF)]_2$ can be obtained from $Sm[N(SiMe_3)_2]_2(THF)_2$, $SmI_2(THF)_2$, and K_2COT in THF (83% yield). The analogous red-brown $(\mu\text{-COT})[Yb\{N(SiMe_3)_2\}(THF)]_2$ can be generated from $KN(SiMe_3)_2$, $YbI_2(THF)_2$, and K_2COT in THF (86% yield). The Sm derivative has been structurally characterized (Fig. 58) [124].

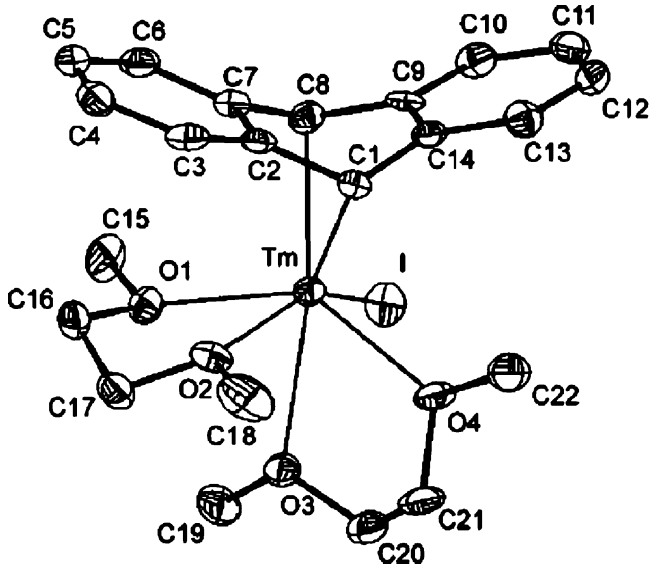

Fig. 55. Molecular structure of $(\eta^2\text{-}C_{14}H_{10})TmI(DME)_2$ [145].

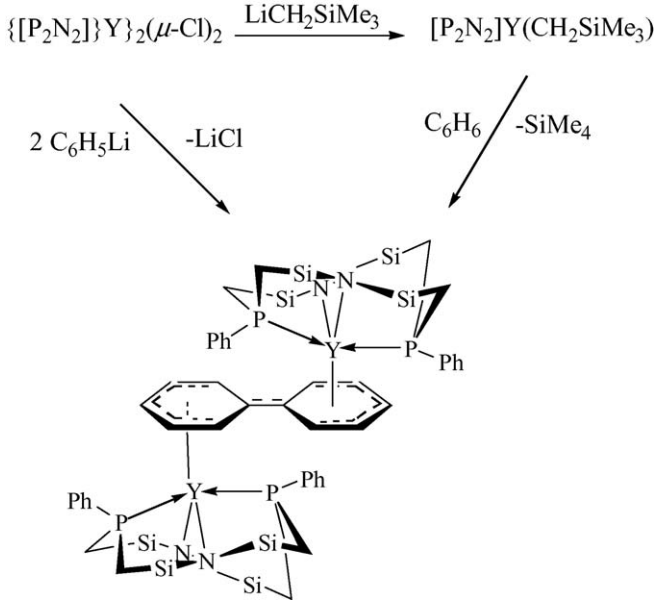

Scheme 61.

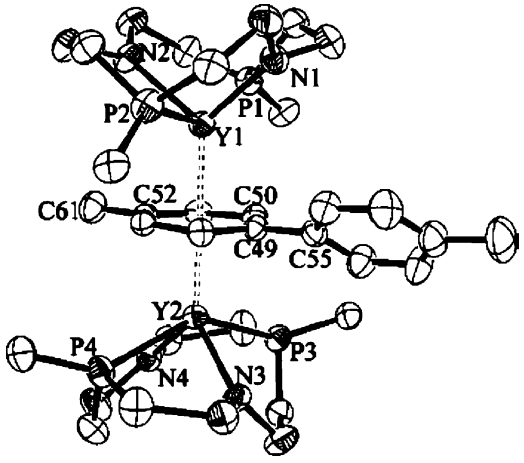

Fig. 56. Molecular structure of [(μ-η6:η6-C6H4-*p*-Me)(C6H4-*p*-Me)][{P2N2}Y]2 [178].

2.8.2. Mono(cyclooctatetraenyl) lanthanide(III) compounds

The dimeric mono(cyclooctatetraenyl)lanthanide chlorides [(COT)Ln(μ-Cl)(THF)2]2 are long known and still represent the most useful precursor in (COT)Ln chemistry. A recently reported alternative preparation of the Sm derivative involves the reaction of samarium metal with cyclooctatetraene in THF in the presence of a small amount of $HgCl_2$. The molecular structure of [(COT)Sm(μ-Cl)(THF)2]2 has been determined [148]. A clean preparation of the monomeric half-sandwich complex (COT)TmI(THF)2 involves treatment of TmI_2 with equimolar amounts of cyclooctatetraene in THF at room temperature (Scheme 63). The product was isolated as red

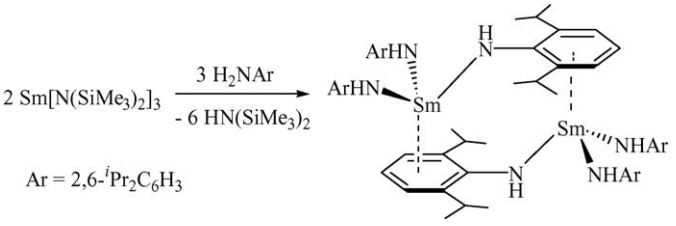

Scheme 62.

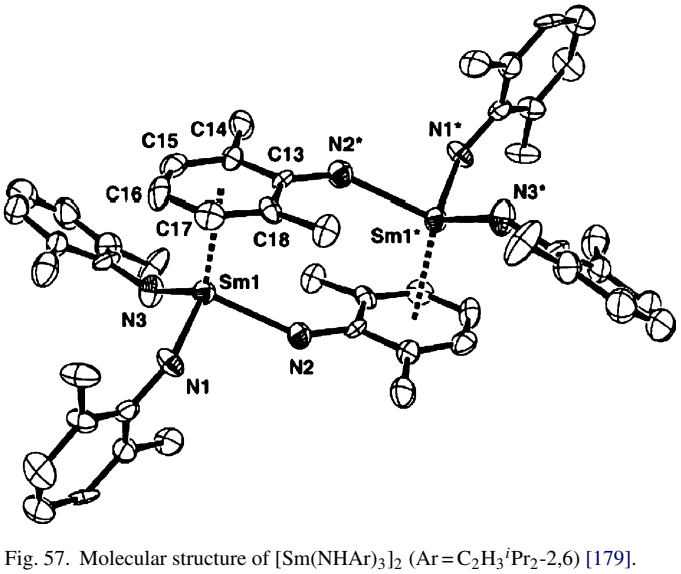

Fig. 57. Molecular structure of [Sm(NHAr)3]2 (Ar = C2H3iPr2-2,6) [179].

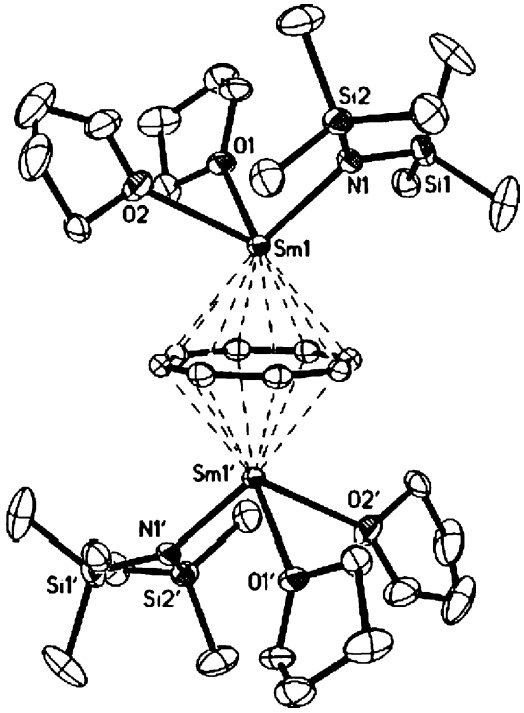

Fig. 58. Molecular structure of (μ-COT)[Sm{N(SiMe3)2}(THF)]2 [124].

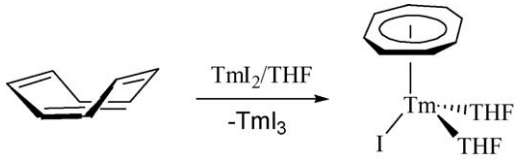

Scheme 63.

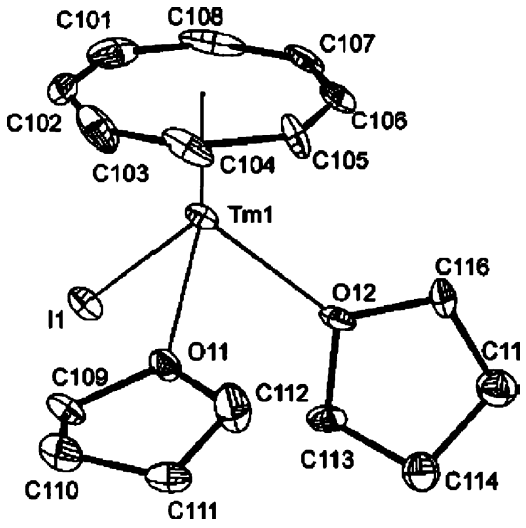

Fig. 59. Molecular structure of (COT)TmI(THF)$_2$ [145].

crystals in 75% yield and structurally characterized by X-ray diffraction (Fig. 59) [145].

Two types of indenyl/cyclooctatetraenyl mixed-sandwich complexes (MeOCH$_2$CH$_2$C$_9$H$_6$)Ln(COT)(THF)$_n$ (Ln = La, Nd, n = 0; Ln = Sm, Dy, Er, n = 1) and (C$_4$H$_7$OCH$_2$C$_9$H$_6$)Ln(COT)(THF) (Ln = La, Nd, Sm, Dy, Er) have been synthesized by the reactions of LnCl$_3$ with 1 equiv. of K$_2$COT, followed by treatment with the corresponding potassium salt of the ether-substituted indenide anion [182]. The novel mixed phospholyl/cyclooctatetraenyl lanthanide sandwich complexes (COT)Sm(Tmp)(THF), (COT)Sm(Dsp), and (COT)Nd(Dsp)(THF) (Tmp = 2,3,4,5-tetramethylphospholyl; Dsp = 3,4-dimethyl-2,5-bis(trimethylsilyl)phospholyl) have been prepared by metathesis of phospholylpotassium salts with the dimeric cyclooctatetraenyllanthanide chloride precursors [(COT)Ln(μ-Cl)(THF)$_2$]$_2$ (Ln = Nd, Sm). The neodymium derivative has been structurally characterized (Fig. 60) [183].

2.9. Metallofullerenes

A lanthanum fullerene complex of the composition C$_{60}$[La(Gly)$_2$]$_2$(ClO$_4$)$_6$ has been reported to contain η^2-coordinated C$_{60}$, though structural evidence is lacking [184]. A photofragmentation study of metal fullerides C$_{60}$Ln$_x$ (Ln = Y, La, Sm) by excimer laser ablation-TOF mass spectrometry showed that many kinds of metallofullerenes have been observed in both the positive and negative ionic modes. For C$_{60}$Sm$_x$, the metal atom is incorporated into the network of the fullerene cage to replace one carbon atom of the cage forming substitutional metallofullerenes. In the case of the metal fullerides C$_{60}$Ln$_x$ (Ln = Y, La), evidence of the encapsulation of Y and La atoms in the fullerene cages forming endohedral fullerenes has been observed [185–187]. The isolation and characterization of an endohedral metallofullerene encapsulating three lanthanide atoms inside a nanoscale C$_{80}$ cage, Lu$_3$N@C$_{80}$, has been reported. Also described were mixed-metal species of gadolinium/lutetium and holmium/lutetium, Lu$_{3-x}$Ln$_x$N@C$_{80}$ (Ln = Gd, Ho; x = 0–2), which may prove useful as multifunctional contrast agents for X-ray, MRI, and radiopharmaceuticals [188].

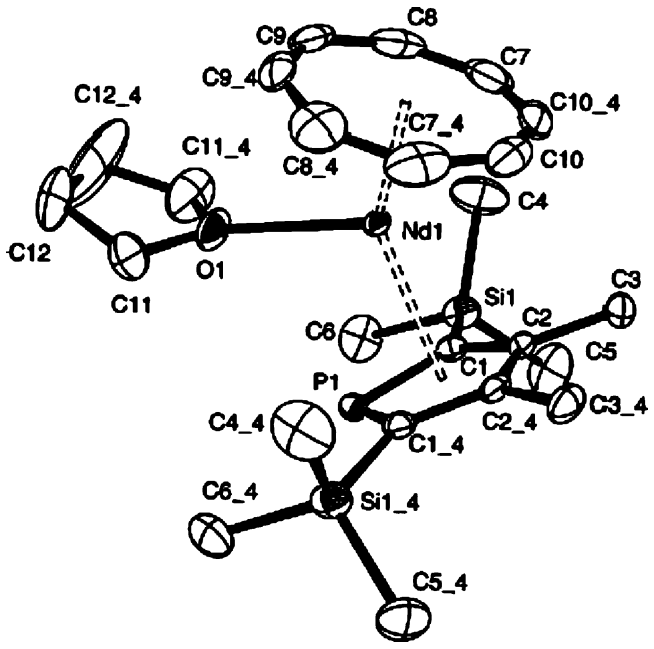

Fig. 60. Molecular structure of (COT)Nd(Dsp)(THF) (Dsp = 3,4-dimethyl-2,5-bis(trimethylsilyl)phospholyl) [183].

2.10. Heterobimetallic organolanthanide complexes

2.10.1. Metal–metal bonded compounds

The gas-phase reactions of lanthanide (Ln$^+$ = La$^+$–Lu$^+$, except Pm$^+$) cations with iron pentacarbonyl, Fe(CO)$_5$, and with ferrocene, Cp$_2$Fe, have been studied by Fourier transform ion cyclotron resonance mass spectrometry (FT-ICR/MS). In the case of Fe(CO)$_5$, the observed primary products were of the type LnFe(CO)$_x^+$ (Ln = La, Ce, Pr, Nd, Gd, Tb: x = 3; Ln = Ho, Er, Lu: x = 3 and 4; Ln = Sm, Eu, Dy, Tm, Yb: x = 4), and evidence was obtained for the presence of direct Ln–Fe bonds in these species. With Cp$_2$Fe the majority of the Ln$^+$ cations reacted by metal exchange, yielding Ln bis(cyclopentadienyl) ions Cp$_2$Ln$^+$, while the less reactive Ln$^+$ cations formed the "adduct" ions LnFeCp$_2^+$ [189].

2.10.2. Heterobimetallic compounds without direct metal–metal bonds

C_2-symmetric tetraalkylaluminate complexes *rac*-[Me$_2$(2-MeC$_9$H$_5$)$_2$]Y(μ-R)AlR$_2$ (R = Me, Et, Bu^i) are quantitatively formed upon treatment of the corresponding indenyl-derived *ansa*-lanthanidocene bis(dimethylsilylamides) with AlR$_3$ [90]. The homoleptic rare earth carboxylate complexes [Ln(O$_2$CC$_6$H$_2$Pr$^i_3$-2,4,6)$_3$]$_n$ (Ln = Y, La, Nd, Lu) react with trimethylaluminum to yield hexane-soluble monolanthanide complexes featuring an η^2-coordinated tetraalkylaluminate ligand and a novel ancillary AlMe$_2$-bridged bis(carboxylate) ligand (Scheme 64). The Nd derivative has been structurally characterized by X-ray diffraction (Fig. 61) [190].

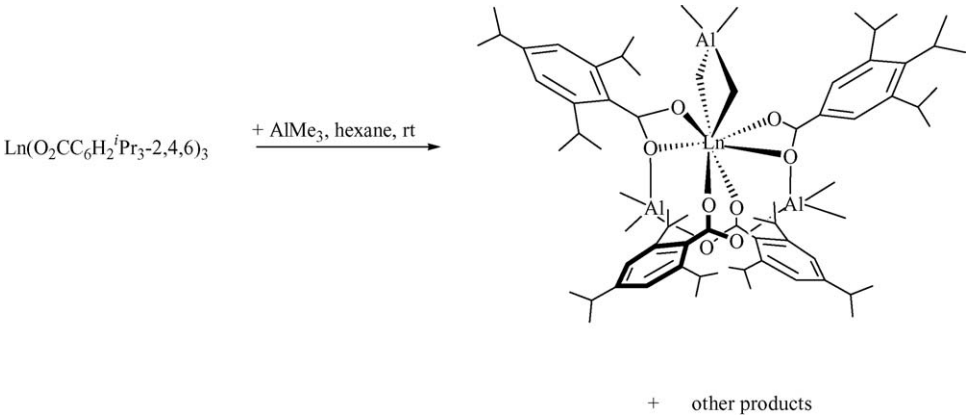

Scheme 64.

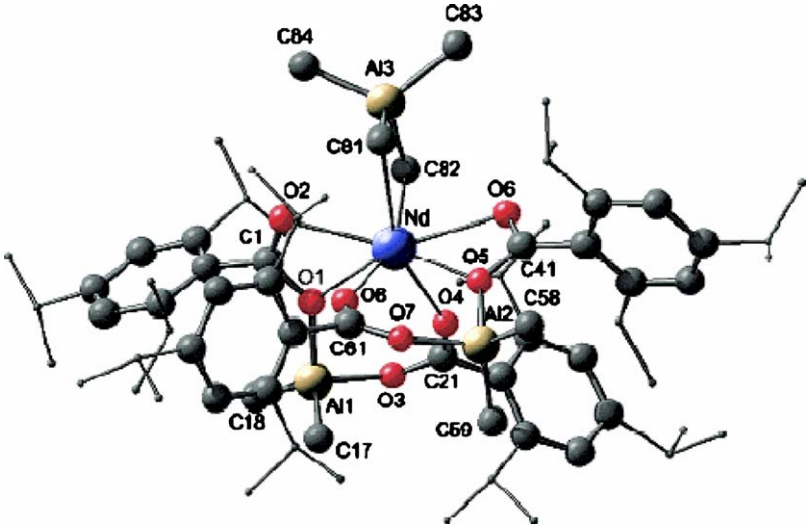

Fig. 61. Molecular structure of $[AlMe_2(O_2CC_6H_2Pr^i{}_3\text{-}2,4,6)_2]_2NdAlMe_4$ [190].

Treatment of the homoleptic aryloxides $Ln(OAr)_3$ (Ar = 2, 6 − $Bu^t{}_2$-4-MeC_6H_2) with 4 equiv. of trialkylaluminum leads to the formation of the bis-trialkylaluminum adducts $(ArO)Ln[(\mu\text{-}OAr)(\mu\text{-}R)AlR_2]_2$ (Ln = La, R = Me; Ln = La, Sm, R = Et), which have been structurally characterized by X-ray analyses [191]. The analogous reaction of $Sm(OAr)_3$ (Ar = 2, 6-$Pr^i{}_2$-4-MeC_6H_2) with 4 equiv. of trimethylaluminum led to formation of the bis-trimethylaluminum adduct $(ArO)Sm[(\mu\text{-}OAr)(\mu\text{-}Me)AlMe_2]_2$ (Scheme 65, Fig. 62), which exhibits very short Sm–C(bridging) distances of 2.620(5) and 2.632(5) Å. A reduced $^1J_{C-H}$ coupling constant of 106 Hz and a low ν(C–H) stretch in the solution and solid-state IR spectrum are indicative of a strong agostic Sm···H–C interaction in solution [192].

Similar treatment of the dimeric arylimido complex $[Sm(NHAr)_3]_2$ (Ar = 2, 6-$Pr^i{}_2C_6H_3$) with trimethylaluminum resulted in an unusual imido-bridged heterobimetallic samarium-aluminum complex (Scheme 66, Fig. 63) [179].

The reaction of bis(diphenylphosphinocyclopentadienyl)ytterbium(II) with tungsten hexacarbonyl in THF yielded $Yb(THF)_3(C_5H_4PPh_2)_2W(CO)_4{\cdot}0.5$ THF as red crystals,

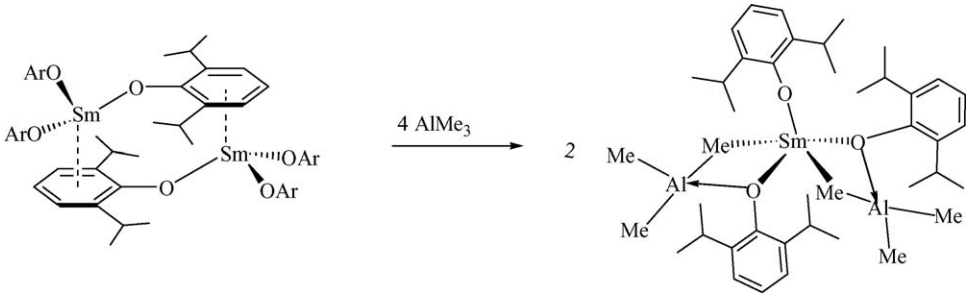

Scheme 65.

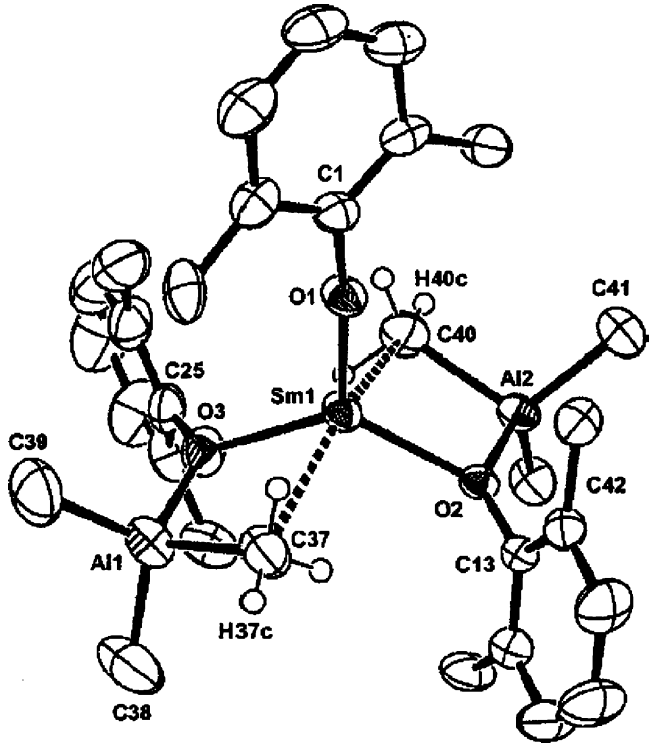

Fig. 62. Molecular structure of (ArO)Sm[(μ-OAr)(μ-Me)AlMe$_2$]$_2$ (Ar = 2, 6-Pr$^i_2$-4-MeC$_6$H$_2$) [192].

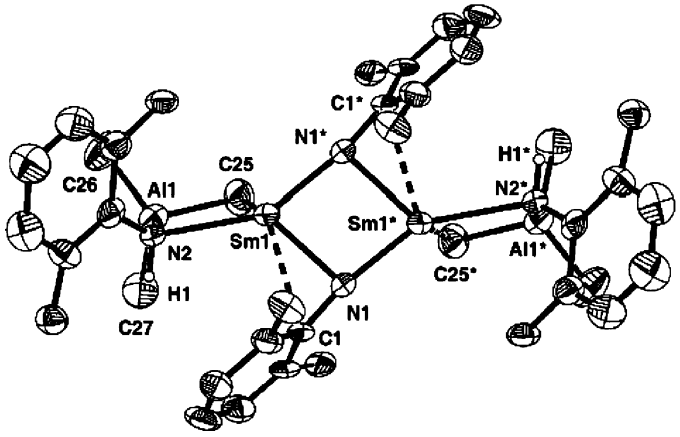

Fig. 63. Molecular structure of [(μ-NC$_6$H$_3$Pr$^i_2$-2,6)Sm(μ-NHC$_6$H$_3$Pr$^i_2$-2,6)(μ-Me)AlMe$_2$]$_2$ [179].

whereas dark red Yb(THF)(C$_5$H$_4$PPh$_2$)$_2$(μ-OC)W(CO)$_3$ was obtained when the same reaction was carried out in boiling toluene. Heating of Yb(THF)$_3$(C$_5$H$_4$PPh$_2$)$_2$W(CO)$_4$·0.5 THF also led to elimination of two THF molecules and conversion to the isocarbonyl-bridged compound [193].

2.11. Organolanthanide catalysis

Asymmetric catalysis with lanthanide complexes, including organometallic compounds, has been reviewed by Mikami et al. [25]. A review on asymmetric catalysis and amplification with chiral lanthanide complexes has been published by Inanaga et al. [12]. Organo-rare-earth-metal initiated living polymerizations of polar and nonpolar monomers have been highlighted by Yasuda [23]. An account on synthesis, structural characterization and catalytic behavior of one-carbon bridged fluorenyl cyclopentadienyl lanthanocene complexes with C_s- and C_1-symmetry has been published by Qian et al. [21]. Molander et al. reviewed the use of lanthanocene catalysts in selective organic synthesis [17]. Okuda reported on rare earth metal-based catalysts for the polymerization of nonpolar and polar monomers [80]. The synthesis of lanthanocene amides and their applications as single-component initiators in polymerization of polar monomers has been reviewed by Shen and Yao [194].

2.11.1. Organolanthanide-catalyzed hydrogenation reactions

A DFT study of H–H activation by Cp$_2$LnH d_0 complexes has been published [195].

2.11.2. Organolanthanide-catalyzed oligomerization reactions

Oligoethylenes with M_n up to 2500 and narrow molecular weight distributions have been prepared using in situ combinations between a chloroneodymocene precursor such as Cp*$_2$Nd(μ-Cl)$_2$Li(OEt$_2$)$_2$ and a dialkylmagnesium reagent [196]. Organolanthanide complexes such as (MeC$_5$H$_4$)$_3$Yb, (MeC$_5$H$_4$)$_2$YbOR and (MeC$_5$H$_4$)$_2$SmSPh have been found to serve as efficient catalyst precursors for the Aldol–Tishchenko reaction of butanal to give 2-ethyl-1,3-hexanediol monobutyrate in good to high yields under mild conditions. The yields are influenced by the structure of the organolanthanide complexes and the reaction conditions. The yield of trimerization of butanal can reach 85% under certain conditions [197]. Silyl-substituted *ansa*-neodymocenes have been utilized as catalysts

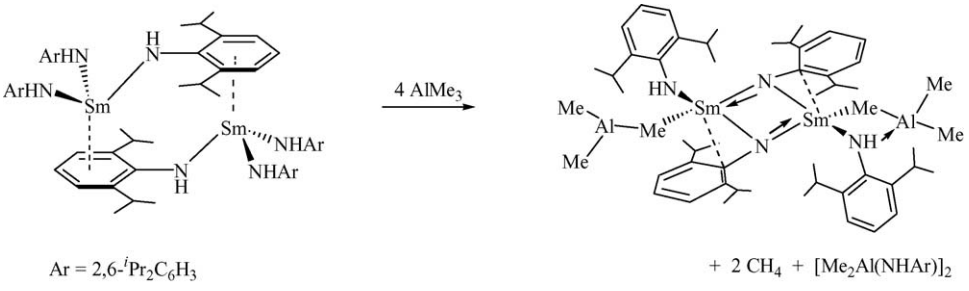

Scheme 66.

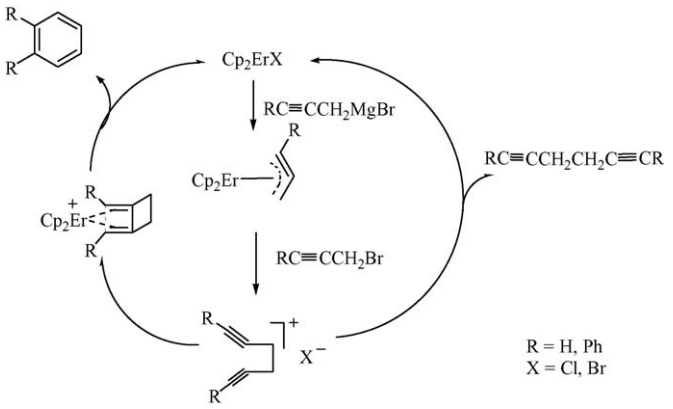

Scheme 67.

for the oligomerization of ethylene (M_n = 400–5000) and 1-octene (M_n = 400–1300) [148].

2.11.3. Organolanthanide-catalyzed cyclization reactions

In the presence of Cp_2LnX–$HgCl_2$, the treatment of RC≡CCH_2Br with Mg leads to the formation of benzene derivatives $C_6H_4R_2$-1,2 (R = H, Ph) in moderate yield. This reaction provides a new method for the construction of the benzene ring skeleton. A plausible reaction pathway is given in Scheme 67 [198].

Samarium(II) complexes or samarium(II) complexes/*n*-hexylamine systems were found to be efficient catalysts for cyclotrimerization of arylnitriles. A variety of nitriles can be converted into the corresponding substituted *s*-triazines under mild conditions in good to high yields by using samarium(II) complexes/*n*-hexylamine as catalysts. The same reaction catalyzed by samarium(II) complexes alone gives *s*-triazines in moderate yields. Among the Sm(II) catalysts employed were SmI_2 (Scheme 68) and $(MeC_5H_4)_2Sm$ [199].

2.11.4. Organolanthanide-catalyzed polymerization reactions

2.11.4.1. Review. Organolanthanides of several classes were examined by Bochkarev et al. as potential styrene and propene polymerization catalysts [200].

2.11.4.2. Monoolefins (ethylene, propene, styrene, etc.). A detailed study addressed the question why propene is not polymerized by $[Cp^*_2Y(\mu\text{-}H)]_2$. Yttrium alkyl complexes of the type Cp^*_2YR react with C–H bonds of alkenes to form wither yttrium allyl complexes or yttrium vinyl complexes. Less substituted alkenes react faster, consistent with prior alkene coordination. The selectivity of the reaction of Cp^*_2R with C–H bonds is allylic $CH_3 \gg$ vinyl C–H ≫ allylic CH_2. Propene is readily metalated by Cp^*_2YR giving the η^3-allyl

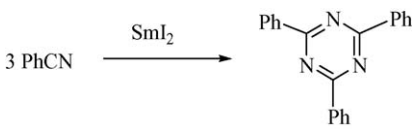

Scheme 68.

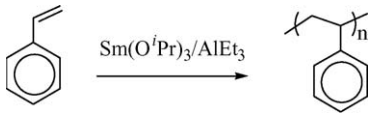

Scheme 69.

complex $Cp^*_2Y(\eta^3\text{-}CH_2CHCH_2)$ which does not react further with propene. This explains why Cp^*_2YR (R = H, alkyl) complexes make poor propene polymerization catalysts [201]. The same problem has also been computationally investigated using approximate density functional theory [202]. Molecular modeling has been utilized to study the regioselectivity in the propene polymerization with *ansa*-metallocenes of scandium and yttrium [203].

Mono(cyclopentadienyl)lanthanide compounds of the type $CpLn(O_3SCF_3)(PzA)_2$ (Ln = Nd, Sm, Eu, Tb; PzA = pyrazinamide) have been found to be active in ethylene polymerization when MAO was used as cocatalyst producing low crystalline polyethylene [204,205]. Other organolanthanide complexes which have been shown to exhibit catalytic activity in ethylene polymerization are $CpLnBr_2(PzA)_2$ (Ln = La, Nd, Sm; PzA = pyrazinamide) [206].

The guanidinate lanthanide methyl complexes $[(Me_3Si)_2NC(NPr^i)_2]_2Ln(\mu\text{-}Me)_2Li(TMEDA)$ (Ln = Nd, Yb) as well as β-diketiminato complexes of Yb(II) have been established as effective single-component initiators for styrene polymerization [207]. The catalytic activity in the polymerization of styrene has been examined using commercially available simple rare earth metal compounds such as $Sm(OPr^i)_3$, $Sm(acac)_3$, $Sm(O_2CMe)_3$, $SmI_2(THF)_2$ or $SmCl_3$ coupled with Et_3Al or methylalumoxane (MAO). Among these compounds, the $Sm(OPr^i)_3/AlEt_3$ system showed the highest catalytic activity, especially in the presence of minor amounts of toluene at 60 °C (Scheme 69) [208].

The catalytic activity of Cp^*/ER-ligated Sm(II) complexes (ER = OAr, SAr) for the one-step block copolymerization of ethylene with styrene has been reported. This is the first example of block-copolymerization of two different simple olefin monomers in a mixture. The catalytically active Cp^*/ER-ligated Sm(II) complexes were easily obtained by reactions of $Cp^*_2Sm(THF)_2$ with 1 equiv. of KER (ER = $OC_6H_3Pr^i_2$-2,6, $OC_6H_2Bu^t_2$-2,6-Me-4, $SC_6H_2Pr^i_3$-2,4,6) in THF yielded in 85–90% (Scheme 70) [209].

2.11.4.3. Dienes (butadiene, isoprene, etc.). Various mono-, di- and triallyl neodymium complexes in combination with trialkylamuminums have been investigated as highly active single-site catalysts for the 1,4-*cis*-polymerization of butadiene [210]. The unsolvated $Nd(\eta^3\text{-}C_3H_5)_3$ catalyzes the 1,4-*trans*-polymerization of butadiene in toluene at 50 °C with a selectivity of 80–85% [211]. In the presence of $AlMe_2Cl$, heterobimetallic complexes of the composition $LnAl_3Me_8(O_2CC_6H_2Pr^i_3\text{-}2,4,6)_4$ transform isoprene to a high-*cis* polymer (>99%) [190]. The bis(allyl)-*ansa*-lanthanide complexes $(Me_2CC_5H_4)_2Ln(allyl)_2Li(DME)$ (Ln = Sm, Nd) have been found to be efficient initiators which not only polymer-

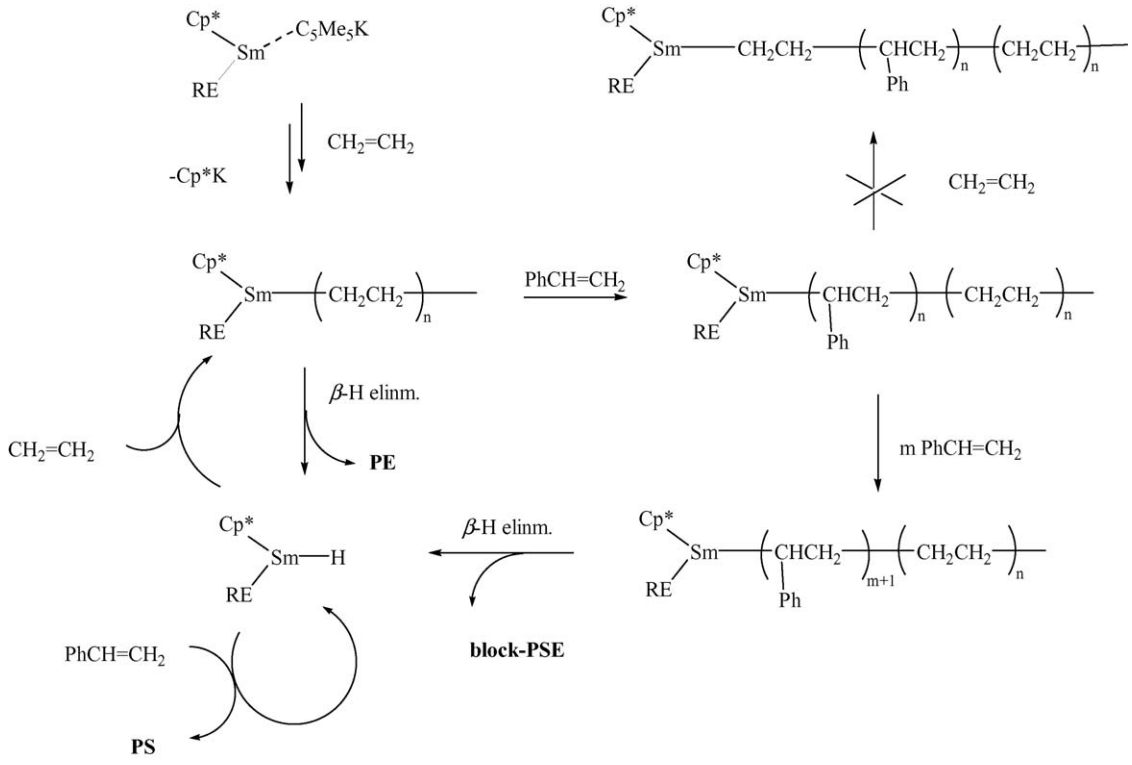

Scheme 70.

ize 1,3-dienes, but also copolymerize dienes and long-chain α-olefins or α,ω-dienes to give functionalizable polymers. They also polymerize caprolactone and allow the controlled diblock copolymerization of isoprene or isoprene/α-olefin copolymer and caprolactone [146,212–214].

Catalytic systems containing an *ansa*-bis(cyclopentadienyl) lanthanide core and lithium and/or magnesium salts have been obtained by reaction of the chloride precursors with allyllithium. These allyl complexes lead to the same active species which polymerizes 1,3-dienes, copolymerizes 1,3-dienes and α-olefines or α,ω-dienes or allows the controlled diblock polyisoprene/polycaprolactone copolymerization [215]. Ethylene and butadiene are copolymerized with neodymocene catalysts. The microstructure of the resulting ethylene/butadiene copolymers has been investigated by ^{1}H and ^{13}C NMR [216]. Random-and block-copolymerization of 1,3-butadiene with styrene has been achieved with the stereospecific system $Cp^*_2Sm(\mu\text{-}Me)_2AlMe_2/AlBu^i_3/[Ph_3C][C(C_6F_5)_4]$. Such random-copolymers of butadiene and styrene are utilized commercially as styrene–butadiene rubbers (SBR) [217]. Addition of appropriate co-catalysts such as MMAO (=modified methylaluminoxane) or $AlR_3/[Ph_3C][B(C_6F_5)_4]$ to the samarocene complexes $Cp^*_2Sm(THF)_2$ or $Cp^*_2Sm(\mu\text{-}Me)_2AlMe_2$ also afforded catalytic systems for stereospecific 1,4-*cis* living polymerization of butadiene and copolymerization of butadiene with styrene [209].

2.11.4.4. Cyclic esters and amides (ε-caprolactone, δ-valerolactone, etc.). The substituted indenyl ytterbium(II) complex $(C_9H_6C_5H_9)_2Yb(THF)_2$ shows high activity to ring-opening polymerization of lactones [118]. Scandium dialkyl complexes containing bulky iminophenolato ligands have been found to be efficient catalysts for the ring-opening polymerization of ε-caprolactone [47]. The ring opening polymerization of cyclic esters (ε-caprolactone and L-lactide) and the cyclic carbonate 1,3-dioxan-2-one (TMC) is initiated by Cp_3Ln complexes (Ln = Ce, Pr, Sm, Gd, Er). The size of the metal ion has an effect on the catalytic activity. Polycarbonate (poly-TMC) was obtained without CO_2 elimination using $LnCp_3$ as initiator [218]. Other complexes which have been found to exhibit high catalytic activity in the ring-opening polymerization of ε-caprolactone include $Cp_3Dy_2(NPPh_3)_3$ [219].

2.11.4.5. Acrylic monomers (methylmethacrylate (MMA), acrylonitrile, etc.). A half-metallocene-type complex, $Cp^*La[CH(SiMe_3)_2]_2(THF)$, showed a dual function of performing the controlled polymerizations of non-polar monomers such as ethylene and styrene as well as polar monomers like methylmethacrylate (MMA), hexylisocyanate, and acrylonitrile in high yields (Scheme 71) [220].

$Cp^*_2SmMe(THF)$ and $Cp^*_2YMe(THF)$ were used as catalysts for living polymerizations and copolymerizations of alkyl acrylates and alkyl methacrylates. $Cp^*_2SmMe(THF)$ also initiated the random living copolymerization of methylacrylate with *n*-butyl acrylate and block-copolymerization of alkyl acrylates with methyl methacrylate to give triblock-copolymers of methylmethacrylate/*n*-butyl acrylate/methylmethacrylate. The obtained copolymers exhibited good mechanical properties. Catalyzed by $Cp^*_2SmMe(THF)$ block-copolymerization of alkyl acrylate with ε-caprolactone yielded unimodal block-copolymers, which contain mainly caprolactone [221].

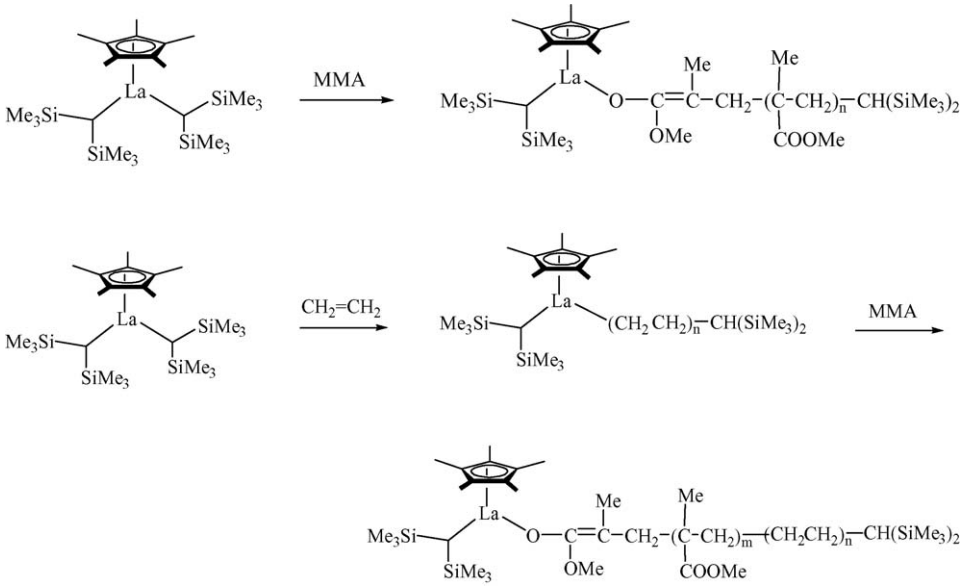

Scheme 71.

In association with $AlBu^t_3$, the complexes $(C_5H_4CH_2CH_2CH{=}CH_2)_2LnCl(THF)_2$ [87] as well as an ethylene-bridged heterodinuclear metallocene of samarium and titanium [222] have shown high activity for the bulk polymerization of MMA. No co-catalyst is required, when allyl-functionalized lanthanocenes containing the 2-propenylcyclopentadienyl ligand are used [223]. Catalytic activity for MMA polymerization has also been reported for the neodymium complex $[(C_5H_4Bu^t)_2Nd(\mu\text{-}Me)]_2$ [224]. The *ansa*-fluorenyl-cyclopentadienyl complex $[Ph_2C(Flu)(Cp)]LuN(SiMe_3)_2$ has been found to catalyze the polymerization of MMA and lactones [158].

Lanthanidocene amide complexes have been established as single-component initiators for the polymerization of (dimethylamino)ethyl methacrylate (DMAEMA), which is one of the most useful nitrogen-functionalized methacrylates [225]. Other complexes which have been found to exhibit high catalytic activity in the polymerization of MMA include $(C_9H_6)_2Y(\mu\text{-}Et)_2AlEt_2$ and $(C_9H_6)_2LnNPr^i_2$ (Ln = Y, Yb) [226], the samarocene derivatives $Cp^*_2SmMe(THF)$ supported on MCM-41 [227], the *ansa*-neodymocene amide $[Me_2Si(Flu)(C_5H_4)]Nd(NPr^i_2)(THF)_n$ [228], 1,1′-(3-oxapentamethylene)-bridged bis(indenyl) ansa-lanthanidocenes [155], and carbene complexes derived from permethylsamarocene and permethylytterbocene [137].

Several 1-cyclopentylindenyl lanthanide(II) complexes have been found to be active for the polymerization of acrylonitrile [152,229–231]. In the case of $(C_5H_4Bu^t)_2Sm(THF)_2$ the catalytic activity can be greatly increased by adding certain sodium phenoxide derivatives [229]. The catalytic activity of $[(C_5H_4Bu^t)_2Nd](\mu\text{-}Me)_2$ was found to be greatly increased by adding quaternary ammonium salts or sodium phenoxides [232]. The heterobimetallic bis(indenyl) complexes $(C_9H_6)_2Y(\mu\text{-}Et)_2AlEt_2$ and $(C_9H_6)_2LnNPr^i_2$ (Ln = Y, Yb) have been used as single-component catalysts for the polymerization of acrylonitrile. These complexes can produce polyacrylonitrile (PAN) with molecular weights from 10,000 to 30,000 [233,234].

2.11.5. Organolanthanide-catalyzed hydroboration reactions

1,5- and 1,6-Dienes undergo a cyclization/hydroboration reaction in the presence of a catalytic amount of $Cp^*_2Sm(THF)$. The resulting organoboranes can be oxidized to the corresponding primary cyclic alcohols using standard conditions (Scheme 72) [235].

2.11.6. Organolanthanide-catalyzed hydrosilylation reactions

A theoretical study of SiH_4 activation by Cp_2LnH complexes for the entire series of lanthanides has been carried out at the DFT-B3PW91 level of theory. The reaction paths corresponding to H/H exchange and silylation, formation of $Cp_2Ln(SiH_3)$, have been computed. They both occur via a single-step σ-bond metathesis mechanism. Both pathways are thermally accessible. The H/H exchange path was calculated to be kinetically more favorable, whereas the silylation reaction is thermodynamically preferred. The reactivity of this family of lanthanide complexes with SiH_4 contrasts strongly with that obtained previously with CH_4. The considerably lower activation barrier for silylation relative to methylation was attributed to the ability of Si to become hypervalent [236].

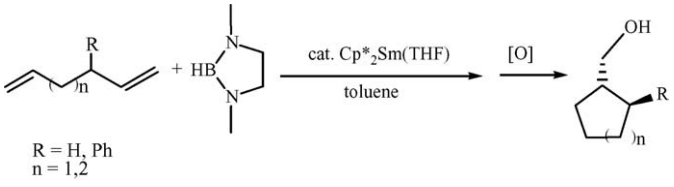

Scheme 72.

Dimeric lanthanide (Tb, Yb, Lu) and yttrium hydrides, $[(C_5H_4Bu^t)_2Ln(\mu\text{-}H)]_2$ and hydrocarbyls $[(C_5H_4Bu^t)_2Ln(\mu\text{-}Me)]_2$, as well as compounds with different bridging $(C_5H_4Bu^t)_2Ln(\mu\text{-}H)(\mu\text{-}Me)Ln(C_5H_4Bu^t)_2$ are efficient and selective catalysts of 1-octene hydrosilylation. Binuclear complexes with $Ln(\mu\text{-}H)_2Ln$ and $Ln(\mu\text{-}H)(\mu\text{-alkyl})Ln$ bridging fragments were found to be the key intermediates in 1-octene hydrosilylation catalyzed by both the hydrides and the mixed compounds in benzene at 75 °C. Therefore, in this case, the dissociation of the starting dimeric organolanthanide into monomeric species is not required for the catalytic reaction to proceed [237].

The organolanthanide metallocene-catalyzed hydrosilylation of alkynylsilanes has been found to provide (*Z*)-1,1-bis(silyl)alkenes. In particular, $Cp^*_2YMe(THF)$, $[(C_5H_4SiMe_3)_2Y(\mu\text{-}Me)]_2$, and $[(C_5H_4SiMe_3)_2Lu(\mu\text{-}Me)]_2$ were shown to be regioselective for the hydrosilylation of various alkynylsilanes. The process was evaluated for diverse substitution patterns and functional groups on the pendant alkyl chain. Silyl ethers and halogens are stable to the catalytic process, affording excellent chemo- and regioselectivities. Competition between "aryl-directed" and "silyl-directed" processes was observed upon hydrosilylation of (phenylethynyl)dimethylsilane [238].

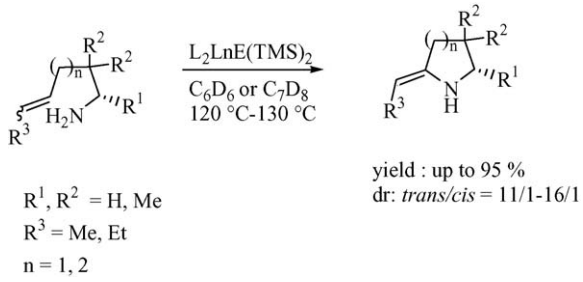

Scheme 73.

2.11.7. Organolanthanide-catalyzed hydroamination reactions

In another contribution the organolanthanide-catalyzed intramolecular hydroamination/cyclization of amines tethered to 1,2-disubstituted alkenes to afford the corresponding mono- and disubstituted pyrrolidines and piperidines (Scheme 73) by using coordinatively unsaturated complexes of the type $Cp^*_2LnCH(SiMe_3)_2$ (Ln = La, Sm), $[Me_2Si(C_5Me_4)_2]NdCH(SiMe_3)_2$, $[Et_2Si(C_5Me_4)(C_5H_4)]NdCH(SiMe_3)_2$, and $[Me_2Si(C_5Me_4)(Bu^tN)]LnE(SiMe_3)_2$ (Ln = Y, Sm, Yb, Lu; E = N, CH) as precatalysts has been reported [239].

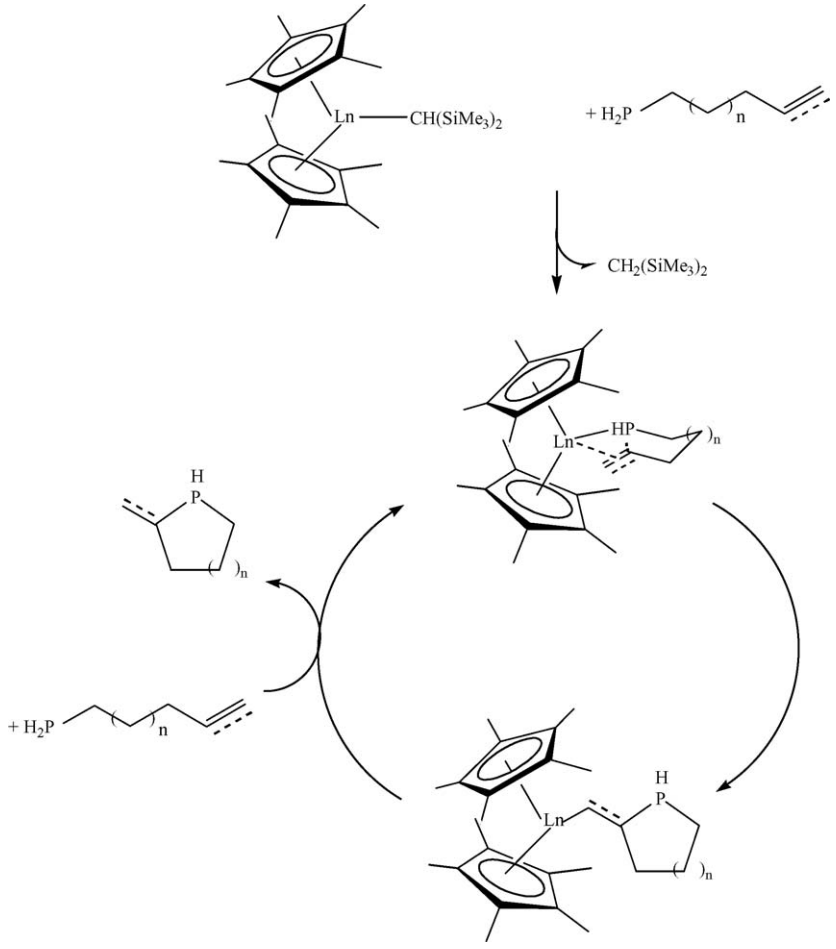

Scheme 74.

The catalytic intramolecular hydrophosphination/cyclization of phosphinoalkenes and phosphinalkynes using organolanthanide precatalysts of the type $Cp^*_2LnCH(SiMe_3)_2$ (Ln = Y, La, Sm, Lu) and $[Me_2Si(C_5Me_4)(NBu^t)]SmN(SiMe_3)_2$ has been studied in detail (Scheme 74) [240].

More recently new chiral C^1-symmetric organolanthanide catalysts of the type $[Me_2Si(OHF)(CpR^*)]LnN(SiMe_3)_2$ (OHF = η^5-octahydrofluorenyl; CpR^* = (−)-menthyl-C_5H_3; Ln = Y, Sm, Lu) have been synthesized, characterized, and implemented in the enantioselective and diastereoselective cyclizations of aminoalkenes and phosphinoalkenes [241].

2.11.8. Other organolanthanide-catalyzed reactions

The monomeric lanthanocene Schiff base complexes $Cp_2Ln(OC_{14}H_{13}NO)$ (Ln = Sm, Er, Dy, Y) in the presence of NaH have been found to catalyze the isomerization of 1,5-hexadiene. The isomerization results in a mixture of 1,4-hexadiene, 2,4-hexadiene, 1,3-hexadiene, methylenecyclopentane, and methylcyclopentane. The ratio of linear to cyclic product depends upon the amount of catalyst used [105].

The lutetium hydride complex $[Cp^*_2Lu(\mu\text{-}H)]_2$ efficiently cleaves the Si–C bond of $PhSiH_3$ to produce benzene and cross-linked polysilanes $(SiH_x)_y$ (Scheme 75) [140]. Formation of Ph_2SiH_2 and SiH_4 has also been observed during the samarium-catalyzed redistribution of $PhSiH_3$ [130].

The Si–C bond cleavage appears to proceed via the lutetium phenyl complex Cp^*_2LuPh. This is supported by the reaction of $PhSiH_3$ with Cp^*_2LuPh, which results in the formation of benzene. A plausible reaction pathway is outlined in Scheme 76 [140]. *N*-(1-Allyl-3-butenyl)-*N*-arylamines have been prepared for the first time in good yields via the direct diallylation reaction of formanilides with an organosamarium reagent under mild conditions.

The Friedel–Crafts acylation of anisole with acetic anhydride using ytterbium(III) tris[tris(nonafluorobutanesulfonyl) methide] has been studied with respect to catalyst loading. A strong inhibitory effect due to the product became apparent from doping experiments and from examination of the kinetic data. This understanding allowed catalyst loadings to be reduced to as little as 0.1 mol% for effective acylation under a suitable temperature and pressure regime [242].

2.12. Organolanthanides in organic synthesis

A comprehensive review on lanthanocene catalysts in selective organic synthesis has been published by Molander and Romero [17]. Petrov et al. have reviewed organolanthanides RLnX (R is alkyl, aryl, X is halogen) and lanthanide compounds with aromatic hydrocarbon dianions: synthesis, structure, and reactivity [19].

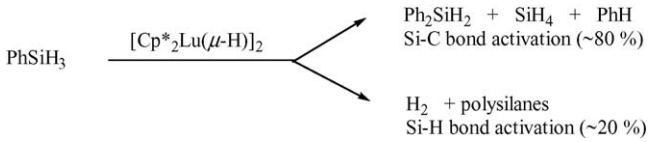

Scheme 75.

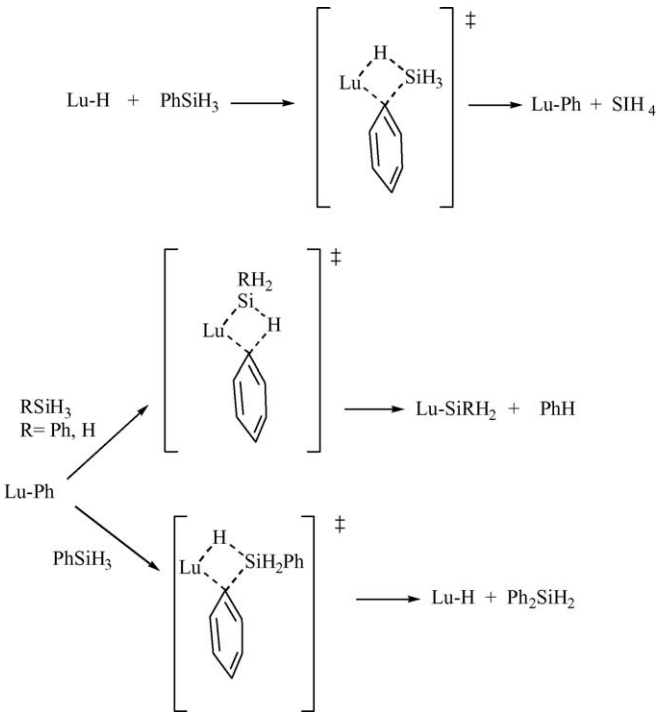

Scheme 76.

N-(1-Allyl-3-butenyl)-*N*-arylamines were prepared for the first time in good yields via the direct diallylation reaction of formanilides with an organosamarium reagent under mild conditions [243].

A THF ring can be opened by in situ generated (acyloxy)phosphonium bromide using allylsamarium bromide as catalyst to afford 4-bromobutyl esters under mild conditions in good to excellent yields [244]. Direct geminal diallylation of ketones, lactams and acyclic amides containing an N–H bond has been achieved in the presence of allylsamarium bromide (Scheme 77). By applying this method, quaternary carbons have been constructed, and 2,2-diallylated cyclic ethers, 2,2-diallylated nitrogen heterocycles, and diallylated amides were synthesized in moderate to good yields under mild conditions [245].

The substitution reaction between gem-diacetates and allylsamarium bromide has also been investigated. Homoallylic

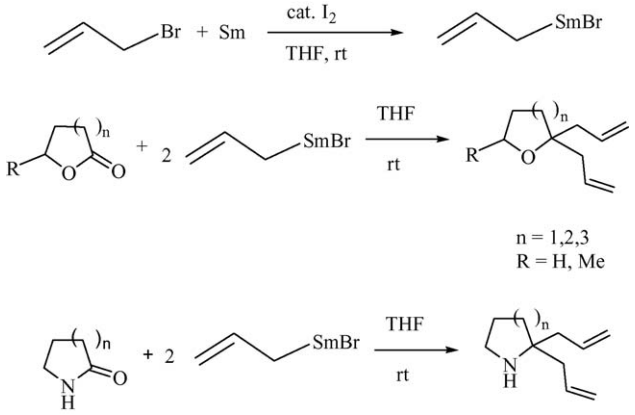

Scheme 77.

Scheme 78.

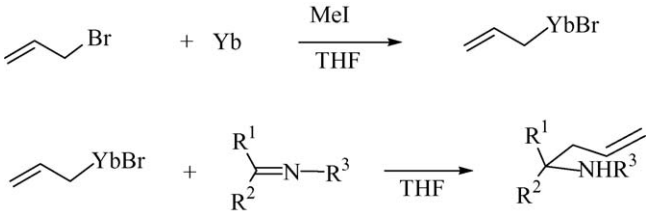

Scheme 79.

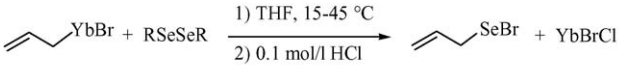

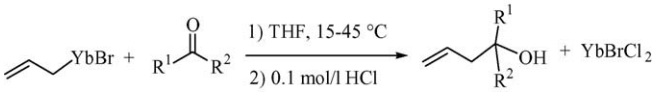

Scheme 80.

alcohol acetates were obtained in moderate to good yields (Scheme 78) [246].

In the presence of methyl iodide, metallic ytterbium can easily react with allylbromide in anhydrous THF to form allylytterbium bromide, which reacts readily with imines to give the corresponding bromoallylamines in satisfactory yields under mild and neutral conditions (Scheme 79) [247].

Allylytterbium bromide has also been reported to react with diselenides, aldehydes, and ketones to afford allylselenides and homoallylic alcohols, respectively, in good yields under neutral and mild conditions (Scheme 80) [248].

Reactions of a vinylcerium species, $Cl_2CeC(=CH_2)Me$, have been employed in the synthesis of vinyl-substituted 4-alkyn-1-ols. The reaction sequence shown in Scheme 81 is part of an efficient synthesis of the biologically active compound (±)-7-*epi*-β-bulnesene [249].

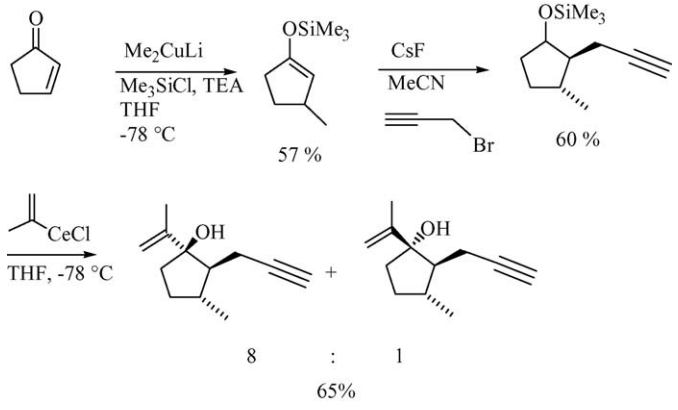

Scheme 81.

3. Actinides

3.1. Actinide carbonyls

While stable binary actinide carbonyls are still unknown, research in this area focusses mainly on the detection and theoretical investigation of unstable molecules such as the monocarbonyl complexes of thorium and uranium. The possible molecular structures UCO, UOC, and CUO of carbon monoxide interacting on a uranium metal surface have been studied by density functional theory (DFT) [250]. In a closely related study the same authors also reported the first identification of the molecules $CThO^-$, OThCCO, $OTh(\eta^3\text{-CCO})$, and $Th(CO)_n$ ($n = 1$–6). The $Th(CO)_n$ ($n = 1$–6) complexes were formed on deposition or on annealing. Relativistic density functional theory (DFT) calculations showed that CThO is an unprecedented actinide-carbene molecule with a triplet ground state and an unusual bent structure ($\angle CThO = 109°$). The CThCCO molecule has a bent structure while its rearranged product $OTh(\eta^3\text{-CCO})$ is found to have a unique exocyclic structure with a side-bonded CCO group. It was also found that both $Th(CO)_2$ and $Th(CO)_2^-$ are, surprisingly, highly bent, with the $\angle CThC$ bond angle being close to 50°. The unusual geometries are the result of extremely strong Th-to-CO back-bonding, which causes significant three-centered bonding among the Th atom and the two C atoms [251]. A comparative density functional study on metal–ligand (M–L) interaction has been performed on $X_3U(CO)$ (X = F, I) species including scalar relativistic effects by means of the zero-order regular approximation (ZORA) Hamiltonian. The role of the halogen atoms in modeling the M–L interactions has been discussed for the π-ligand CO [26].

3.2. Actinide hydrocarbyls

3.2.1. Homoleptic compounds

A theoretical investigation of structural and vibrational properties of the gas-phase molecule $U(CH_3)_3$ by density functional methodologies or with a post-Hartree–Fock MP2 perturbative approach has been published, The optimized geometries for $U(CH_3)_3$ have been compared with the experimental solid-state structural data for $U[CH(SiMe_3)_2]_3$ [252]. Similarly, organoberkelium and organocalifornium ions were produced for the first time by laser ablation of $^{249}Bk_2O_3$ and $^{249}Cf_2O_3$ dispersions in polyimide, followed by time-of-flight mass spectrometry. The primary organometallic products were: $BkCH_3^+$, AnC_2H^+, and AnC_4H^+ (An = Bk, Cf) [253]. Gas-phase reactions of the bare monopositive berkelium ion, Bk^+, with several reagents have been examined by a mass spectrometric technique adapted for the highly radioactive transuranium actinides. Organometallic products were observed with several alkenes such as ethylene, propene, 1- and 2-butene, isobutene, cyclohexene, 1,5-cyclooctadiene, cyclooctatetraene, and pentamethylcyclopentadiene. The products included π-bonded organoberkelium ions such as $BkCOT^+$, presumable the berkelium-cyclooctatetraenyl half-sandwich complex ion [254].

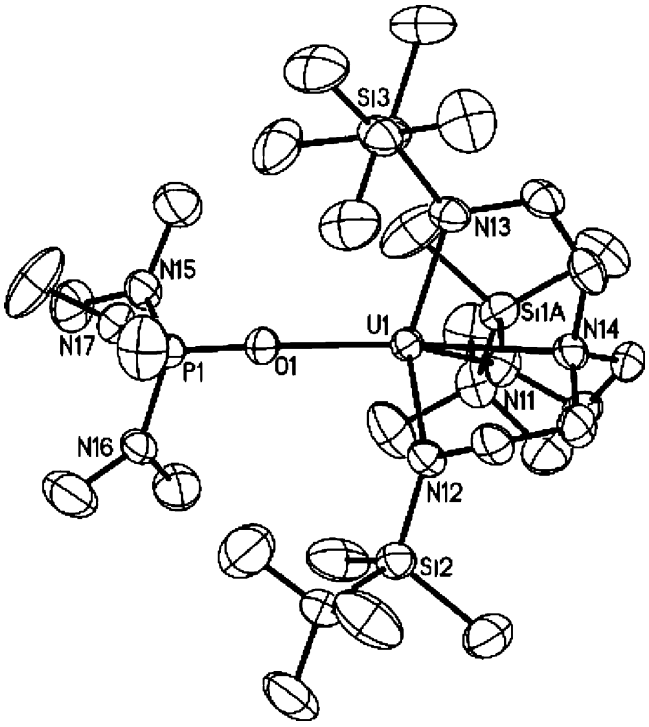

Fig. 64. Molecular structure of $U(NN'_3)$(HMPA) [255].

3.2.2. Heteroleptic compounds

Reduction of $U(NN'_3)I$ [$NN'_3 = N(CH_2CH_2NSiMe_2Bu^t)_3$] with potassium in pentane gave the purple trivalent monomer $U(NN'_3)$, this compound having previously been synthesized via fractional vacuum sublimation of mixed-valent $(\mu\text{-Cl})[U(NN'_3)]_2$. The derivative chemistry of $U(NN'_3)$ towards various reagents (pyridine, HMPA (Fig. 64), trimethylsilylazide, trimethylsilyldiazomethane, Me_3NO) has been studied in detail. While the reaction products in these cases should not be considered "real" organometallic compounds, the reaction with methylenetrimethylphosphorane led to formation of the adduct $U(NN'_3)(CH_2PMe_3)$ containing a uranium–carbon bond. Reaction of this complex with air gave a few crystals of the unusual hydroxo complex $U(NN'_3)(OH)(CH_2PMe_3)$, which was structurally characterized (Fig. 65) [255].

Treatment of $UO_2Cl_2(THF)_3$ in THF with 1 equiv. of $Na[CH(Ph_2P{=}NSiMe_3)_2]$ led to formation of an unusual red uranyl chloro-bridged dimer (70% yield) containing a uranium(VI)–carbon bond as part of a tridentate bis(iminophosphorano)methanide chelate complex (Scheme 82). This was the first example of a uranyl–methine carbon bond. The methine carbon is displaced significantly from the uranyl equatorial plane (Fig. 66) [256].

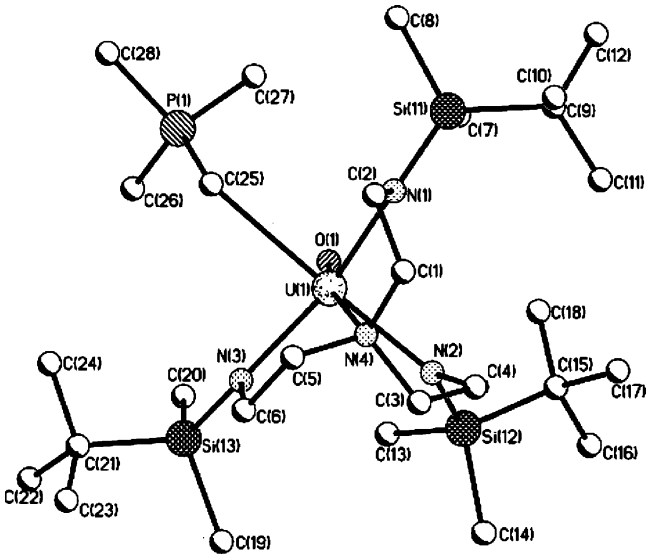

Fig. 65. Molecular structure of $U(NN'_3)(OH)(CH_2PMe_3)$ [255].

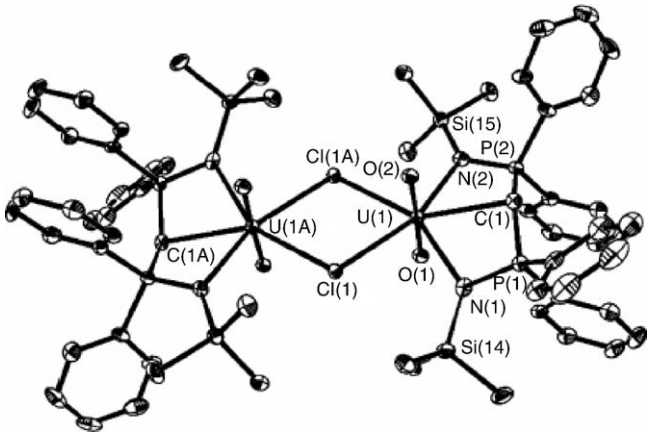

Fig. 66. Molecular structure of $[UO_2Cl\{CH(Ph_2P{=}NSiMe_3)_2\}]_2$ [256].

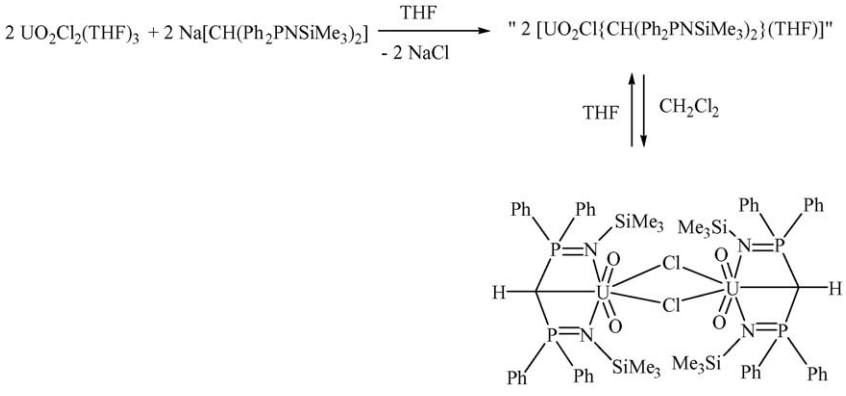

Scheme 82.

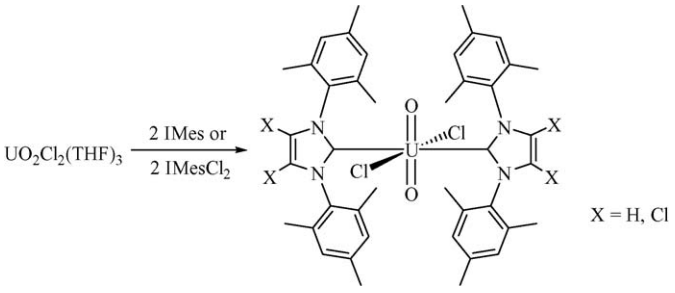

Scheme 83.

Treatment of $UO_2Cl_2(THF)_2$ in THF with 2 equiv. of 1,3-dimesitylimidazole-2-ylidene (IMes) or 1,3-dimesityl-4,5-dichloroimidazole-2-ylidene ($IMesCl_2$) as depicted in Scheme 83 afforded novel monomeric uranyl *N*-heterocyclic carbene complexes, representing the first examples of actinyl carbon bonds. The complexes were isolated in 74 and 62% yield, respectively, as pale yellow crystalline solids, which were both structurally characterized by X-ray diffraction. The uranium-carbene bond lengths are 2.626(7) and 2.609(4) Å, respectively [257].

3.3. Actinide cyclopentadienyl compounds

3.3.1. Cp_2AnX, Cp_3An and Cp_3AnL compounds

A remarkable achievement was the synthesis and characterization of tris(cyclopentadienyl)thorium(III) complexes. The homoleptic dark blue, crystalline (disubstituted-cyclopentadienyl)thorium(III) complexes $Th[C_5H_3(SiMe_2R)_2\text{-}1,3]_3$ (R = Me, Bu^t) were obtained in good yield from the appropriate tris(cyclopentadienyl)thorium(IV) chloride by treatment with an excess of Na–K alloy in toluene at 20–35 °C with sonification (Scheme 84). The complex with R = Me is also accessible by a similar reduction of Cp''_2ThCl_2 ($Cp'' = C_5H_3(SiMe_3)_2$-1,3). Fig. 67 illustrates the molecular structure of $Cp^{tt}{}_3Th$ [258].

3.3.2. $CpAnX_3$ and Cp_2AnX_2 compounds

The reaction of the uranium(IV) triflate $U(OTf)_4$ ($OTf = OSO_2CF_3$) with 2 equiv. of KCp afforded a mixture of $Cp_3U(OTf)$ and $Cp_2U(OTf)_2$ in a ratio of 73:27. Thus, pure $Cp_2U(OTf)_2$ could not be obtained by this synthetic route [259]. The synthesis and structural characterization of the first uranium cluster containing an isopolyoxometalate core has been achieved. Reduction of $(1,2,4\text{-}Bu^t{}_3C_5H_2)_2UCl_2$ with 2 equiv. of KC_8 in THF, followed by an addition of 2 equiv. of pyridine *N*-oxide was conducted in an attempt to produce the organometallic dioxo species $(1,2,4\text{-}Bu^t{}_3C_5H_2)_2UO_2$. However, the cluster compound $(1,2,4\text{-}Bu^t{}_3C_5H_2)_4U_6O_{13}(bipy)_2$ was isolated as the main product (54% yield) from this reaction. In the molecular structure, six uranium atoms are arranged in approximate octahedral symmetry, with an interstitial μ_6-oxo group situated in the center of the cluster. Twelve other oxo ligands form μ_2-O bridging interactions to uranium centers around the cluster framework to furnish the U_6O_{13} core that mimics the isopolyoxometalate Lindqvist structure [260].

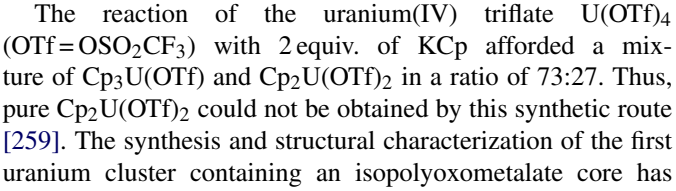

Scheme 84.

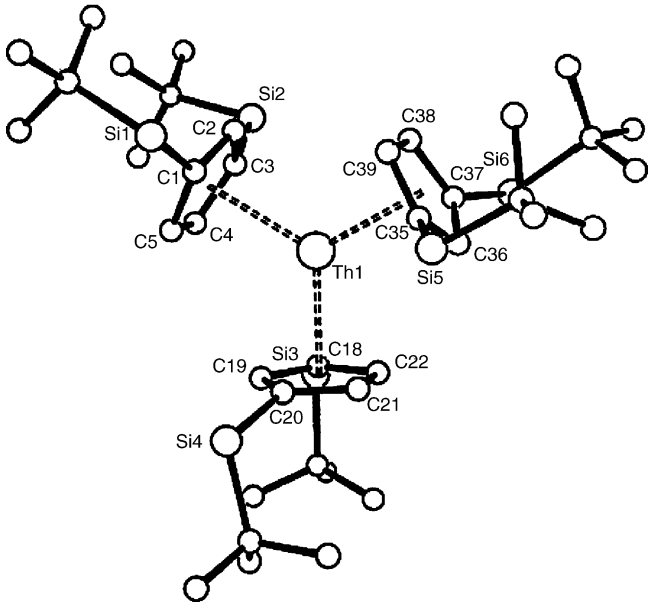

Fig. 67. Molecular structure of $Cp^{tt}{}_3Th$ (Me groups on Si atoms omitted for clarity) [258].

3.3.3. Cp_3AnX and $Cp_3AnX(L)$ compounds

$Cp_3U(OTf)$ has been prepared from $U(OTf)_4$ and KCp ($OTf = CF_3OSO_2{}^-$) [259].

3.3.4. Pentamethylcyclopentadienyl compounds

The pentamethylcyclopentadienyl ligand remains the most important ligand in organoactinide chemistry. It has been very successfully employed in the stabilization of novel organoactinide complexes and in organoactinide catalysis.

3.3.4.1. Cp^*AnX_2 and $Cp^*{}_2AnX$ compounds. Reduction of the uranium(IV) thiolates $Cp^*{}_2U(SR)_2$ (R = Me, Pr^i, Bu^t, Ph) with sodium amalgam afforded the corresponding U(III) complexes $Na[Cp^*{}_2U(SR)_2]$ or the U(IV) sulfide $Na[Cp^*{}_2U(SBu^t)(S)]$. C–S bond cleavage of a thiolate ligand was also observed during the thermal decomposition of $Na[Cp^*{}_2U(SPr^i)_2]$, whereas $Na[Cp^*{}_2U(SMe)_2]$ was transformed in refluxing THF into the thiametallacyclopropane complex $Na[Cp^*{}_2U(SMe)(SCH_2)]$, resulting from C–H bond activation of a SMe group. The X-ray crystal structures of $[Na(18\text{-crown-6})(THF)_2][Cp^*{}_2U(SPr^i)_2]$, $[Na(18\text{-crown-6})][Cp^*{}_2U(SBu^t)(S)]$, and $[Na(18\text{-crown-6})(THF)_2][Cp^*{}_2U(SMe)(SCH_2)]$ (Fig. 68) have been determined [261].

3.3.4.2. $Cp^*{}_3An$ compounds. Several new methods leading to the sterically crowded $Cp^*{}_3U$ complex have been devel-

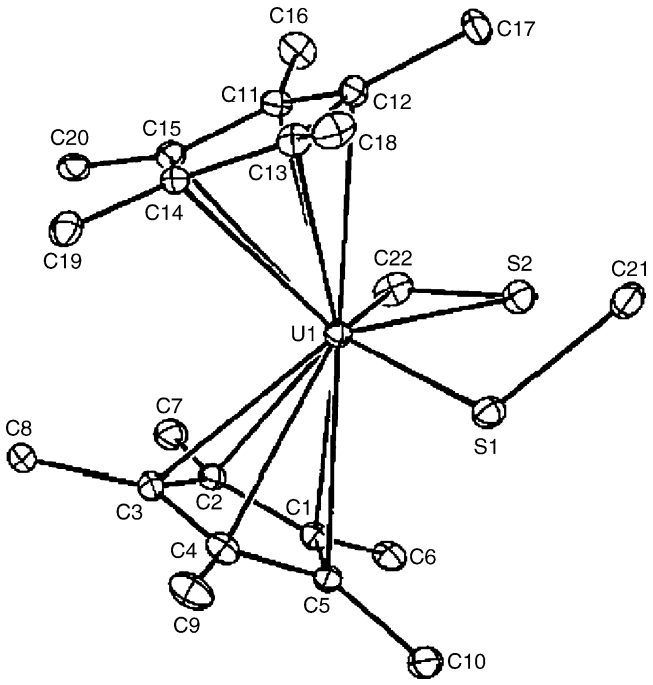

Fig. 68. Molecular structure of the $[Cp^*_2U(SMe)(SCH_2)]$ anion [261].

oped (Scheme 85). Cp^*_3U can be prepared by (a) reaction of $[Cp^*_2U(\mu\text{-}H)]_2$ with tetramethylfulvene, (b) reduction of Cp^*_2Pb with $Cp^*_2UH(dmpe)$, (c) reaction of $[Cp^*_2U(L)]^+$ (L = THF, dmpe) with K(18-crown-6)Cp^*, and (d) reaction of $[Cp^*_2U][BPh_4]$ with KCp^* [262].

3.3.4.3. Mono(pentamethylcyclopentadienyl)actinide(IV)-compounds. A high-yield one-pot synthesis of the tribenzyl complex $Cp^*U(CH_2Ph)_3$ has been developed (Scheme 86). It circumvents the isolation of Cp^*UCl_3 and employs the commercially available reagent benzylmagnesium chloride. Dark brown $Cp^*U(CH_2Ph)_3$ (Fig. 69) can be isolated in typically 80–90% yield using this synthetic route. The uranium atom interacts with the three benzyl ligands in a decidedly multihapto fashion. The reaction of $Cp^*U(CH_2Ph)_3$ with excess cyclopentadiene led to elimination of 2 equiv. of toluene and formation of $Cp^*Cp_2UCH_2Ph$ (black crystals, 89%) [263].

3.3.4.4. Bis(pentamethylcyclopentadienyl) actinide(IV)-, (V)-, and (VI)-compounds. Diphenyldiazomethane effects a two-electron oxidation of the uranium(IV) monoimido complex $Cp^*_2U{=}NC_6H_2Bu^t_3$-2,4,6 to give the uranium(VI) mixed bis(imido) complex $Cp^*_2U(=NC_6H_2Bu^t_3\text{-}2,4,6)(=N{-}N{=}CPh_2)$ (brown crystals, 97% yield), which undergoes a rare cyclometalation reaction upon mild thermolysis to afford

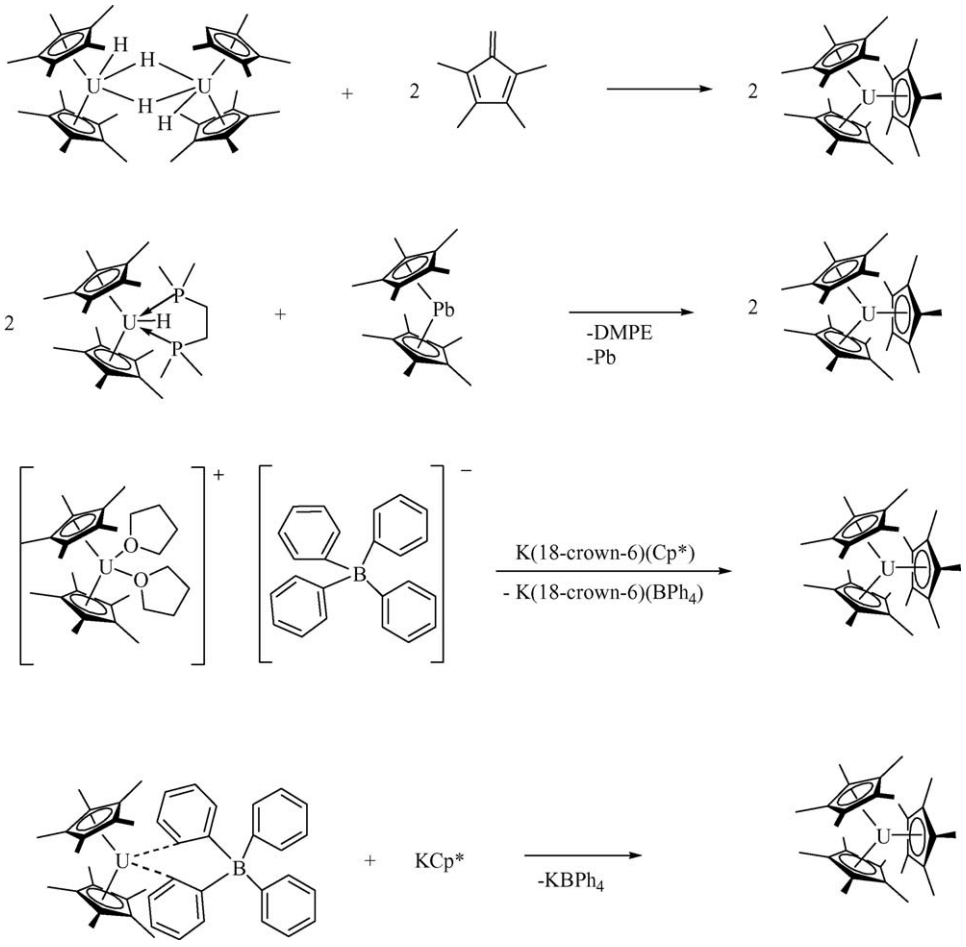

Scheme 85.

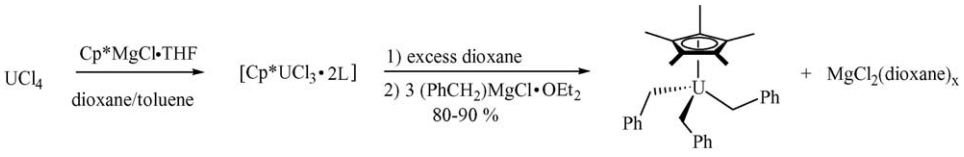

Scheme 86.

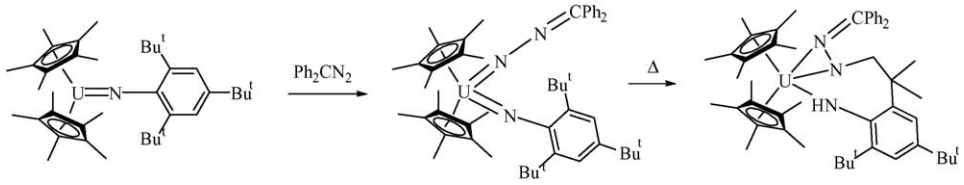

Scheme 87.

a cherry red uranium(IV) bis(amide) complex that results from net addition of a C–H bond of an *ortho-t*-butyl group across the N=U=N core (Scheme 87) [264] (Fig. 70).

The first example of a 5*f*-element ketimido complex has been prepared by the reaction sequence shown in Scheme 88. The product is surprisingly unreactive and displays unusual electronic properties. The physical properties and chemical stability of this complex suggest higher U–N bond order due to significant ligand to metal π-bonding in the uranium ketimido interactions (Fig. 71) [265].

Closely related are the sulfilimido complexes $Cp^*_2UCl(N{=}SPh_2)$ (Scheme 89) and $Cp^*_2U(N{=}SPh_2)_2$, which have been prepared in high yield from $Cp^*_2UCl_2$ and various stoichiometry amounts of $LiNSPh_2$. The same compounds can also be synthesized by treating $Cp^*_2UCl[(CH_2)_2PPh_2]$ with anhydrous $HNSPh_2$. $Cp^*_2U(N{=}SPh_2)_2$ was the first structurally characterized uranium bis(sulfilimide) complex. Its short U–N distance suggests significant uranium-imido multiple-bond character. The molecular structure of $Cp^*_2U(N{=}SPh_2)_2$ is illustrated in Fig. 72 [266].

A bis(pentamethylcyclopentadienyl)uranium triflate has been established as a new reagent for uranium metallocene chemistry. The synthesis and characterization of the first actinide hydrazonato complex, $Cp^*_2U[\eta^2\text{-}(N, N') - MeNN{=}C{=}Ph_2](OTf)$, has been made possible by the use of the organouranium(IV) trifluoromethanesulfonate (triflate)

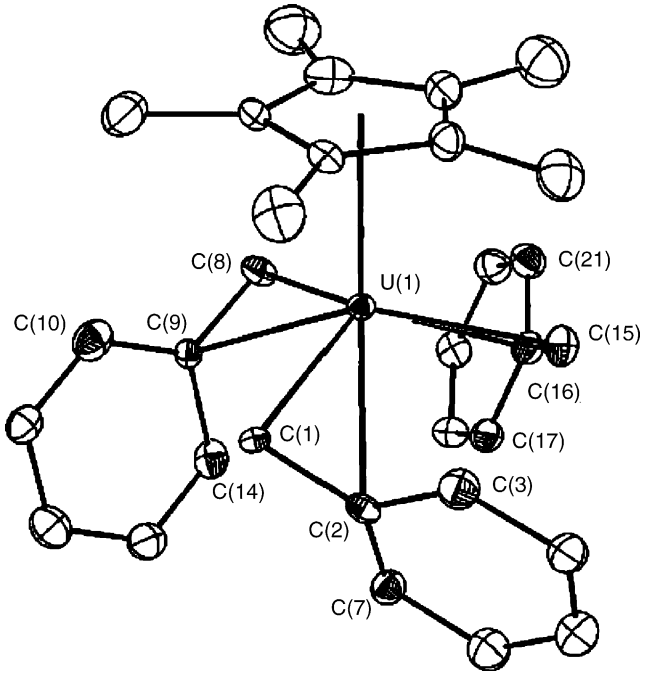

Fig. 69. Molecular structure of $Cp^*U(CH_2Ph)_3$ [163].

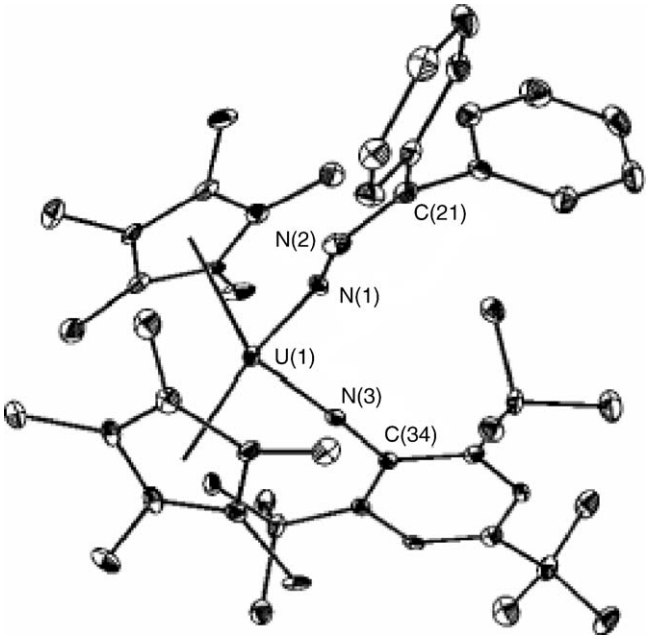

Fig. 70. Molecular structure of $Cp^*_2U(=NC_6H_2Bu^t_3\text{-}2,4,6)(=N{-}N{=}CPh_2)$ [264].

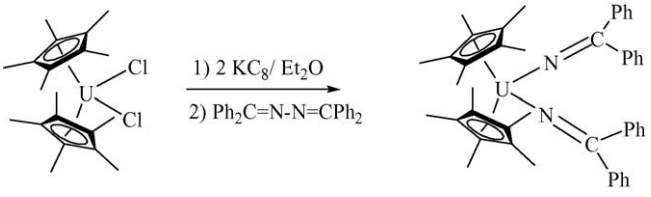

Scheme 88.

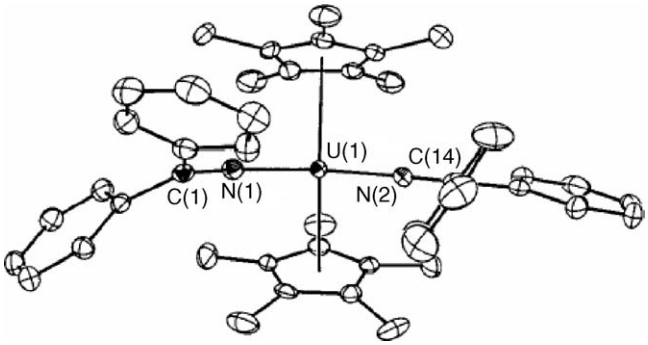

Fig. 71. Molecular structure of $Cp^*_2U(N{=}CPh_2)_2$ [265].

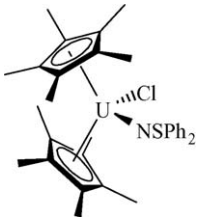

Scheme 89.

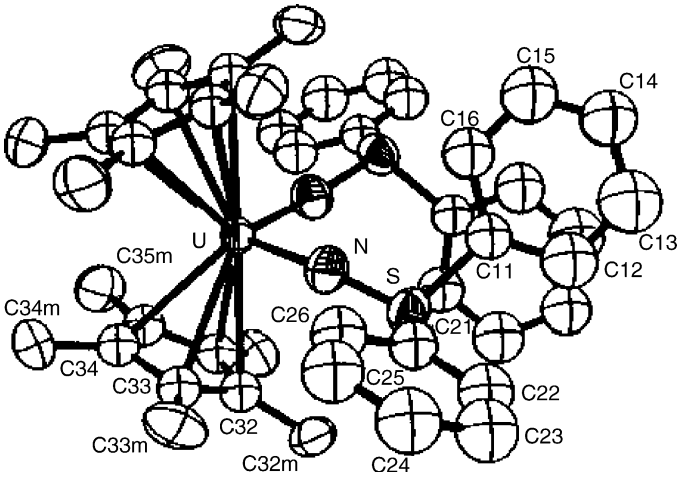

Fig. 72. Molecular structure of $Cp^*_2U(N{=}SPh_2)_2$ [266].

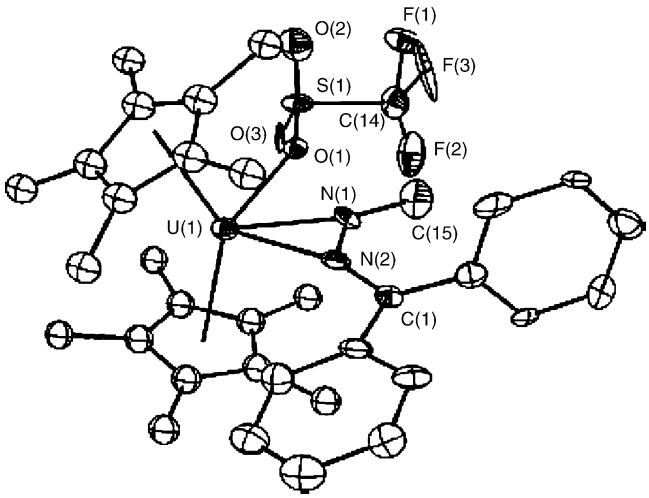

Fig. 73. Molecular structure of $Cp^*_2U[\eta^2\text{-}(N,N')\text{-}MeNN{=}C{=}Ph_2](OTf)$ [267].

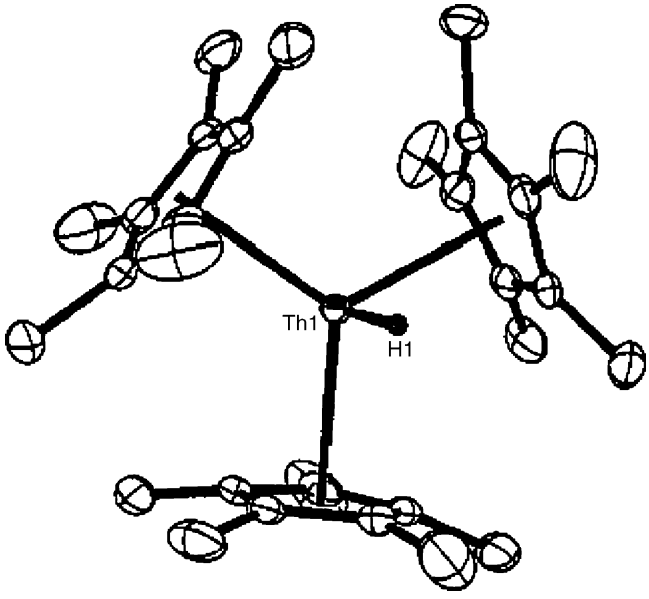

Fig. 74. Molecular structure of Cp^*_3ThH [268].

complex $[Cp^*_2UMe(OTf)]_2$ ($OTf = OSO_2CF_3$), which is derived from the reaction between $Cp^*_2UMe_2$ and Ph_3COTf (Scheme 90, Fig. 73) [267].

3.3.4.5. Tris(pentamethylcyclopentadienyl) actinide(IV)-compounds. In order to determine if tris(pentamethylcyclopentadienyl) chemistry could be extended to thorium, the reaction of a cationic organothorium hydride, $[Cp^*_4Th_2H_2(DMPE)][BPh_4]$ with 2 equiv. of K(18-crown-6)Cp^* was examined and found to produce Cp^*_3ThH as a pale yellow powder in 70% yield (Fig. 74). The precursor was obtained by protonation of $[Cp^*_2ThH(\mu-H)]_2$ with $[Et_3NH][BPh_4]$. Preliminary reactivity studies of Cp^*_3ThH showed that its chemistry is surprisingly limited [268].

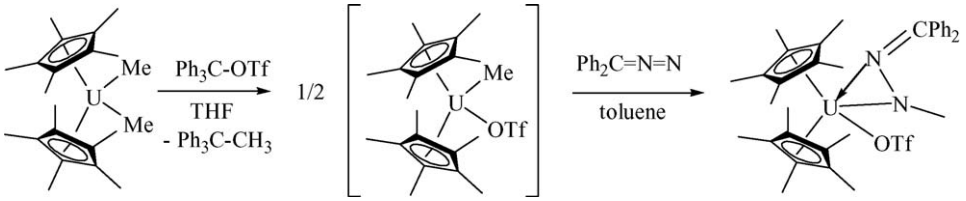

Scheme 90.

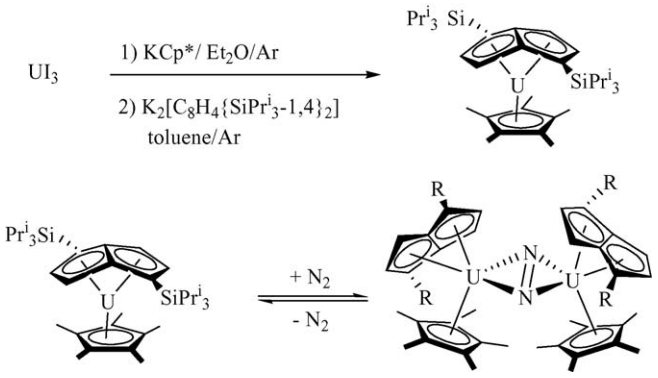

Scheme 91.

3.3.5. Indenyl and pentalenediyl compounds

Exciting uranium(III) chemistry has been developed around a silyl-substituted pentalene ligand. The reaction of UI_3 with 1 equiv. of KCp^* in diethyl ether afforded a dark green material assumed to be $[Cp^*UI_2]_n$ or an etherate thereof. This material was not isolated but reacted directly with $K_2[C_8H_4(SiPr^i_3)_2\text{-}1, 4]$ in toluene under argon to afford purple-black, crystalline $Cp^*U[\eta^8\text{-}C_8H_4(SiPr^i_3)_2\text{-}1, 4]$ in moderate yield (40%) (Scheme 91). According to an X-ray diffraction study, the compound adopts a slightly bent sandwich structure (Fig. 75). Exposure of a sample of $Cp^*U[\eta^8\text{-}C_8H_4(SiPr^i_3)_2\text{-}1, 4]$ led to formation of an N_2 complex which could be isolated as green-black, X-ray quality crystals by fractional crystallization from a pentane solution of $Cp^*U[\eta^8\text{-}C_8H_4(SiPr^i_3)_2\text{-}1, 4]$ under a 5 psi overpressure of N_2 at −20 °C. $(\mu\text{-}N_2)[Cp^*U\{\eta^8\text{-}C_8H_4(SiPr^i_3)_2\text{-}1, 4\}]_2$ has a binuclear structure, in which two units of the precursor are bridged by a sideways-bound dinitrogen unit (Fig. 76). The key structural feature of the latter is the N–N bond length of 1.232(10) Å, consistent with an N–N double bond. The complex loses dinitrogen extremely easily both in solution and the solid state [269].

A variety of thorium complexes incorporating the bulky permethylindenyl ligand ($Ind^* = C_9Me_7$) have been synthesized and characterized. Specifically, the dichloride $Ind^*{}_2ThCl_2$ was obtained by reaction of $ThCl_4$ with $LiInd^*$ in toluene

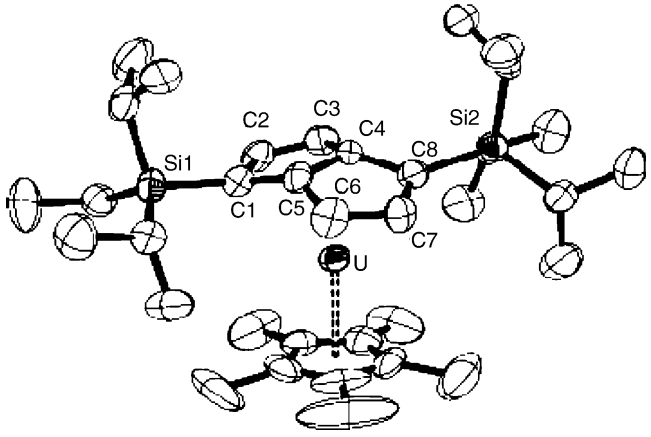

Fig. 75. Molecular structure of $Cp^*U[\eta^8\text{-}C_8H_4(SiPr^i_3)_2\text{-}1, 4]$ [269].

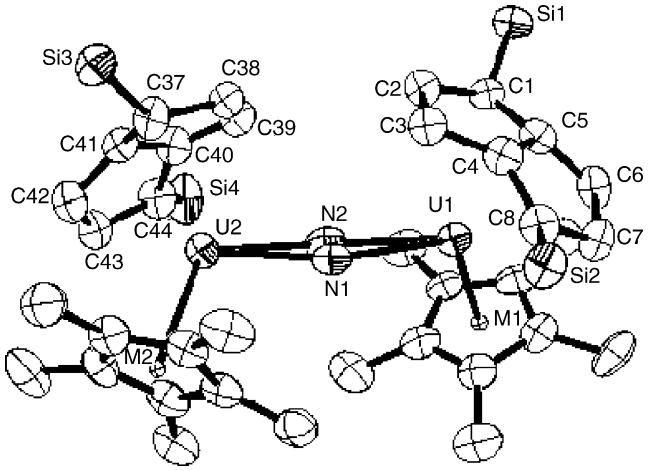

Fig. 76. Molecular structure of $(\mu\text{-}N_2)[Cp^*U\{\eta^8\text{-}C_8H_4(SiPr^i_3)_2\text{-}1, 4\}]_2$ [269].

(Scheme 92). The yellow, crystalline product was isolated in 67% yield [270].

With $Ind^*{}_2ThCl_2$ as precursor, the derivatives $Ind^*{}_2ThMe_2$, $Ind^*{}_2Th(NC_4H_4)_2$, and $Ind^*{}_2Th(BH_4)_2$ could be obtained by metathesis with MeLi, $LiNC_4H_4$, and $Ca(BH_4)_2$, respectively (Scheme 93). As a representative example, the molecular structure of the bis(tetrahydroborate) derivative is shown in Fig. 77 [270].

In the same manner, $Ind^*{}_2ThCl_2$ reacted with 2 equiv. of $LiNMe_2$ to give the regular bis(dimethylamide) $Ind^*{}_2Th(NMe_2)_2$ (Scheme 94). In contrast to simple metathesis, reaction of $Ind^*{}_2ThCl_2$ with $KN(SiMe_3)_2$ yielded the metallacycle $Ind^*{}_2Th(\eta^2\text{-}CH_2SiMe_2NSiMe_3)$ (Scheme 94). X-Ray crystal structure determination on several bis(permethylindenyl)thorium complexes indicated that the permethylindenyl ligands in these complexes exhibit a variety of conformations [270].

$Ind^*{}_2ThMe_2$ undergoes several insertion reactions. For example, it reacts rapidly with CO_2 to yield the acetate complex $Ind^*{}_2Th(\eta^2\text{-}O_2CMe)_2$ as a pale orange solid in 88% yield (Scheme 95) [270].

3.4. Actinide complexes with heteroatom five-membered ring ligands

A highly reactive uranium complex supported by the Et_8-calix-[4]-tetrapyrrole tetraanion ligand has been reported. The compound was found to effect dinitrogen cleavage, solvent

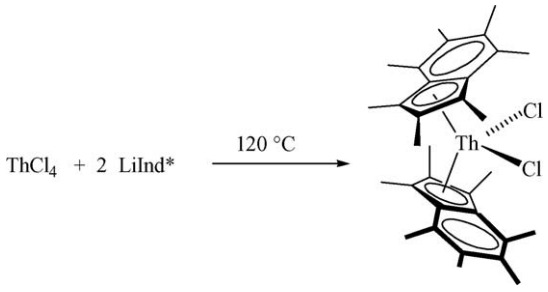

Scheme 92.

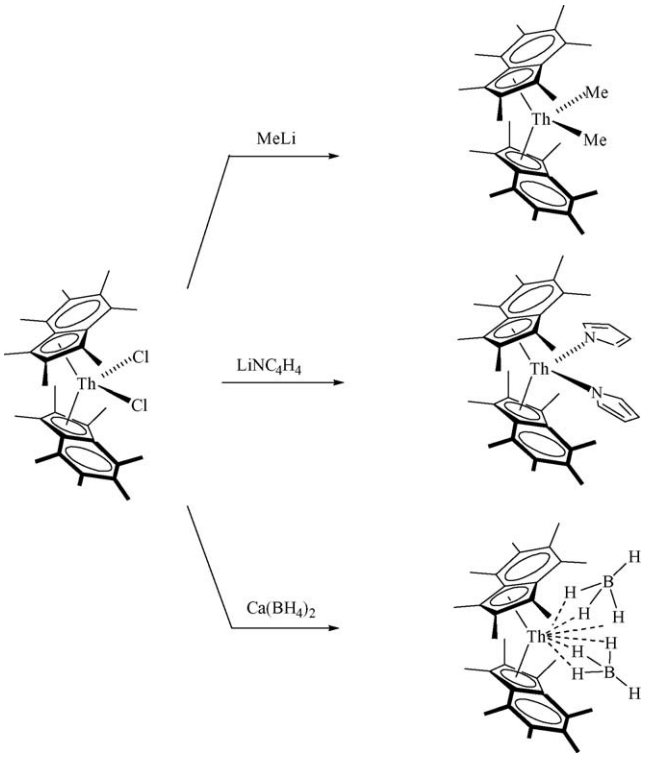

Scheme 93.

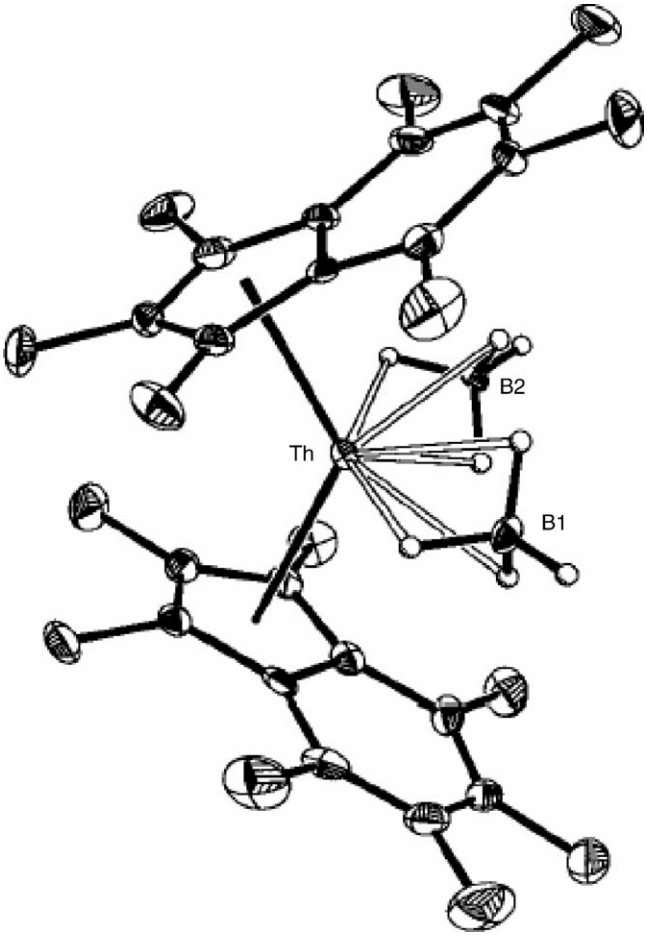

Fig. 77. Molecular structure of $Ind^*_2Th(BH_4)_2$ [270].

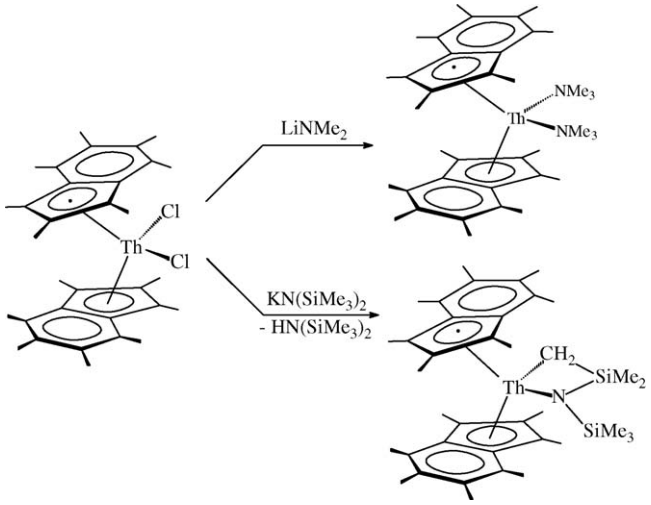

Scheme 94.

desoxygenation, and polysilanol depolymerization. These compounds are mentioned here because they involve π-bonding interactions between the pyrrole units and the uranium centers [271].

3.5. Actinide cyclooctatetraenyl complexes

The chemistry of mono(cyclooctatetraenyl)uranium complexes has been reviewed by Ephritikhine et al. [181] Gas-phase reactions of the bare monopositive berkelium ion, Bk^+, with several reagents including cyclooctatetraene have been examined by a mass spectrometric technique adapted for the highly radioactive transuranium actinides. The products included π-bonded organoberkelium ions such as $BkCOT^+$, presumable the berkelium-cyclooctatetraenyl half-sandwich complex ion [254].

A cyclooctatetraenyl uranium(IV) triflate complex $(COT)U(OTf)_2(py)$ is accessible from the uranium(IV) triflate precursor $U(OTf)_4$ and K_2COT in pyridine [259].

Diuranium inverted sandwich complexes involving naphthalene and cyclooctatetraene have been synthesized with the use of bulky ketimide ancillary ligands. Reaction of readily available $UI_3(DME)_2$ with $KN{=}C(Bu^t)Mes$ in DME led to the isolation of dark green-brown $IU(DME)[N{=}C(Bu^t)Mes]_3$ (=2-I-DME) in 30% yield. In this compound one DME ligand coordinates to the uranium center in the pocket formed by the mesityl groups. Treatment of $IU(DME)[N{=}C(Bu^t)Mes]_3$ with 4 equiv. of KC_8 and 0.5 equiv. of naphthalene in DME allowed the isolation of a naphthalene-bridged com-

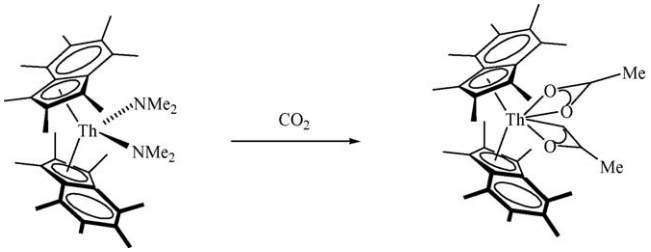

Scheme 95.

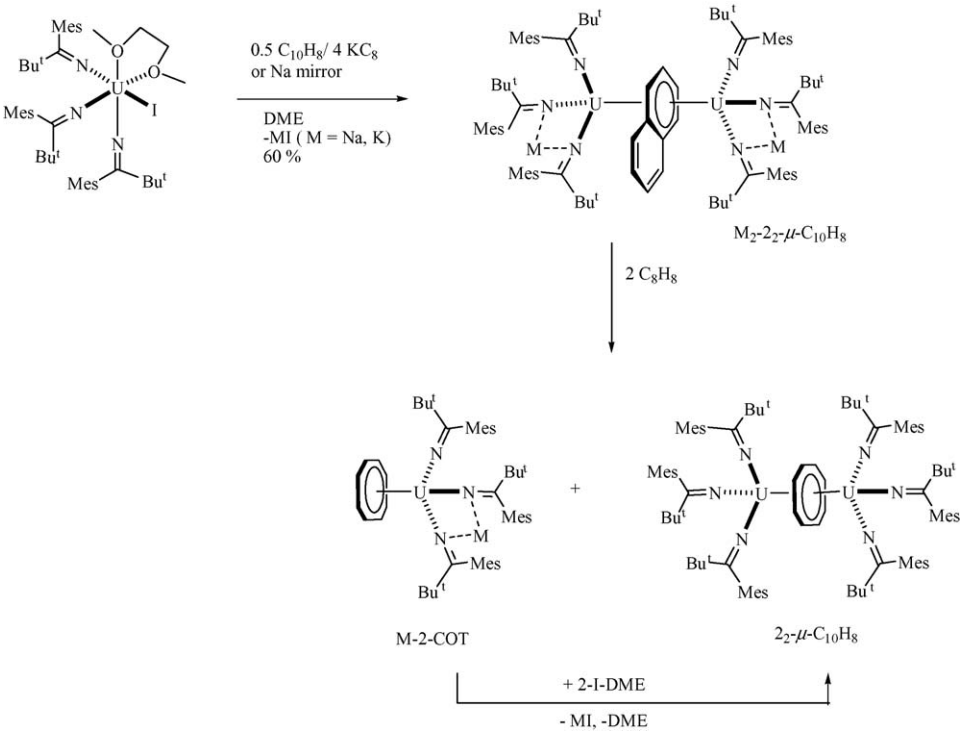

Scheme 96.

pound, $K_2(\mu\text{-}\eta^6{:}\eta^6\text{-}C_{10}H_8)[U\{N{=}C(Bu^t)Mes\}_3]_2$ (=K_2-2_2-μ-$C_{10}H_8$). The corresponding sodium derivative, $Na_2(\mu\text{-}\eta^6{:}\eta^6\text{-}C_{10}H_8)[U\{N{=}C(Bu^t)Mes\}_3]_2$ (=Na_2-2_2-μ-$C_{10}H_8$), was obtained as dark green-brown crystals in 40% yield by reducing 2-I-DME over a sodium mirror in THF in the presence of 0.6 equiv. of naphthalene (Scheme 84). Treatment of M_2-2_2-μ-$C_{10}H_8$ (M = Na, K) with 2 equiv. of cyclooctatetraene afforded a mixture of two products (Scheme 96). The ionic compounds $K[(COT)U\{N{=}C(Bu^t)Mes\}_3]$ (=K-2-COT) and $[Na(Et_2O)][(COT)U\{N{=}C(Bu^t)Mes\}_3]$ (=Na-2-COT) are insoluble in pentane, facilitating their separation from the neutral inverted sandwich complex ($\mu\text{-}\eta^8{:}\eta^8$-COT)$[U\{N{=}C(Bu^t)Mes\}_3]_2$ (=2_2-μ-COT). Interestingly, the latter compound can also be assembled independently in 90% yield by salt elimination upon reaction of M-2-COT with theiodide 2-I-DME [272].

Treatment of $(COT)U(BH_4)_2(THF)$ or $[(COT)U(BH_4)(THF)_2][BPh_4]$ with Ttmp (tmp = C_5Me_4P) afforded the mixed cyclooctatetraenyl–phospholyl uranium complex $(COT)U(tmp)(BH_4)(THF)$ as a brown solid in 89% yield (Fig. 78). Further reaction with Ktmp with $(COT)U(tmp)(BH_4)(THF)$ gave the "*ate*"-type addition derivative $K[(COT)U(tmp)_2(BH_4)(THF)_x]$. In the presence of NaOEt $(COT)U(tmp)(BH_4)(THF)$ was transformed into orange-red (COT)U(tmp)(OEt) (69% yield). The cationic compound $[(COT)U(tmp)(HMPA)_2][BPh_4]$ was isolated from the reaction of $[(COT)U(HMPA)_3][BPh_4]$ with Ktmp [273].

The synthesis of $(\mu\text{-}COT)[Cp^*(COT)U]_2$ from $Cp^*{}_3U$ and cyclooctatetraene has been achieved. Treatment of $Cp^*{}_3U$ with COT in a 1:1 stoichiometry afforded $(C_5Me_5)_2$ and $(\mu\text{-}COT)[Cp^*(COT)U]_2$ (Scheme 97) [262].

3.6. Heterobimetallic organoactinide complexes

The gas-phase reactions of actinide ($An^+ = Th^+, U^+$) cations with iron pentacarbonyl, $Fe(CO)_5$, and with ferrocene, Cp_2Fe,

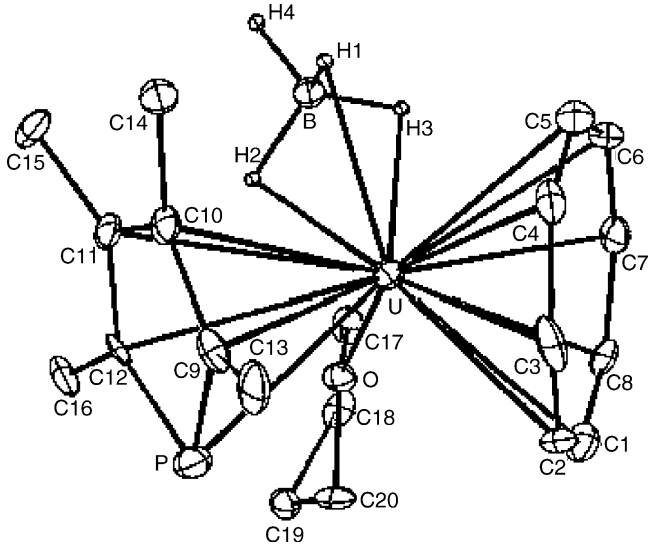

Fig. 78. Molecular structure of $(COT)U(tmp)(BH_4)(THF)$ [273].

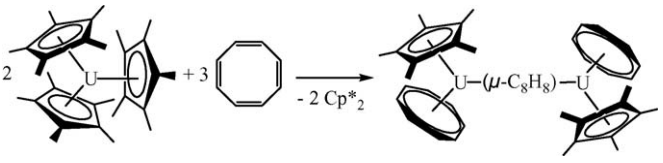

Scheme 97.

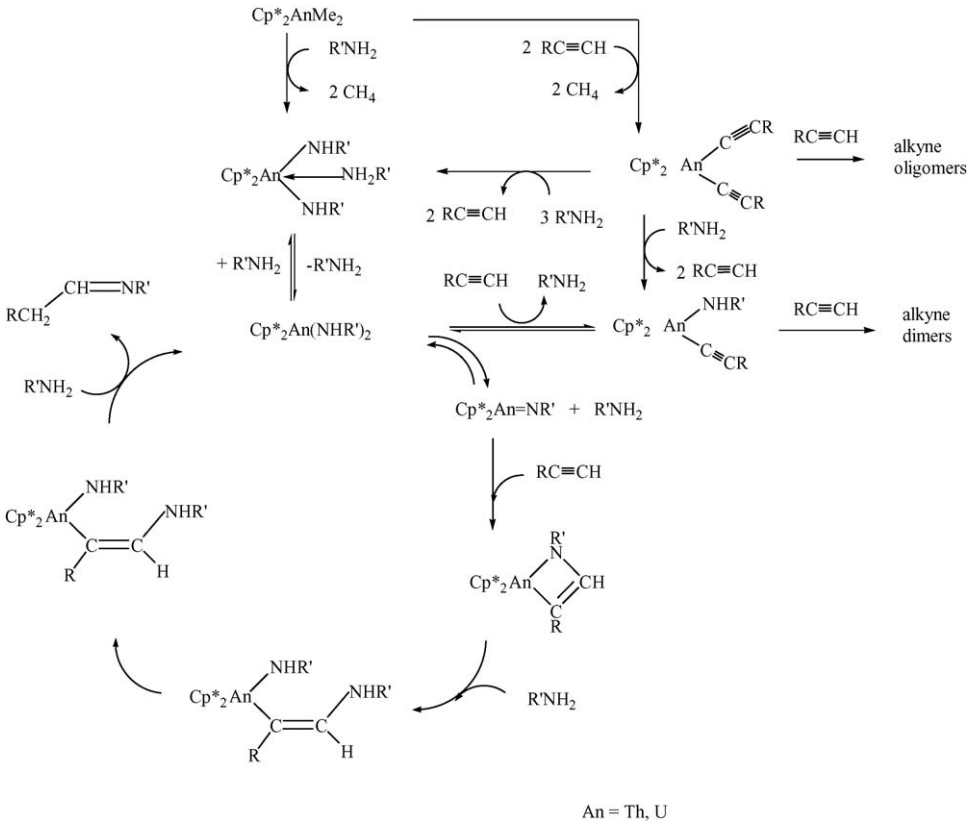

Scheme 98.

have been studied by Fourier transform ion cyclotron resonance mass spectrometry (FT-ICR/MS). In the case of $Fe(CO)_5$, the observed primary products were of the type $AnFe(CO)_x^+$ (An = Th, U; $x = 2$ and 3), and evidence was obtained for the presence of direct Ln–Fe bonds in these species. With Cp_2Fe the An^+ cations reacted by metal exchange, yielding the An-bis(cyclopentadienyl) ions Cp_2An^+ [189].

3.7. Organoactinide catalysis

Several review articles on special aspects of organoactinide catalysts have been published. Eisen et al. gave an account on "Organoactinides—novel catalysts for demanding chemical transformations" [274]. The topic "Organoactinides—new type of catalysts for carbon–silicon bond formation" has also been reviewed by Eisen et al. [275]. The same authors also published a comparative study of the catalytic effect in opening an organoactinide metal coordination sphere (permethylmetallocene versus *ansa*-metallocene derivatives) using the regioselective dimerization of terminal alkynes and hydrosilylation of alkynes and alkenes with $PhSiH_3$ promoted by $[Me_2Si(C_5Me_4)_2]ThBu^n{}_2$ as examples [276].

3.7.1. Organoactinide-catalyzed hydrogenation reactions

Structural studies including ^{13}C CPMAS NMR spectroscopy of the $^{13}C_\alpha$-enriched model adsorbate $Cp^*{}_2Th(^{13}CH_3)_2$ chemisorbed on superacidic sulfated zirconia revealed that the adsorbate undergoes a new molecular chemisorptive process: protonolytic M–C σ-bond cleavage at the very strong Brønsted acid sites to yield "cation-like" organometallic electrophiles [277].

3.7.2. Organoactinide-catalyzed hydroamination reactions

Organoactinide complexes of the type $Cp^*{}_2AnMe_2$ (An = Th, U) have been found to be efficient catalysts for the hydroamination of terminal alkynes with aliphatic primary amines. The chemoselectivity and regioselectivity of the reactions depend strongly on the nature of the catalysts and the nature of the amine and show no major dependence on the nature of the alkyne. The hydroamination reaction of terminal alkynes with aliphatic primary amines catalyzed by organouranium complexes produces the corresponding imines where the amine and the alkyne are regioselectively disposed in a syn-regiochemistry, whereas for similar reactions with the organothorium complexes besides the methyl alkylated imine, dimeric and trimeric alkyne oligomers are also produced. The key organoactinide intermediate for the intermolecular hydroamination reaction was found to be the corresponding actinide-imido complex. A plausible scenario is illustrated in Scheme 98 [278].

References

[1] H.B. Kagan, Chem. Rev. 102 (2002) 1805.
[2] H.C. Aspinall, Chem. Rev. 102 (2002) 1807.
[3] M.N. Bochkarev, Chem. Rev. 102 (2002) 2089.
[4] G.B. Deacon, C.M. Forsyth, S. Nickel, J. Organomet. Chem. 647 (2002) 50.

[5] F.T. Edelmann, D.M.M. Freckmann, H. Schumann, Chem. Rev. 102 (2002) 1851.
[6] W.J. Evans, B.L. Davis, Chem. Rev. 102 (2002) 2119.
[7] W.J. Evans, J. Organomet. Chem. 647 (2002) 2.
[8] W.J. Evans, J. Organomet. Chem. 652 (2002) 61.
[9] O. Eisenstein, L. Maron, J. Organomet. Chem. 647 (2002) 190.
[10] G.M. Ferrence, J. Takats, J. Organomet. Chem. 647 (2002) 84.
[11] Z. Hou, Y. Wakatsuki, J. Organomet. Chem. 647 (2002) 61.
[12] J. Inanaga, H. Furuno, T. Hayano, Chem. Rev. 102 (2002) 2211.
[13] K. Izod, Angew. Chem. 114 (2002) 769;
K. Izod, Angew. Chem. Int. Ed. 41 (2002) 743.
[14] M.C. Cassani, Y.K. Gun'ko, P.B. Hitchcock, A.G. Hulkes, A.V. Khvostov, M.F. Lappert, A.V. Protchenko, J. Organomet. Chem. 647 (2002) 71.
[15] J. Marçalo, A. Pires de Matos, J. Organomet. Chem. 647 (2002) 216.
[16] N. Marques, A. Sella, J. Takats, Chem. Rev. 102 (2002) 2137.
[17] G.A. Molander, J.A.C. Romero, Chem. Rev. 102 (2002) 2161.
[18] S. Arndt, J. Okuda, Chem. Rev. 102 (2002) 1953.
[19] E.S. Petrov, D.M. Roitershtein, L.F. Rybakova, J. Organomet. Chem. 647 (2002) 21.
[20] Y. Qian, J. Huang, J. Organomet. Chem. 647 (2002) 100.
[21] W. Nie, C. Qian, Y. Chen, S. Jie, J. Organomet. Chem. 647 (2002) 114.
[22] Q. Shen, Y. Yao, J. Organomet. Chem. 647 (2002) 180.
[23] H. Yasuda, J. Organomet. Chem. 647 (2002) 128.
[24] X. Zhou, M. Zhu, J. Organomet. Chem. 647 (2002) 28.
[25] K. Mikami, M. Terada, H. Matsuzawa, Angew. Chem. 114 (2002) 3704;
K. Mikami, M. Terada, H. Matsuzawa, Angew. Chem. Int. Ed. 41 (2002) 3554.
[26] V. Vetere, P. Maldivi, C. Adamo, Int. J. Quant. Chem. 91 (2002) 321.
[27] J.J. Schroeden, M. Teo, H.F. Davis, J. Chem. Phys. 117 (2002) 9258.
[28] C.A. Bayse, J. Phys. Chem. A 106 (2002) 4226.
[29] J.J. Schroeden, M. Teo, H.F. Davis, J. Phys. Chem. A 106 (2002) 11695.
[30] D.-Y. Hwang, A.M. Mebel, J. Phys. Chem. A 106 (2002) 12072.
[31] L. Maron, L. Perrin, O. Eisenstein, J. Chem. Soc., Dalton Trans. (2002) 534.
[32] D.J. Zhang, C.B. Liu, Chin. Chem. Lett. 13 (2002) 359.
[33] M. Niemeyer, Acta Cryst. E57 (2001) m553.
[34] H. Schumann, D.M.M. Freckmann, S. Dechert, Z. Anorg. Allgem. Chem. 628 (2002) 2422.
[35] D.L. Clark, J.C. Gordon, P.J. Hay, R.L. Martin, R. Poli, Organometallics 21 (2002) 5000.
[36] M.V. Metz, Y. Sun, C.L. Stern, T.J. Marks, Organometallics 21 (2002) 3691.
[37] M. Westerhausen, S. Schmeiderbauer, M. Hartmann, M. Warchhold, H. Nöth, Z. Anorg. Allgem. Chem. 628 (2002) 330.
[38] P.B. Hitchcock, A.V. Khvostov, M.F. Lappert, J. Organomet. Chem. 663 (2002) 263.
[39] A. Wacker, C.G. Yan, G. Kaltenpoth, A. Ginsberg, A.M. Arif, R.D. Ernst, H. Pritzkow, W. Siebert, J. Organomet. Chem. 641 (2002) 195.
[40] G.W. Rabe, C.D. Bérubé, G.P.A. Yap, K.-C. Lam, T.E. Concolino, A.L. Rheingold, Inorg. Chem. 41 (2002) 1446.
[41] G.W. Rabe, C.D. Berube, G.P.A. Yap, Inorg. Chem. 40 (2001) 2682.
[42] S. Arndt, T.P. Spaniol, J. Okuda, Chem. Commun. (2001) 896.
[43] D.J.H. Emslie, W.E. Piers, R. McDonald, J. Chem. Soc., Dalton Trans. (2002) 293.
[44] F.G.N. Cloke, B.R. Elvidge, P.B. Hitchcock, V.M.E. Lamarche, J. Chem. Soc., Dalton Trans. (2002) 2413.
[45] B.D. Ward, S.R. Dubberley, A. Maisse-François, L.H. Gade, P. Mountford, J. Chem. Soc., Dalton Trans. (2002) 4649.
[46] A. Lara-Sanchez, A. Rodriguez, L. Hughes, M. Schormann, M. Bochmann, J. Organomet. Chem. 663 (2002) 63.
[47] D.J.H. Emslie, W.E. Piers, M. Parvez, R. McDonalds, Organometallics 21 (2002) 4226.
[48] P.G. Hayes, W.E. Piers, L.W. Lee, L.K. Knight, M. Parvez, M.R.J. Elsegood, W. Clegg, Organometallics 20 (2001) 2533.
[49] P.G. Hayes, W.E. Piers, R. McDonald, J. Am. Chem. Soc. 124 (2002) 2132.
[50] A.M. Neculai, D. Neculai, H.W. Roesky, J. Magull, M. Baldus, O. Andromesi, M. Jansen, Organometallics 21 (2002) 2590.
[51] S. Bambirra, D. van Leusen, A. Meetsma, B. Hessen, J.H. Teuben, J. Chem. Soc., Chem Commun. (2001) 637.
[52] M.E.G. Skinner, B.R. Tyrrell, B.D. Ward, P. Mountford, J. Organomet. Chem. 647 (2002) 145.
[53] M.E.G. Skinner, P. Mountford, J. Chem. Soc., Dalton Trans. (2002) 1694.
[54] Z. Lu, G.P.A. Yap, D.S. Richeson, Organometallics 20 (2001) 706.
[55] I. Lopes, B. Monteiro, G. Lin, A. Domingos, N. Marques, J. Takats, J. Organomet. Chem. 632 (2001) 119.
[56] S. Jank, J. Hanss, H. Reddmann, H.-D. Amberger, N.M. Edelstein, Z. Anorg. Allgem. Chem. 628 (2002) 1355.
[57] H.-D. Amberger, S. Jank, H. Reddmann, N.M. Edelstein, Spectrochim. Acta A 58 (2002) 379.
[58] E.D. Glendening, M.L. Strange, J. Phys. Chem. A 106 (2002) 7338.
[59] T. Dube, J. Guan, S. Gambarotta, Chem. Eur. J. 7 (2001) 374.
[60] R. Taube, S. Maiwald, J. Sieler, J. Organomet. Chem. 621 (2001) 327.
[61] A.A. Trifonov, E.N. Kirillov, A. Fischer, F.T. Edelmann, M.N. Bochkarev, J. Organomet. Chem. 647 (2002) 94.
[62] Z. Hou, T. Koizumi, M. Nishiura, Y. Wakatsuki, Organometallics 20 (2001) 3323.
[63] O. Tardif, Z. Hou, M. Nishiura, T. Koizumi, Y. Wakatsuki, Organometallics 20 (2001) 4565.
[64] D. Barbier-Baudry, S. Heiner, M.M. Kubicki, E. Vigier, M. Visseaux, Organometallics 20 (2001) 4207.
[65] G.R. Giesbrecht, C. Cui, A. Shafir, J.A.R. Schmidt, J. Arnold, Organometallics 21 (2002) 3841.
[66] S.S. Jagannatha, Indian J. Chem. 41A (2002) 1850.
[67] A.N. Shoshkin, L.N. Bochkarev, S.Y. Khorshev, Russ. J. Gen. Chem. 72 (2002) 715.
[68] F. Weber, H. Sitzmann, M. Schultz, C.D. Sofield, R.A. Andersen, Organometallics 21 (2002) 3139.
[69] P. Selg, H.H. Brintzinger, M. Schultz, R.A. Andersen, Organometallics 21 (2002) 3100.
[70] L. Maron, L. Perrin, O. Eisenstein, R.A. Andersen, J. Am. Chem. Soc. 124 (2002) 5614.
[71] M. Schultz, C.J. Burns, D.J. Schwartz, R.A. Andersen, Organometallics 20 (2001) 5690.
[72] W.J. Evans, N.T. Allen, J.W. Ziller, Angew. Chem. 114 (2002) 369; W.J. Evans, N.T. Allen, J.W. Ziller, Angew. Chem. Int. Ed. 41 (2002) 359.
[73] G.V. Khoroshenkov, T.V. Petrovskaya, I.L. Fedushkin, M.N.Z. Bochkarev, Anorg. Allgem. Chem. 628 (2002) 1355.
[74] G.B. Deacon, C.M. Forsyth, D.L. Wilkinson, Chem. Eur. J. 7 (2001) 1784.
[75] Y. Yao, Y. Zhang, Q. Shen, K. Yu, Organometallics 21 (2002) 819.
[76] P.W. Roesky, Organometallics 21 (2002) 4756.
[77] Y.-P. Cia, H.-Z. Ma, B.-S. Kang, C.-Y. Su, W. Zhang, J. Sun, Y.-L. Xiong, J. Organomet. Chem. 628 (2001) 99.
[78] W. Zhang, Y.-P. Cai, H.-X. Li, H.-Z. Ma, Jiegou Huaxue 21 (2002) 378.
[79] Y. Cheng, G.-X. Jin, Q. Shen, Y. Lin, J. Organomet. Chem. 631 (2001) 94.
[80] J. Okuda, S. Arndt, K. Beckerle, K.C. Hultzsch, P. Voth, T.P. Spaniol, Pure Appl. Chem. 73 (2001) 351.
[81] G. Lin, R. McDonald, J. Takats, J. Organomet. Chem. 626 (2001) 76.
[82] S. Arndt, T.P. Spaniol, J. Okuda, Eur. J. Inorg. Chem. (2001) 73.
[83] S. Arndt, A. Trifonov, T.P. Spaniol, J. Okuda, M. Kitamura, T. Takahashi, J. Organomet. Chem. 647 (2002) 158.
[84] A. Gapeev, R.C. Dunbar, J. Am. Soc. Mass Spectrom. 13 (2002) 477.
[85] W.J. Evans, J.C. Brady, J.W. Ziller, J. Am. Chem. Soc. 123 (2001) 7711.
[86] D. Stellfeldt, G. Meyer, G.B. Deacon, Z. Anorg. Allgem. Chem. 627 (2001) 1659.

[87] M.D. Bala, J. Huang, H. Zhang, Y. Qian, J. Sun, C. Liang, J. Organomet. Chem. 647 (2002) 105.
[88] H. Schumann, A. Heim, J. Demtschuk, S.H. Mühle, Organometallics 21 (2002) 3334.
[89] Y.-X. Cheng, G.-X. Jin, H.-Q. Jia, Y. Xing, Y.-H. Lin, Chin. J. Struct. Chem. 20 (2001) 31.
[90] T. Jiang, Q. Shen, J. Ocean Univ. Qiangdao 31 (2001) 173.
[91] C.-F. Liang, J.-Q. Sun, W.-Q. Hu, Y.-R. Yang, H. Schumann, Zhejiang Daxue Xuebao Gongxueban 36 (2002) 109.
[92] I.L. Fedushkin, F. Girgsdies, H. Schumann, M.N. Bochkarev, Eur. J. Inorg. Chem. (2001) 2405.
[93] H. Schumann, M.R. Kreitsch, S.H. Mühle, Z. Anorg. Allgem. Chem. 628 (2002) 1311.
[94] C.D. Abernethy, C.L.B. Macdonald, J.A.C. Clyburne, A.H. Cowley, J. Chem. Soc., Chem. Commun. (2001) 61.
[95] H. Sitzmann, O. Schmitt, F. Weber, G.Z. Wolmershäuser, Anorg. Allgem. Chem. 627 (2001) 12.
[96] R.A.L. Gendron, D.J. Berg, T. Barclay, Can. J. Chem. 80 (2002) 1285.
[97] M.M. Corradi, M.A.D. McGowan, P.C. McGowan, M. Thornton-Pett, Eur. J. Inorg. Chem. (2002) 2362.
[98] D.M. Roitershtein, D.P. Krut'ko, E.N. Veksler, D.A. Lemenovskii, W. Nie, C. Qian, Russ. Chem. Bull. 50 (2001) 1295.
[99] G.B. Deacon, C.C. Quitmann, K. Müller-Buschbaum, G. Meyer, Z. Anorg. Allgem. Chem. 627 (2001) 1431.
[100] Y.-M. Sun, Q. Ling, Y.-B. Wan, X.-R. Wang, H.-Y. Yu, Chin. J. Chem. 20 (2002) 996.
[101] Q. Ling, G.-X. Shen, H.-Y. Yu, Y. Zhang, Y.-M. Sun, Hecheng Huaxue 10 (2002) 263.
[102] M. Luo, H.-Z. Ma, Q.-D. Su, Q.-R. Li, N.-L. Hu, Asian J. Chem. 14 (2002) 1463.
[103] Y. Wang, Q. Shen, L. Wu, Y. Zhang, J. Sun, J. Organomet. Chem. 626 (2001) 176.
[104] F.-G. Yuan, Q. Shen, J. Sun, Chem. J. Chin. Univ. 22 (2001) 1501.
[105] Y. Muhammad, J. Huang, Z. Feng, Y. Qian, Huadong Ligong Daxue Xuebao 27 (2001) 211.
[106] L.-G. Zhang, X.-G. Zhou, Z.-E. Huang, R.-F. Cai, L.-B. Zhang, Chin. J. Struct. Chem. 20 (2001) 40.
[107] L.-X. Zhang, M.-H. Xie, H.-Z. Ma, Hecheng Huaxue 9 (2001) 156.
[108] X.-G. Zhou, L.-X. Zhang, C.-M. Zhang, J. Zhang, M. Zhu, R.-F. Cai, Z.-E. Huang, Z.-X. Huang, Q.-J. Wu, J. Organomet. Chem. 655 (2002) 120.
[109] Y.-B. Wan, X.-R. Wang, J. Anhui Univ. Technol. 18 (2001) 235.
[110] X.R. Wang, Y.-B. Wan, J.-P. Hu, Hecheng Huaxue 9 (2001) 452.
[111] M.T. Gamer, P.W. Roesky, J. Organomet. Chem. 647 (2002) 123.
[112] H. Li, Y. Yao, Q. Shen, L. Weng, Organometallics 21 (2002) 2529.
[113] J. Zhang, R. Ruan, Z. Shao, R. Cai, L. Weng, X. Zhou, Organometallics 21 (2002) 1420.
[114] X.-G. Zhou, L.-B. Zhang, M. Zhu, R.-F. Cai, L.-H. Weng, Organometallics 20 (2001) 5700.
[115] A.K. Dash, A. Razavi, A. Mortreux, C.W. Lehmann, J.-F. Carpentier, Organometallics 21 (2002) 3238.
[116] Q. Shen, H. Li, C. Yao, Y. Yao, L. Zhang, K. Yu, Organometallics 20 (2001) 3070.
[117] M. Westerhausen, S. Schneiderbauer, N. Makropoulos, M. Warchhold, H. Nöth, H. Piotrowski, K. Karaghiosoff, Organometallics 21 (2002) 4335.
[118] D. Cui, T. Tang, J. Cheng, N. Hu, W. Chen, B. Huang, J. Organomet. Chem. 650 (2002) 84.
[119] L. Maron, O. Eisenstein, F. Alary, R. Poteau, J. Phys. Chem. A 106 (2002) 1797.
[120] H.-D. Amberger, H. Reddmann, S. Jank, L. Zhang, N.M. Edelstein, J. Organomet. Chem. 656 (2002) 18.
[121] T. Liu, Crystallogr. Rep. 47 (2002) 425.
[122] D.-M. Cui, J.-H. Cheng, X.-L. Zhuang, N.-H. Hu, J.-Z. Jin, W.-Q. Chen, T. Tang, B.-T. Huang, Jiegou Huaxue 21 (2002) 78.
[123] J. Guan, R.D. Fischer, Eur. J. Inorg. Chem. (2001) 2497.
[124] W.J. Evans, M.A. Johnston, R.D. Clark, R. Anwander, J.W. Ziller, Polyhedron 20 (2001) 2483.
[125] N. Kaltsoyannis, M.R. Russo, J. Nucl. Sci. Technol. (Suppl. 3) (2002) 393.
[126] Z. Hou, Y. Zhang, O. Tardif, Y. Wakatsuki, J. Am. Chem. Soc. 123 (2001) 9216.
[127] W.J. Evans, N.T. Allen, M.A. Greci, J.W. Ziller, Organometallics 20 (2001) 2936.
[128] W.J. Evans, C.H. Fujimoto, J.W. Ziller, Polyhedron 21 (2002) 1683.
[129] M.G. Klimpel, H.W. Görlitzer, M. Tafipolsky, M. Spiegler, W. Scherer, R. Anwander, J. Organomet. Chem. 647 (2002) 236.
[130] I. Castillo, T.D. Tilley, J. Am. Chem. Soc. 123 (2001) 10526.
[131] W.J. Evans, C.H. Fujimoto, M.A. Johnston, J.W. Ziller, Organometallics 21 (2002) 1825.
[132] V. Lorenz, A. Fischer, F.T. Edelmann, J. Organomet. Chem. 647 (2002) 245.
[133] W.J. Evans, N.T. Allen, J.W. Ziller, J. Am. Chem. Soc. 123 (2001) 7927.
[134] M. Schultz, J.M. Boncella, D.J. Berg, T.D. Tilley, R.A. Andersen, Organometallics 21 (2002) 460.
[135] D.J. Berg, J.M. Boncella, R.A. Andersen, Organometallics 21 (2002) 4622.
[136] W.J. Evans, J.C. Brady, J.W. Ziller, Inorg. Chem. 41 (2002) 3340.
[137] H. Schumann, M. Glanz, J. Gottfriedsen, S. Dechert, D. Wolff, Pure Appl. Chem. 73 (2001) 279.
[138] C.P. Casey, J.A. Tunge, T.-Y. Lee, D.W. Carpenetti II, Organometallics 21 (2002) 389.
[139] W.J. Evans, D.G. Giarikos, C.B. Robledo, V.S. Leong, J.W. Ziller, Organometallics 20 (2001) 5648.
[140] I. Castillo, T.D. Tilley, Organometallics 20 (2001) 5598.
[141] W.J. Evans, B.L. Davis, J.W. Ziller, Inorg. Chem. 40 (2001) 6341.
[142] I.L. Fedushkin, T.V. Petrovskaya, M.N. Bochkarev, S. Dechert, H. Schumann, Angew. Chem. 113 (2001) 2540;
I.L. Fedushkin, T.V. Petrovskaya, M.N. Bochkarev, S. Dechert, H. Schumann, Angew. Chem. Int. Ed. 40 (2001) 2474.
[143] I.L. Fedushkin, Y.A. Kurskii, V.I. Nevodchikov, M.N. Bochkarev, S. Mühle, H. Schumann, Russ. Chem. Bull. 51 (2002) 160.
[144] I.L. Fedushkin, S. Dechert, H. Schumann, Angew. Chem. 113 (2001) 584;
I.L. Fedushkin, S. Dechert, H. Schumann, Angew. Chem. Int. Ed. 40 (2001) 561.
[145] I.L. Fedushkin, M.N. Bochkarev, S. Dechert, H. Schumann, Chem. Eur. J. 7 (2001) 3558.
[146] D. Barbier-Baudry, F. Bonnet, A. Dormond, A. Hafid, A. Nyassi, M. Visseaux, J. Alloys Compd. 323/324 (2001) 592.
[147] E. Ihara, S. Yoshioka, M. Furo, K. Katsura, H. Yasuda, S. Mohri, N. Kanehisa, Y. Kai, Organometallics 20 (2001) 1752.
[148] S. Bogaert, T. Chenal, A. Mortreux, G. Nowogrocki, C.W. Lehmann, J.-F. Carpentier, Organometallics 20 (2001) 199.
[149] G. Paolucci, J. Zanon, V. Lucchini, W.-E. Damrau, E. Siebel, R.D. Fischer, Organometallics 21 (2002) 1088.
[150] A.A. Trifonov, E.N. Kirillov, S. Dechert, H. Schumann, M.N. Bochkarev, Eur. J. Inorg. Chem. (2001) 3055.
[151] A.A. Trifonov, E.N. Kirillov, S. Dechert, H. Schumann, M.N. Bochkarev, Eur. J. Inorg. Chem. (2001) 2509.
[152] M.-H. Qi, X.-Q. Shen, X.-Q. Gong, Z.-Q. Shen, L.-H. Weng, Chin. J. Chem. 20 (2002) 564.
[153] Y. Ge, Z.-Y. Yue, J.-S. Gao, P.-F. Yan, Chem. Res. Chin. Univ. 17 (2001) 338.
[154] J. Cheng, D. Cui, W. Chen, T. Tang, B. Huang, J. Organomet. Chem. 658 (2002) 153.
[155] C. Qian, G. Zou, Y. Chen, J. Sun, Organometallics 20 (2001) 3106.
[156] W. Zhang, Y.-P. Cai, H.-X. Li, H.-Z. Ma, Hecheng Huaxue 10 (2002) 268.
[157] M. Luo, H.-Z. Ma, Q.-D. Su, N.-L. Hu, B.-J. Du, Asian J. Chem. 14 (2002) 1469.
[158] C. Qian, W. Me, Y. Chen, J. Sun, J. Organomet. Chem. 645 (2002) 82.
[159] C. Qian, W. Me, J. Sun, J. Organomet. Chem. 626 (2001) 171.
[160] F. Nief, Eur. J. Inorg. Chem. (2001) 891.

[161] M. Ganesan, C.D. Bérubé, S. Gambarotta, G.P.A. Yap, Organometallics 21 (2002) 1707.
[162] I. Korobkov, G. Aharonian, S. Gambarotta, G.P.A. Yap, Organometallics 21 (2002) 4899.
[163] D.M.M. Freckmann, T. Dubé, C.D. Bérubé, S. Gambarotta, G.P.A. Yap, Organometallics 21 (2002) 1240.
[164] F. Nief, L. Ricard, Organometallics 20 (2001) 3884.
[165] S.M. Cendrowski-Guillaume, G. Le Gland, M. Ephritikhine, M. Nierlich, Z. Kristallogr. New Cryst. Struct. 217 (2002) 35.
[166] J. Wang, S. Li, C. Zheng, J.A. Maguire, N.S. Hosmane, Organometallics 21 (2002) 5149.
[167] J. Wang, S. Li, C. Zheng, J.A. Maguire, N.S. Hosmane, Organometallics 21 (2002) 3314.
[168] J. Wang, S. Li, C. Zheng, J.A. Maguire, N.S. Hosmane, Inorg. Chem. Commun. 5 (2002) 602.
[169] G. Zi, Q. Yang, T.C.W. Mak, Z. Xie, Organometallics 20 (2001) 2359.
[170] G. Zi, H.-W. Li, Z. Xie, Organometallics 21 (2002) 3464.
[171] S. Wang, H.-W. Li, Z. Xie, Organometallics 20 (2001) 3624.
[172] G. Zi, H.-W. Li, Z. Xie, Organometallics 21 (2002) 1136.
[173] X.-Y. Yu, G.-X. Jin, L.-H. Wenig, Chin. J. Chem. 20 (2002) 1256.
[174] X.-Y. Yu, G.-X. Jin, N.-H. Hu, L.-H. Weng, Organometallics 21 (2002) 5540.
[175] S. Tobisch, T. Nowak, H. Bögel, J. Organomet. Chem. 619 (2001) 24.
[176] D. Caraiman, D.K. Bohme, J. Phys. Chem. A 106 (2002) 9705.
[177] R.C. Dunbar, J. Phys. Chem. A 106 (2002) 7328.
[178] M.D. Fryzuk, L. Jafarpour, F.M. Kerton, J. Love, B.O. Patrick, S.J. Rettig, Organometallics 20 (2001) 1387.
[179] J.C. Gordon, G.R. Giesbrecht, D.L. Clark, P.J. Hay, D.W. Keogh, R. Poli, B.L. Scott, J.G. Watkin, Organometallics 21 (2002) 4726.
[180] X. Zheng, B. Wang, U. Englert, G.E. Herberich, Inorg. Chem. 40 (2001) 3117.
[181] S.M. Cendrowski-Guillaume, G. Le Gland, M. Lance, M. Nierlich, M. Ephritikhine, Comptes Rendus Chimie 5 (2002) 73.
[182] J.-L. Huang, X.-Q. Shen, Q.-C. Liu, Y.-L. Qian, A.S.-C. Chan, Chin. J. Chem. 19 (2001) 102.
[183] M. Visseaux, F. Nief, L. Ricard, J. Organomet. Chem. 647 (2002) 139.
[184] J.-L. Li, Y.-S. Lin, Z.-Y. Wu, S.-G. Yang, D.-D. Cheng, M.-X. Zhan, Xiamen Daxue Xuebao Ziran Kexueban 41 (2002) 453.
[185] Q. Kong, Y. Shen, L. Zhao, J. Zhuang, S. Qian, Y. Li, R. Lin, R. Cai, J. Chem. Phys. 116 (2002) 128.
[186] Q. Kong, J. Zhuang, X. Li, R. Cai, L. Zhao, S. Qian, Y. Li, Appl. Phys. A: Mater. Sci. Process. 75 (2002) 367.
[187] C.-F. Liang, J.-Q. Sun, W.-Q. Hu, Y.-R. Yang, H. Schumann, Zhejiang Daxue Xuebao Gongxueban 36 (2002) 109.
[188] E.B. Iezzi, J.C. Duchamp, K.R. Fletcher, T.E. Glass, H.C. Dorn, Nano Lett. 2 (2002) 1187.
[189] M. da Conceicao Vieira, J. Marcalo, A.P. de Matos, J. Organomet. Chem. 632 (2001) 126.
[190] A. Fischbach, F. Perdih, P. Sirsch, W. Scherer, R. Anwander, Organometallics 21 (2002) 4569.
[191] G.R. Giesbrecht, J.C. Gordon, J.T. Brady, D.L. Clark, D.W. Keogh, R. Michalcyk, L. Scott, J.G. Watkin, Eur. J. Inorg. Chem. (2002) 723.
[192] J.C. Gordon, G.R. Giesbrecht, J.T. Brady, D.L. Clark, D.W. Keogh, B.L. Scott, J.G. Watkin, Organometallics 21 (2002) 127.
[193] K. Müller-Buschbaum, G.B. Deacon, C.M. Forsyth, Eur. J. Inorg. Chem. (2002) 3172.
[194] Q. Shen, Y.-M. Yao, Chin. J. Org. Chem. 21 (2002) 1018.
[195] L. Maron, O. Eisenstein, J. Am. Chem. Soc. 123 (2001) 1036.
[196] S. Bogaert, T. Chenal, A. Morttreux, J.-F. Carpentier, J. Mol. Catal. A 190 (2002) 207.
[197] J. Chen, Y.-M. Zhang, Chin. J. Chem. 20 (2002) 103.
[198] R. Ruan, X. Zhou, R. Cai, Chem. Commun. (2002) 538.
[199] F. Xu, X.-H. Zhu, Q. Shen, J. Lu, J.-Q. Li, Chin. J. Chem. 20 (2002) 1334.
[200] E.N. Kirillov, A.E. Fedorova, A.A. Trifonov, M.N. Bochkarev, Appl. Organomet. Chem. 15 (2001) 151.
[201] C.P. Casey, J. Tunge, M.A. Fagan, J. Organomet. Chem. 663 (2002) 91.
[202] N. Sändig, W. Koch, Organometallics 21 (2002) 1861.
[203] L. Cavallo, G. Talarico, Polym. Mater. Sci. Eng. 87 (2002) 38.
[204] R.D. Miotti, A. de Souza Maia, I.S. Paulino, U. Schuchardt, W. de Oliveira, J. Alloys Compd. 344 (2002) 92.
[205] R.D. Miotti, A. de Souza Maia, W. de Oliveira, I.S. Paulino, U. Schuchardt, Quim. Nova 25 (2002) 762.
[206] V. Lavini, A. de Souza Maia, I.S. Paulino, U. Schuchardt, W. de Oliveira, Inorg. Chem. Commun. 4 (2001) 582.
[207] Y. Lou, Y. Yao, Q. Shen, Macromolecules 35 (2002) 8670.
[208] T. Hayakawa, Y. Nakayama, H. Yasuda, Polym. Int. 50 (2001) 1260.
[209] Z. Hou, S. Kaita, Y. Wakatsuki, Pure Appl. Chem. 73 (2001) 291.
[210] S. Maiwald, C. Sommer, G. Müller, R. Taube, Macromol. Chem. Phys. 203 (2002) 1029.
[211] S. Maiwald, H. Weissenborn, C. Sommer, G. Müller, R. Taube, J. Organomet. Chem. 640 (2001) 1.
[212] D. Barbier-Baudry, F. Bonnet, A. Dormond, M. Visseaux, Entropie (2001) 96.
[213] F. Bonnet, D. Barbier-Baudry, A. Dormond, M. Visseaux, Polym. Int. 51 (2002) 986.
[214] F. Bonnet, M. Visseaux, D. Barbier-Baudry, A. Dormond, Macromolecules 35 (2002) 1143.
[215] D. Barbier-Baudry, F. Bonnet, B. Domenichini, A. Dormond, M. Visseaux, J. Organomet. Chem. 647 (2002) 167.
[216] M.F. Llauro, C. Monnet, F. Barbotin, V. Monteil, R. Spitz, C. Boisson, Macromolecules 34 (2001) 6304.
[217] S. Kaita, Z. Hou, Y. Wakatsuki, Macromolecules 34 (2001) 1536.
[218] S. Agarwal, M. Puchner, Eur. Polym. J. 38 (2002) 2365.
[219] P. Ravi, T. Gröb, D. Dehnicke, A. Greiner, Macromol. Chem. Phys. 202 (2001) 2641.
[220] K. Tanaka, M. Furo, E. Ihara, H. Yasuda, J. Polym. Sci. A: Polym. Chem. 39 (2001) 1382.
[221] M. Tanabe, T. Sugimura, H. Yasuda, React. Funct. Polym. 52 (2002) 135.
[222] J. Sun, Z. Pan, W. Hu, S. Yang, Eur. Polym. J. 38 (2002) 545.
[223] Y. Qian, M.D. Bala, M. Yousaf, H. Zhang, J. Huang, J. Sun, C. Liang, J. Mol. Catal. A 188 (2002) 1.
[224] Y. Zhang, Y.-M. Yao, Q. Shen, Q.-J. Meng, J.-S. Ren, Y.-H. Lin, Yingyong Huaxue 19 (2002) 173.
[225] Q. Shen, Y. Wang, K. Zhang, Y. Yao, J. Polym. Sci. 40 (2002) 612.
[226] L.-Q. Ying, X.-W. Ba, Y.-Y. Zhao, G. Li, T. Tang, Y.-T. Jin, Chin. J. Polym. Sci. 19 (2001) 85.
[227] X.F. Ni, Z.Q. Shen, H. Yasuda, Chin. Chem. Lett. 12 (2001) 821.
[228] H.-X. Teng, L.-Q. Yingt, S.-C. Han, W.-H. Tang, X.-W. Ba, Y.Y. Zhao, G. Li, T. Tang, Y.-T. Jin, Chin. J. Appl. Chem. 18 (2001) 246.
[229] Y. Yao, Q. Shen, L. Zhang, Chin. Sci. Bull. 46 (2001) 1443.
[230] M. Qi, S. Qi, Z. Shen, Zhongguo Xitu Xuebao 20 (2002) 279.
[231] D.-M. Cui, T. Tang, J.-H. Cheng, N.-H. Hu, W.-Q. Chen, B. Huang, Gaodeng Xuexiao Huaxue Xuebao 23 (2002) 188.
[232] Y.-J. Luo, Y.-M. Yao, Q. Shen, Chin. J. Appl. Chem. 18 (2001) 392.
[233] L.-Q. Ying, X.-W. Ba, Y.-Y. Zhao, G. Li, T. Tang, Y.-T. Jin, Chin. J. Polym. Sci. 19 (2001) 89.
[234] L.-Q. Ying, G. Li, Y.-Y. Zhao, X.-W. Ba, D.-M. Cui, T. Tang, Y.-T. Jin, J. Chin. Rare Earth Soc. 19 (2001) 275.
[235] G.A. Molander, D. Pfeiffer, Org. Lett. 3 (2001) 361.
[236] L. Perrin, L. Maron, O. Eisenstein, Inorg. Chem. 41 (2002) 4355.
[237] A.Z. Voskoboynikov, A.K. Shestakova, I.P. Beletskaya, Organometallics 20 (2001) 2794.
[238] G.A. Molander, J.A.C. Romero, C.P. Corrette, J. Organomet. Chem. 647 (2002) 225.
[239] J.-S. Ryu, T.J. Marks, F.E. McDonald, Org. Lett. 3 (2001) 3091.
[240] M.R. Douglass, C.L. Stern, T.J. Marks, J. Am. Chem. Soc. 123 (2001) 10221.
[241] M.R. Douglass, M. Ogasawara, S. Hong, M.V. Metz, T.J. Marks, Organometallics 21 (2002) 283.
[242] A.G.M. Barrett, N. Bouloc, C.D. Braddock, D. Chadwick, D.A. Henderson, Synlett (2002) 653.
[243] Z. Li, Y. Zhang, J. Chem. Res. Synopses (2002) 297.
[244] Y. Liu, Y. Zhang, J. Chem. Res. Synopses (2002) 15.

[245] Z. Li, Y. Zhang, Tetrahedron 58 (2002) 5301.
[246] X.X. Wang, Y.M. Zhang, Chin. Chem. Lett. 12 (2001) 943.
[247] W.-K. Su, Y.-M. Zhang, Y.-S. Li, Chin. J. Chem. 19 (2001) 205.
[248] W.-K. Su, Y.-M. Zhang, Y.-S. Li, Chin. J. Chem. 19 (2001) 381.
[249] J.S. Ravi Kumar, M.F. O'Sullivan, S.E. Reismann, C.A. Hulford, T.V. Ovaska, Tetrahedron Lett. 43 (2002) 1939.
[250] G.-F. Zhang, W.-D. Xue, X.-L. Wang, Z.-H. Zhu, H.-Y. Wang, L.-X. Zou, Y. Sun, Chin. J. Atom. Mol. Phys. 18 (2001) 372.
[251] J. Li, B.E. Bursten, M. Zhou, L. Andrews, Inorg. Chem. 40 (2001) 5448.
[252] L. Joubert, P. Maldivi, J. Phys. Chem. A 105 (2001) 9068.
[253] J.K. Gibson, R.G. Haire, Radiochim. Acta 89 (2001) 363.
[254] J.K. Gibson, R.G. Haire, Radiochim. Acta 89 (2001) 709.
[255] P. Roussel, R. Boaretto, A.J. Kingsley, N.W. Alcock, P. Scott, J. Chem. Soc., Dalton Trans. (2002) 1423.
[256] M.J. Sarsfield, M. Helliwell, D. Collison, Chem. Commun. (2002) 2264.
[257] W.J. Oldham Jr., S.M. Oldham, B.L. Scott, K.D. Abney, W.H. Smith, D.A. Costa, J. Chem. Soc., Chem. Commun. (2001) 1348.
[258] P.C. Blake, N.M. Edelstein, P.B. Hitchcock, W.K. Kot, M.F. Lappert, G.V. Shalimoff, S. Tian, J. Organomet. Chem. 636 (2001) 124.
[259] J.C. Berthet, M. Nierlich, M. Ephritikhine, Eur. J. Inorg. Chem. (2002) 840.
[260] P.B. Duval, C.J. Burns, D.L. Clark, D.E. Morris, B.L. Scott, J.D. Thompson, E.L. Werkema, L. Jia, R.A. Andersen, Angew. Chem. 113 (2001) 3461;
P.B. Duval, C.J. Burns, D.L. Clark, D.E. Morris, B.L. Scott, J.D. Thompson, E.L. Werkema, L. Jia, R.A. Andersen, Angew. Chem. Int. Ed. 40 (2001) 3357.
[261] T. Arliguie, C. Lescop, L. Ventelon, P.C. Leverd, P. Thuery, M. Nierlich, M. Ephritikhine, Organometallics 20 (2001) 3698.
[262] W.J. Evans, G.W. Nyce, K.J. Forrestal, J.W. Ziller, Organometallics 21 (2002) 1050.
[263] J.L. Kipplinger, D.E. Morris, B.L. Scott, C.J. Burns, Organometallics 21 (2002) 5978.
[264] J.L. Kiplinger, D.E. Morris, B.L. Scott, C.J. Burns, Chem. Commun. (2002) 30.
[265] J.L. Kiplinger, D.E. Morris, B.L. Scott, C.J. Burns, Organometallics 21 (2002) 3073.
[266] K.A.N.S. Ariyaratne, R.E. Cramer, J.W. Gilje, Organometallics 21 (2002) 5799.
[267] J.L. Kiplinger, K.D. John, D.E. Morris, B.L. Scott, C.J. Burns, Organometallics 21 (2002) 4306.
[268] W.J. Evans, G.W. Nyce, J.W. Ziller, Organometallics 20 (2001) 5489.
[269] F.G.N. Cloke, P.B. Hitchcock, J. Am. Chem. Soc. 124 (2002) 9352.
[270] T.M. Trnka, J.B. Bonanno, B.M. Bridgewater, G. Perkin, Organometallics 20 (2001) 3255.
[271] I. Korobkov, S. Gambarotta, G.P.A. Yap, Angew. Chem. 114 (2002) 3583;
I. Korobkov, S. Gambarotta, G.P.A. Yap, Angew. Chem. Int. Ed. 41 (2002) 3433.
[272] P.L. Diaconescu, C.C. Cummins, J. Am. Chem. Soc. 124 (2002) 7660.
[273] S.M. Cendrowski-Guillaume, M. Nierlich, M. Ephritikhine, J. Organomet. Chem. 643/644 (2002) 209.
[274] A.K. Dash, Y. Gurevizt, J.Q. Wang, J. Wang, M. Kapon, M.S. Eisen, J. Alloys Compd. 344 (2002) 65.
[275] A. Dash, J.Q. Wang, J. Wang, I. Gourevich, M.S. Eisen, J. Nucl. Sci. Technol. (Suppl. 3) (2002) 386.
[276] A.K. Dash, I. Gourevich, J.Q. Wang, J. Wang, M. Kapon, M.S. Eisen, Organometallics 20 (2001) 5084.
[277] H. Ahn, C.P. Nicholas, T.J. Marks, Organometallics 21 (2002) 1788.
[278] T. Straub, A. Haskel, T. Gueta Neyroud, M. Kapon, M. Botoshansky, M.S. Eisen, Organometallics 20 (2001) 5017.